View metadata, citation and similar papers at core.ac.uk

brought to you by CORE

provided by NASA Technical Reports Server

NASA Technical Memorandum 85679

VERTICAL DROP TEST OF A TRANSPORT FUSELAGE SECTION LOCATED FORWARD OF THE WING

M. Susan Williams
Robert J. Hayduk

August 1983

(NASA-TM-85679) VERTICAL DROP TEST OF A TRANSPORT FUSELAGE SECTION LOCATED FORWARD OF THE WING (NASA) 57 p HC A04/MF A01 CSCL 20K

N84-10611

Unclas
G3/39 42333

National Aeronautics and Space Administration

Langley Research Center
Hampton, Virginia 23665

VERTICAL DROP TEST OF A TRANSPORT FUSELAGE SECTION LOCATED FORWARD OF THE WING

M. Susan Williams
Robert J. Hayduk

Langley Research Center

SUMMARY

A 12-foot long Boeing 707 fuselage section was drop tested at the NASA Langley Research Center to measure structural, seat, and occupant response to vertical crash loads. Occupant response was simulated with anthropomorphic dummies. The specimen had nominally zero pitch, roll, and yaw at impact with a sink speed of 20 ft/sec. Results from this drop test and future drop tests of other transport sections will be used to prepare for a full-scale crash test of a B-720 in July, 1984.

Post-test inspection showed that the section bottom collapsed inward approximately 2 ft. Preliminary data traces indicated maximum normal accelerations of 20 g at the fuselage bottom, 10 to 12 g at the cabin floor, and 6.5 to 8 g at the dummy pelvises.

INTRODUCTION

As part of the NASA LaRC Transport Crash Test program, reference 1, various fuselage sections from Boeing 707 transport aircraft were acquired for dynamic drop testing. The structural response data from these tests will be used to corroborate the DYCAST computer program, reference 2, being developed for crash analysis of aircraft structures. Another purpose of these tests is to determine structural, seat, and occupant response to vertical crash loads in preparation for a full-scale crash test of remotely piloted B-720 to be conducted at NASA/Dryden in July, 1984 as part ot a joint NASA/FAA program.

This report presents photographs and preliminary data traces from the first Transport Section Drop Test conducted April 26, 1983. This 12 foot long, 14.2 foot high section located just forward of the wing, was drop tested at 20 ft/sec using the Vertical Test Apparatus at NASA Langley Research Center. Results from this test provide an indication of vertical loads and accelerations to be expected in the full-scale crash test.

TEST SPECIMEN

The fuselage section is shown suspended in the Vertical Test Apparatus at the Impact Dynamics Research Facility in figure 1. The 12

foot-long section was cut from a Boeing 707 10 in. forward of Body Station (BS) 600 to 10 in. aft of BS 600J (Fig.2) (Ref. 3). After removing nonstructural items, such as interior paneling, insulation, storage bins, ducting, etc., the bare section weighed 1870 lbs. The section weighed 5051 lbs when loaded with seats, anthropomorphic dummies, and instrumentation. The structural beams and paneling, which form the lower bulkhead closing off the cargo bay at BS 600J, were removed in order to make the subfloor structural strength uniform lengthwise.

As can be seen in Figure 1, the fuselage section is open on both ends. In a crash the response of this fuselage section would depend on the transmission of forces and moments between the section and the rest of the structure. This interaction is very difficult to predict and simulate. Consequently, a very simple end restraint tension cable system was used to provide outward radial restraint only.

Figure 3 is a floor layout of seats, instrumentation junction box, a simulated power distribution pallet (for weight simulation) and a battery for camera power. Seats were located on the test section approximately as they are to be located on the full-scale airplane test. Seats A, B, D, and F were modified with two aluminum strips to reinforce the seat pans and help prevent seat pan failure. Each strip was three inches wide, 6064 - TO aluminum sheet metal, 0.100 inch thick and ran the entire width of the seat. For comparison, seat C was not modified and was left with its original rubberized fabric seat pan. Eight 50th percentile, 165 lb, Part 572 anthropomorphic dummies (Ref. 4) were distributed among the five triple seats as follows:

Seat	Anthropomorphic Dummy Location
A	Center
B	Center
C	Outboard, Center, Inboard
D	Center, Outboard
F	Center

All dummies had normal (aligned with the spine) and longitudinal (fore-and-aft perpendicular to the spine) accelerometers in their head and pelvis and were restrained with standard lap belts. A 95th percentile dummy (195 lb) sat in the inboard location of seat F, restrained with a standard lap belt, but was not instrumented with accelerometers. Weights (see Fig. 4) were used to load the remaining six occupant locations. Table I gives the weight and coordinates of all articles and ballast onboard the section at test time. The origin (0,0,0) was chosen to be along the centerline of the fuselage (X), BS 600F (Y), and on top of the floor (Z). Figure 5 gives the seat leg locations in inches relative to the front edge of the test section floor.

TEST APPARATUS AND METHODS

The NASA Vertical Test Apparatus (VTA) (Fig. 1) was used to drop test the transport section and to provide a stable guide mechanism for the vertical impact test. The VTA was designed for the following conditions:

1. Maximum impact velocity - 50 ft/sec
2. Maximum specimen dimensions - 12 ft diameter, 26 ft long, 10,000 lb weight

Test conditions for the transport section test fell below these limits.

The VTA is located at the north west leg of the gantry structure at the Impact Dynamics Research Facility (Ref. 5). The gantry provides support through lateral ties to the VTA. The VTA (70 ft high) consists of a 7 1/2 ton hoist platform on two support columns. Each column has rails to guide the vertical motion of a lift frame to which a specimen can be attached for drop testing. The specimen impacts a steel reinforced concrete pad at the bottom of the VTA while the support frame is decelerated by impacting shock absorbers. A power quick-release hook is used to lift the support frame and specimen to the desired drop height.

For the transport section test, the section was connected to the support frame by a series of cables with turnbuckles to adjust cable length and control the impact attitude. The impact attitude for the test was 0 degree pitch, 0 degree yaw, and 0 degree roll. The section was raised 6 ft 2.5 in above the impact surface to obtain a vertical impact velocity of 20 ft/sec. The section contacted the concrete prior to the support frame impacting the shock absorbers.

INSTRUMENTATION AND DATA REDUCTION

DC accelerometers were used in the dummies and on the aircraft structure to obtain continuous recordings during the dynamic drop test. The accelerometers were mounted on aluminum blocks, which were then mounted to the structure (Fig. 6). Strain gages were located on the support frames beneath the floor. Figures 7a and 7b show the location of the accelerometers and strain gages and also show the positive axis directions. Four extensometers (see Fig. 6) were mounted on the section, two above the floor and two below to measure deflection of the fuselage relative to the floor. All data were transmitted to a tape recorder through an umbilical cable that was hard-wired to the data acquisition system.

The analog signals were filtered during recording at 600 Hz and subsequently digitized at 4000 samples per second. The digitized accelerometer data were passed through the following digital filters:

Dummy Head	180 Hz

Dummy Pelvis	180 Hz
Aircraft Structure	20 Hz

The extensometer data and strain gage data are not presented in this preliminary data report.

Motion pictures were taken at 400 pictures per second during the experiment. The cameras were located onboard the test section and on the ground. Still photographs were taken before and after the test.

GENERAL RESULTS

Figures 8a through 8d show post-test damage to the transport section. The frontal view of the section in figure 8a shows that the fuselage beneath the floor collapsed approximately 2 ft. No apparent damage occurred to the upper fuselage. floor, or seats during the test.

Bending failure of the frames occurred on both sides of the fuselage at approximately one third the vertical height from the fuselage bottom to the top of the floor. On the port side, the skin folded between bays at the bending failure (Fig. 8b). The floor in the baggage compartment buckled inward and upward, and bolt holes were sheared through on the port side where the edge of the floor was fastened down (Fig. 8c). Tensile failures due to bending occurred along access holes beneath the baggage compartment floor (Figs. 8b and 8c). Figure 8d shows a frame on the starboard side approximately 2 ft below the floor at BS 600H, which failed in bending where the cross sectional thickness of the frame was decreasing.

Acceleration time histories for the structure and anthropomorphic dummies are given in figures 9a through 9s and 10a through 10p, respectively. The locations of the acceleration traces are identified by word descriptions and by numbers, which are shown in figures 7a and 7b. The locations of the acceleration traces in the dummies are also identified by word descriptions and by numbers referring to figure 3. These data traces are presented in an unrefined form in order to make them available quickly. Futher refinement will correct for zero shifts.

The maximum normal acceleration of the first pulse was measured on the bottom of the fuselage and was approximately 20 g (20 Hz filter) with a time duration of 0.03 sec. Secondary pulses were in the 6 to 12 g range. Normal accelerations measured on the frames approximately one-third and two-thirds the vertical distance between the bottom of the fuselage and floor on the starboard side were characterized by two pulses. The first pulse ranged from 8 to 10 g for approximately 0.03 sec. The acceleration levels dropped soon after the buckling failure occurred and began increasing again as the structure stiffened to a maximum of 10 to 12 g for approximately 0.05 sec (second pulse).

Crushing of the fuselage structure in the baggage area resulted in

lower accelerations at the floor level as compared to the measured acceleration of the fuselage bottom. The normal acceleration traces at the floor beam / frame intersection had a first pulse of about 10 g for 0.03 to 0.04 sec followed by a second pulse of 12 g for 0.06 sec. Maximum normal accelerations measured under the inboard seat rails on the floor beams were approximately 8 g for 0.04 sec for the first pulse and 6 g for 0.12 sec for the second pulse.

The highest normal acceleration level measured occurred, surprisingly, at the roof. The roof normal accelerometers at BS 600D and 600H (figures 9r and 9s) show an oscillatory rather than pulse response, as exhibited on the floor and undercarriage. Nearly 24 g for 0.04 sec was measured during the first half wave at BS 600H. This oscillatory response at the roof is in the 10 to 12 cycle per second range, clearly at structural vibration levels.

The maximum normal pelvis accelerations for the dummies in the modified seats (reinforcing straps under the seat pan) were approximately 8 g (filtered at 180 Hz) for both the first and second pulses; however, the duration of the second pulse was longer (0.09 sec as compared to 0.06 sec). The same type of trace with two distinct acceleration peaks was also seen in the normal pelvis acceleration of the dummies in the unmodified seat. The maximum normal acceleration was approximately 6.5 g for each pulse, and the total time duration for both pulses was about 0.24 sec. The accelerations were lower in the unmodified seat, since the loads experienced during the test were not high enough to cause seat pan failure. The unmodified seat was not nearly as stiff as the modified seats with reinforced aluminum seat pans and consequently allowed the dummy occupants to stop over a longer distance with less acceleration.

CONCLUDING REMARKS

A Boeing 707 fuselage section was drop tested at the Impact Dynamics Research Facility, NASA Langley Research Center, to study structural, seat, and occupant response to vertical crash loads. The section, located just forward of the wing, was tested at 20 ft/sec vertical impact velocity without roll, pitch, or yaw.

From post-test inspection of the fuselage section and preliminary data traces the following were concluded:

1. The lower fuselage section (baggage compartment) collapsed inward approximately 2 ft during the test.

2. Bending failures developed along both sides of the section at one third the vertical height between the fuselage bottom and floor.

3. No damage occurred to the upper fuselage, floor, or seats.

4. A maximum normal acceleration of 20 g (20 Hz filter) was measured on the fuselage bottom.

5. Due to the crushing of the lower fuselage, the maximum normal accelerations on the floor were 10 to 12 g (20 Hz filter).

6. Maximum normal pelvic accelerations measured in the anthropomorphic dummies ranged from 6.5 to 8 g (180 Hz filter).

This report is a quick release of technical information before complete refinement and evaluation. Consequently, the above conclusions are preliminary and subject to reconsideration.

REFERENCES

1. Thomson, Robert G.; and Caiafa, Caesar: Designing for Aircraft Structural Crashworthiness. J. of Aircraft, Vol. 19, Number 10, Oct. 1982, Page 868.

2. Pifko, A.B.; and Winter, R.: Theory and Application of Finite Element Analysis to Structural Crash Simulation. Computers and Structures, Vol. 13, pp. 227-285.

3. Boeing 707-720 Reference Guide D6-40942, March 1980, Boeing Commercial Airplane Company.

4. U.S. Code of Federal Regulations, Title 49, Chapter 5, Part 572: Anthropomorphic Test Dummy. Government Printing Office, Washington, D.C., (Rev.) 978.

5. Vaughan, Victor L., Jr.; and Alfaro-Bou, Emilio: Impact Dynamics Research Facility for Full-Scale Aircraft Crash Testing. NASA TN D-8179, 1976.

TABLE I.- TRANSPORT SECTION TEST WEIGHT DISTRIBUTION

Item	Weight(lbs.)	X(in)	Y(in)	Z(in)
Empty weight	1870	0	0	0
Seat A: inboard	146	42	-19	-24
center	188	42	-38	-24
outboard	154	42	-57	-24
Seat B: inboard	154	42	19	-24
center	188	42	38	-24
outboard	148	42	57	-24
Seat C: inboard	187	-18	-19	-24
center	188	-18	-38	-24
outboard	187	-18	-57	-24
Seat D: inboard	154	12	19	-24
center	188	12	38	-24
outboard	187	12	57	-24
Seat F: inboard	217	-47	19	-24
center	188	-47	38	-24
outboard	148	-47	57	-24
Junction box	60	21	-36	-4
Pallet	145	-48	-36	-5
Camera 1 & mount	30	50	-31	-78
Light 1	6	54	-23	-84
Camera 2 & mount	30	50	47	-66
Light 2	6	54	38	-78
Camera 3 & mount	30	0	-42	-60
Light 3	6	14	-45	-72
Camera 4 & mount	30	0	43	-60
Light 4	6	6	44	-72
Time code box & battery	8	30	-70	-12
Battery	18	28	-55	-3
Camera timing panel	4	10	-70	-12
Ballast	20	-65	-54	43
Ballast	20	-50	-54	43
Ballast	40	-65	-48	50
Ballast	20	-50	-48	50
Ballast	40	-65	-37	61
Ballast	40	-65	0	72

ORIGINAL PAGE IS
OF POOR QUALITY

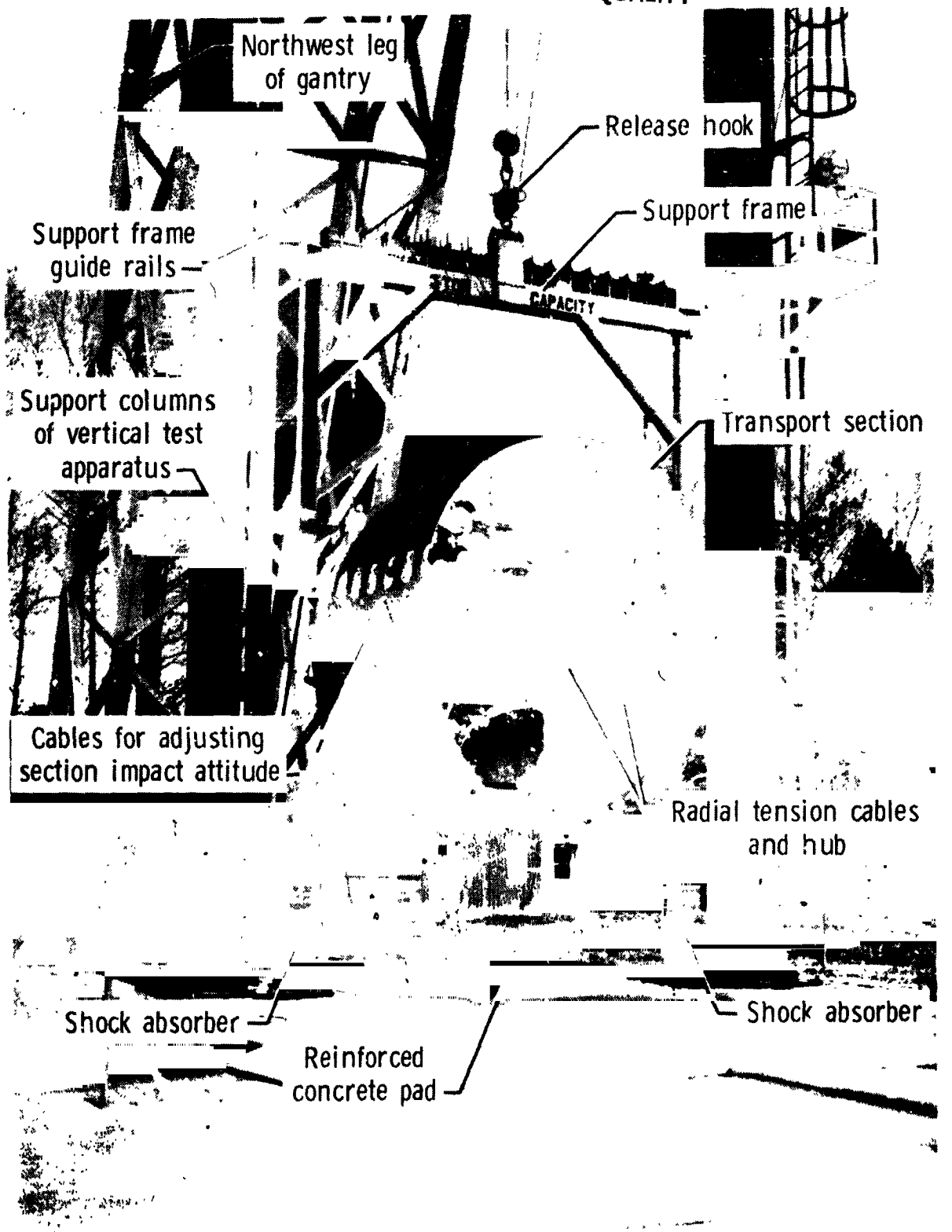

NASA L-83-4,199

Figure 1.- Transport section suspended in Vertical Test Apparatus.

ORIGINAL PAGE IS
OF POOR QUALITY

Figure 2.- B-720 fuselage showing location of test section.

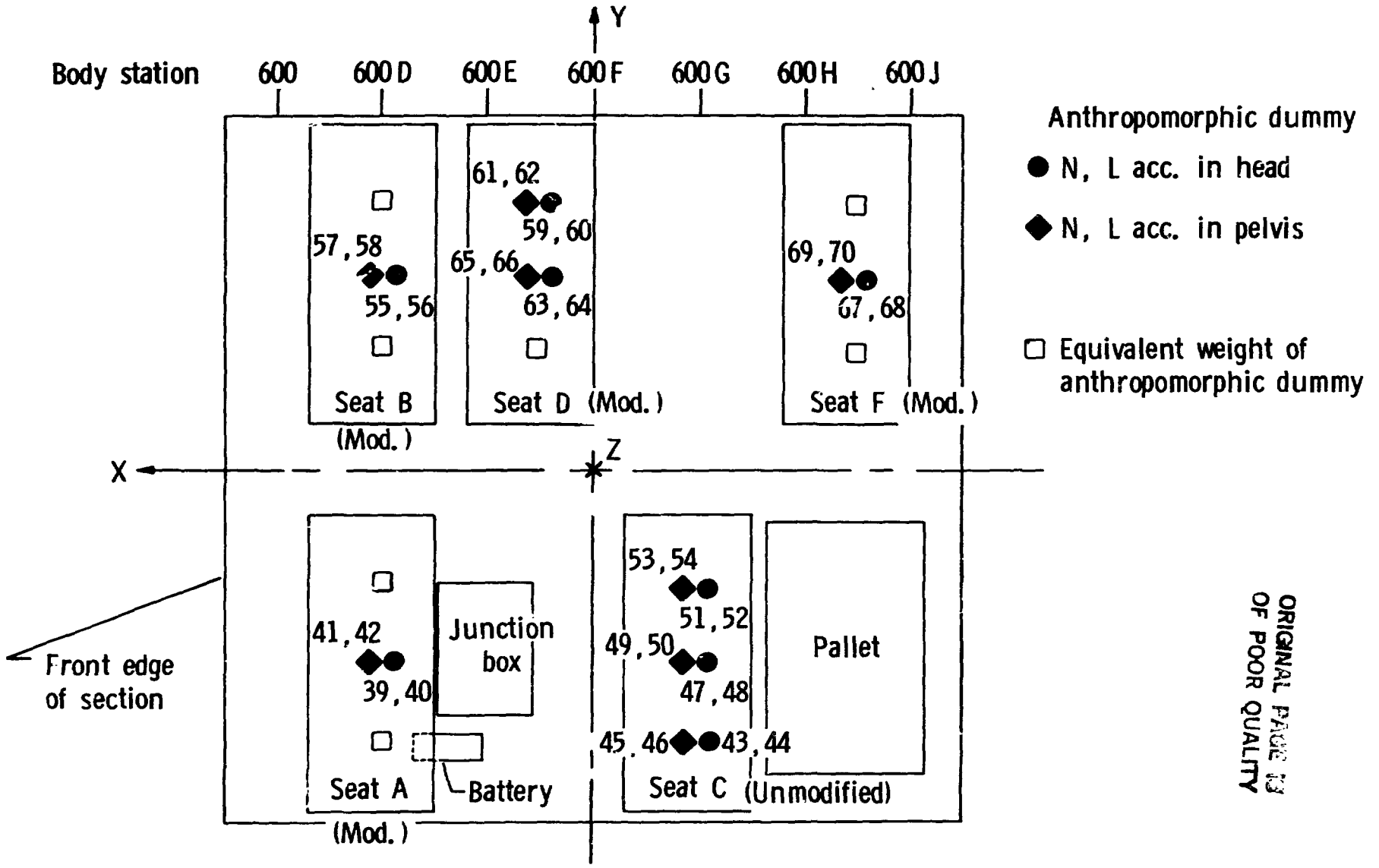

Figure 3.- Transport section test seat arrangement and accelerometer channel number identification for dummies.

ORIGINAL PAGE IS OF POOR QUALITY

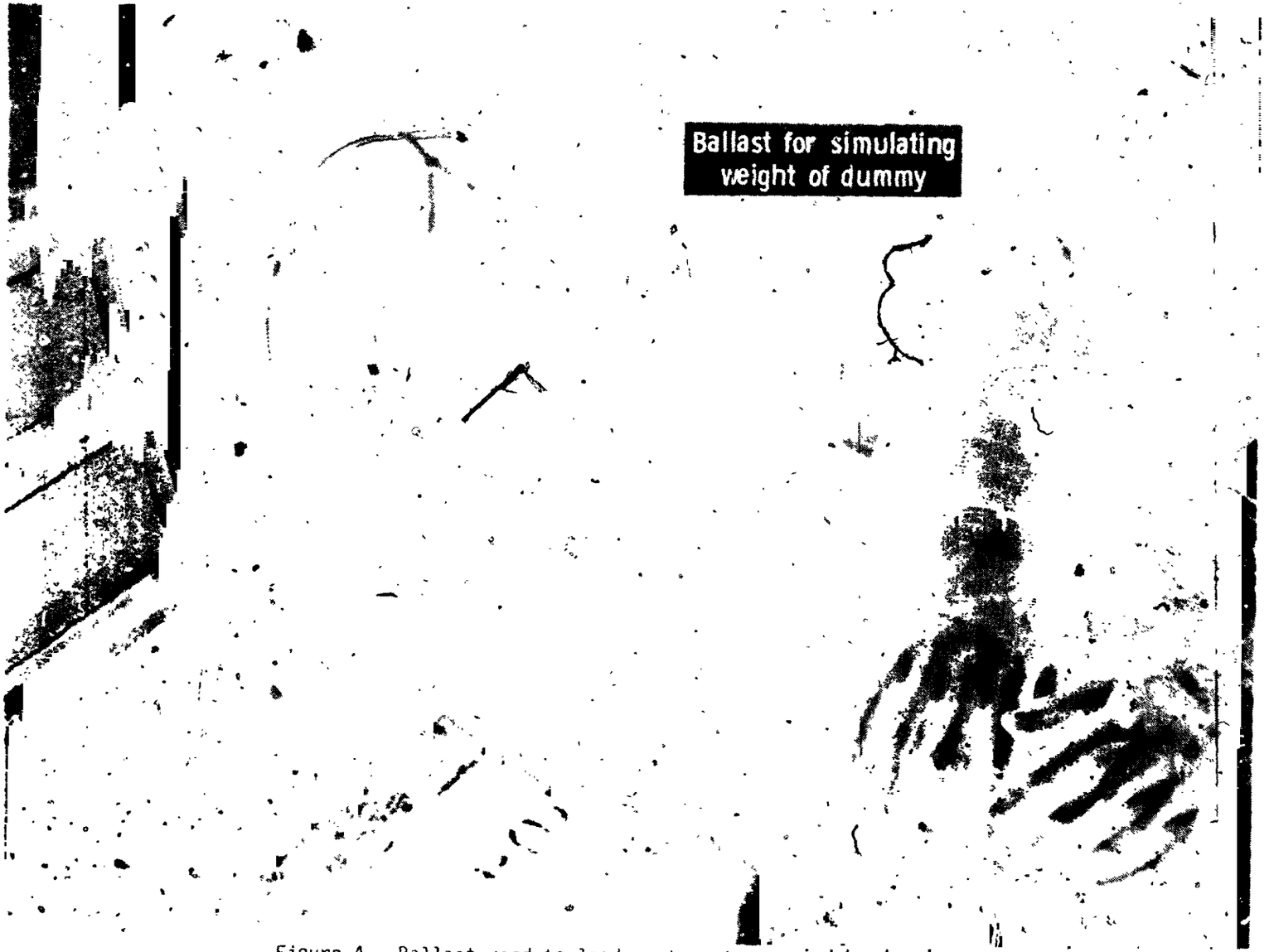

ORIGINAL PAGE IS
OF POOR QUALITY

Figure 4.- Ballast used to load seats not occupied by dummies.

ORIGINAL PAGE IS
OF POOR QUALITY

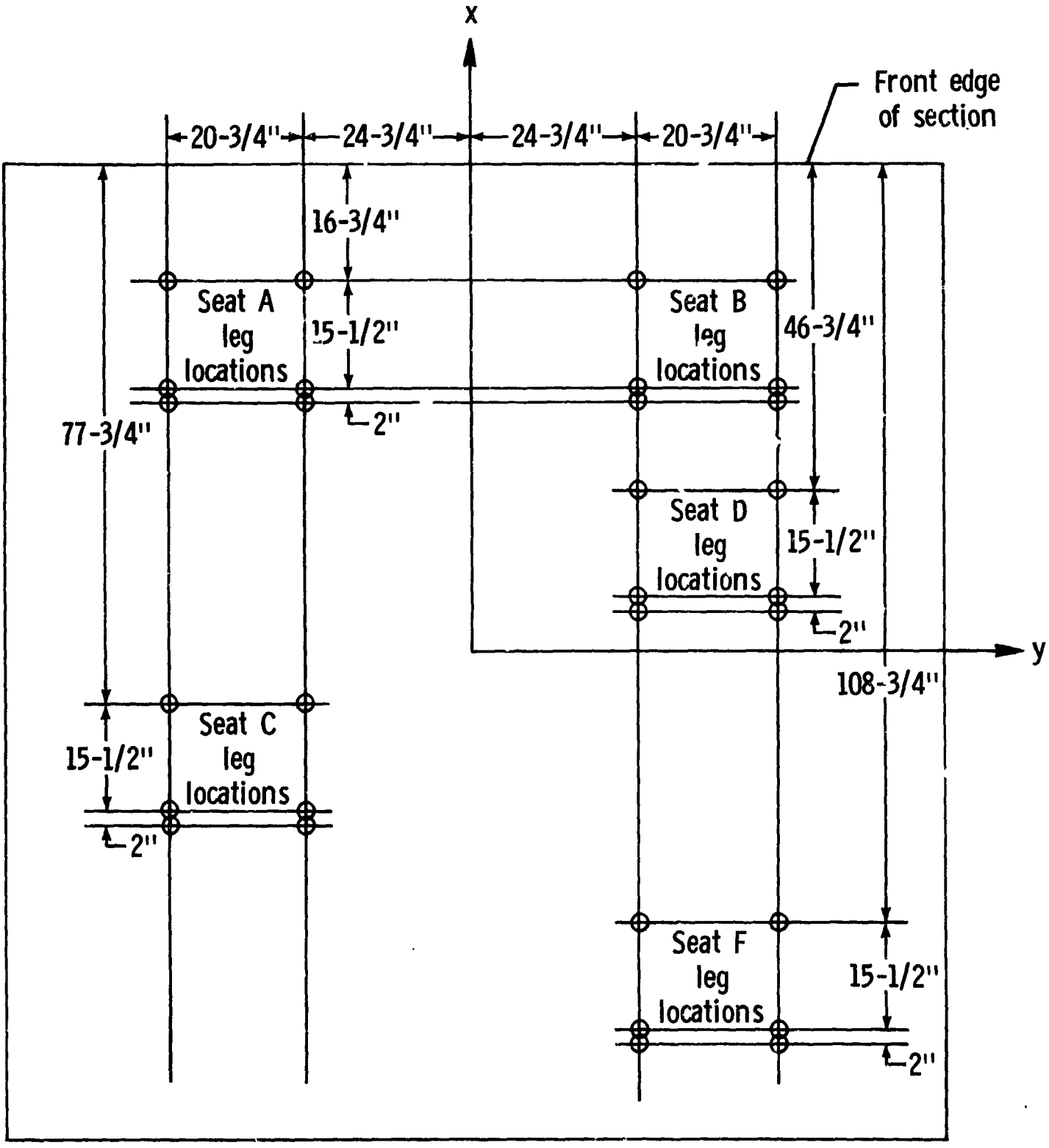

Figure 5.- Seat leg locations relative to front edge of section.

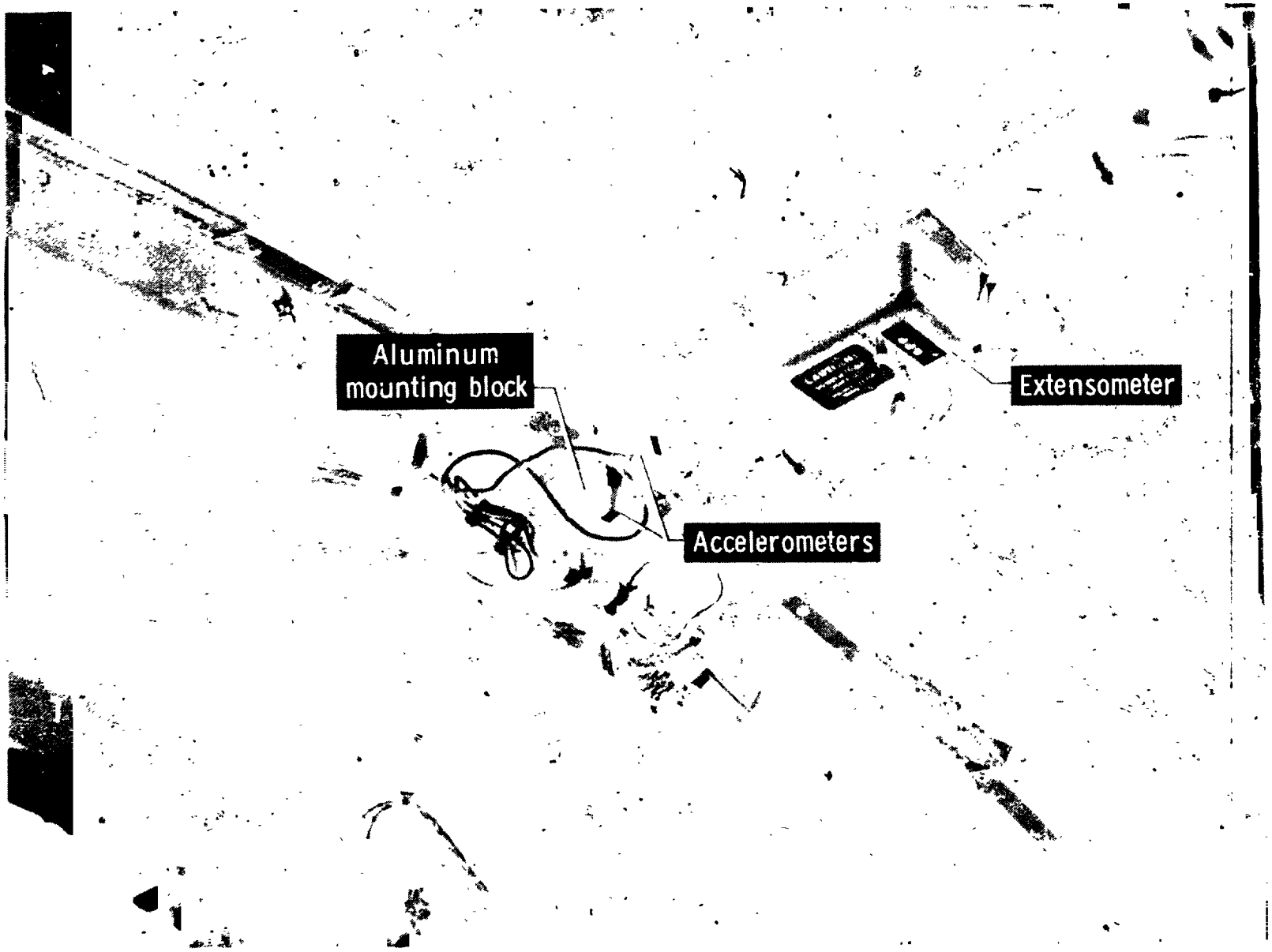

ORIGINAL PAGE IS
OF POOR QUALITY

Figure 6.- Method of mounting accelerometers and extensometers.

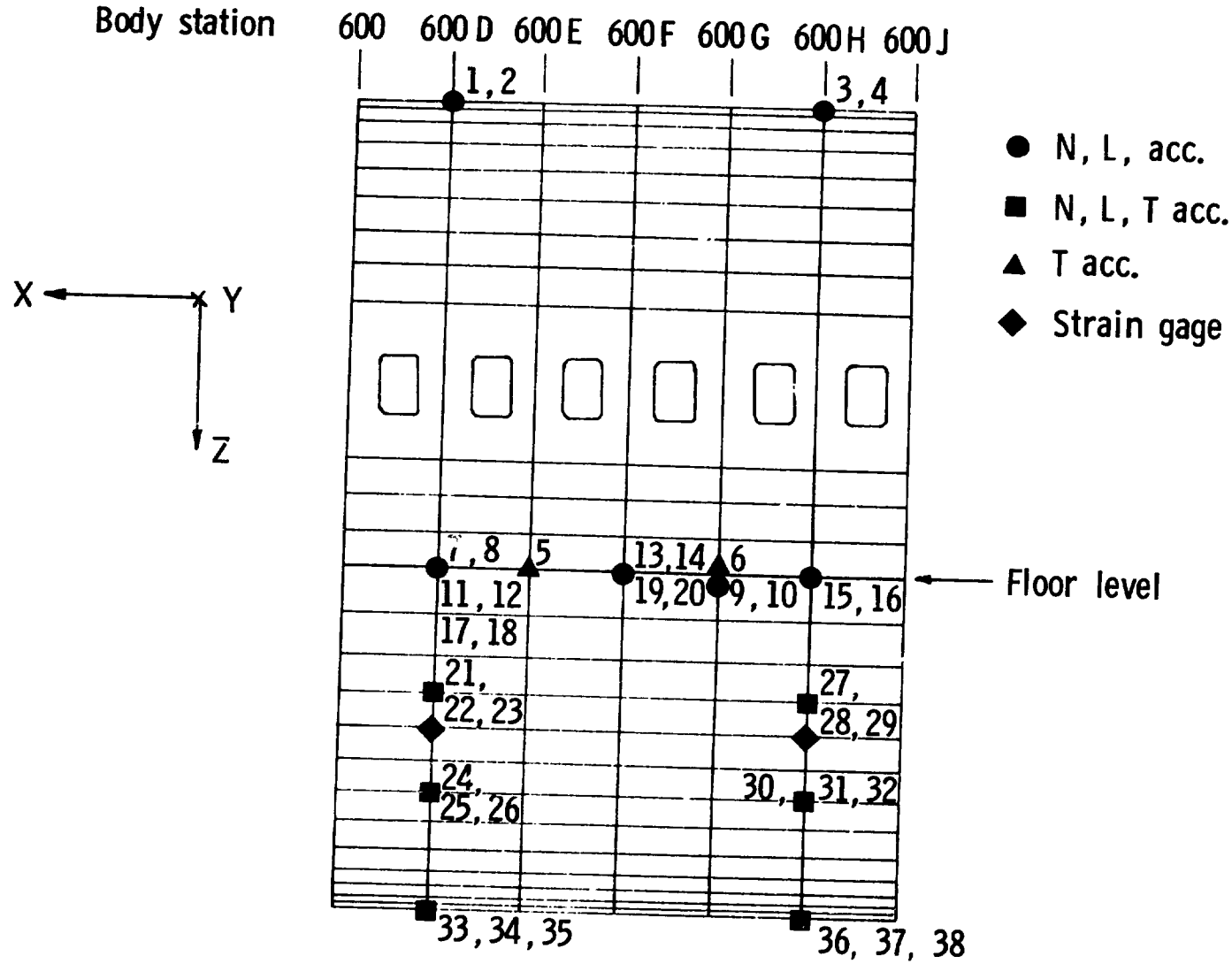

(a) Side view.

Figure 7.- Instrumentation locations for transport section test.

ORIGINAL PAGE IS
OF POOR QUALITY

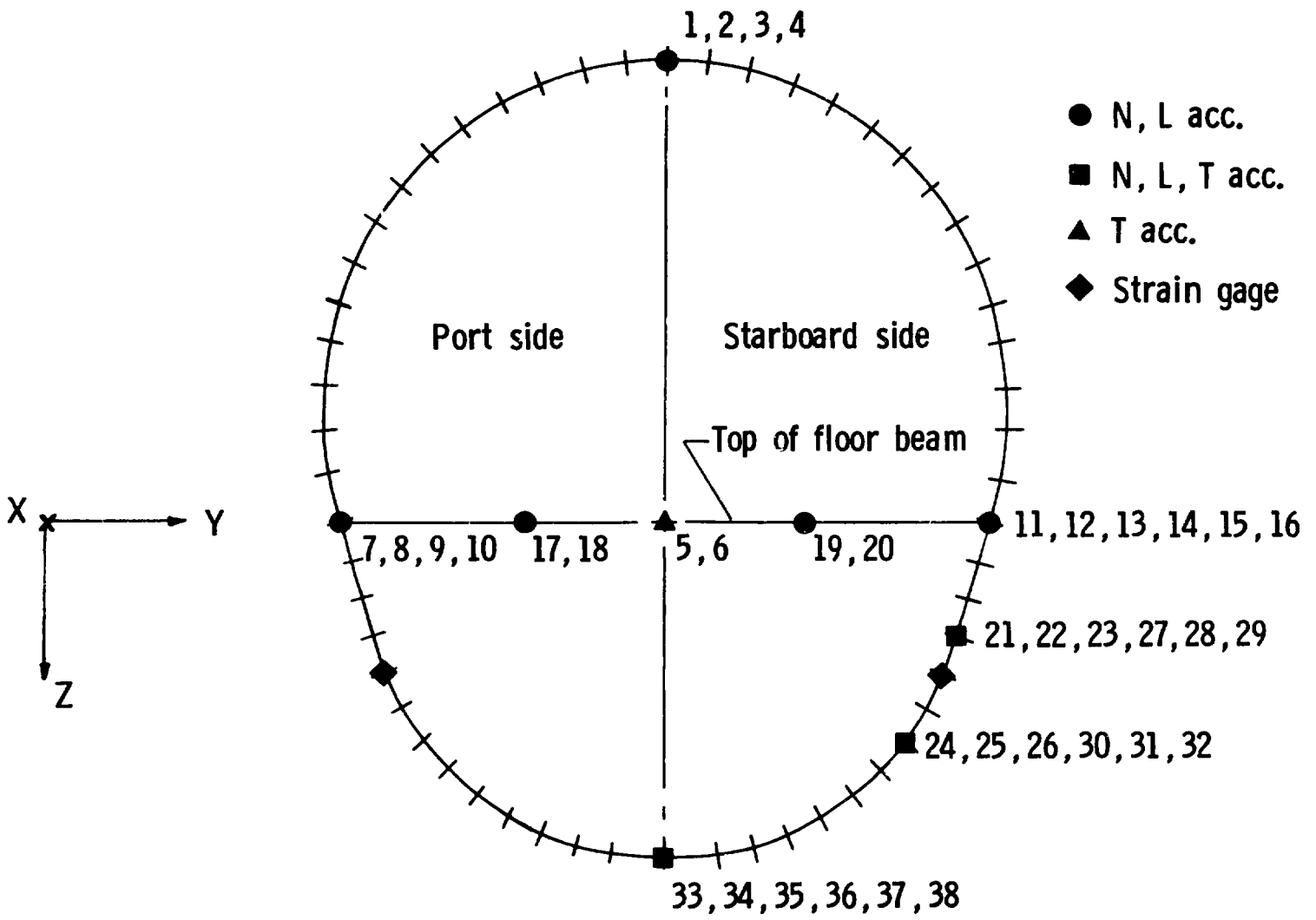

ORIGINAL PAGE IS
OF POOR QUALITY

(b) End view.

Figure 7.- Concluded.

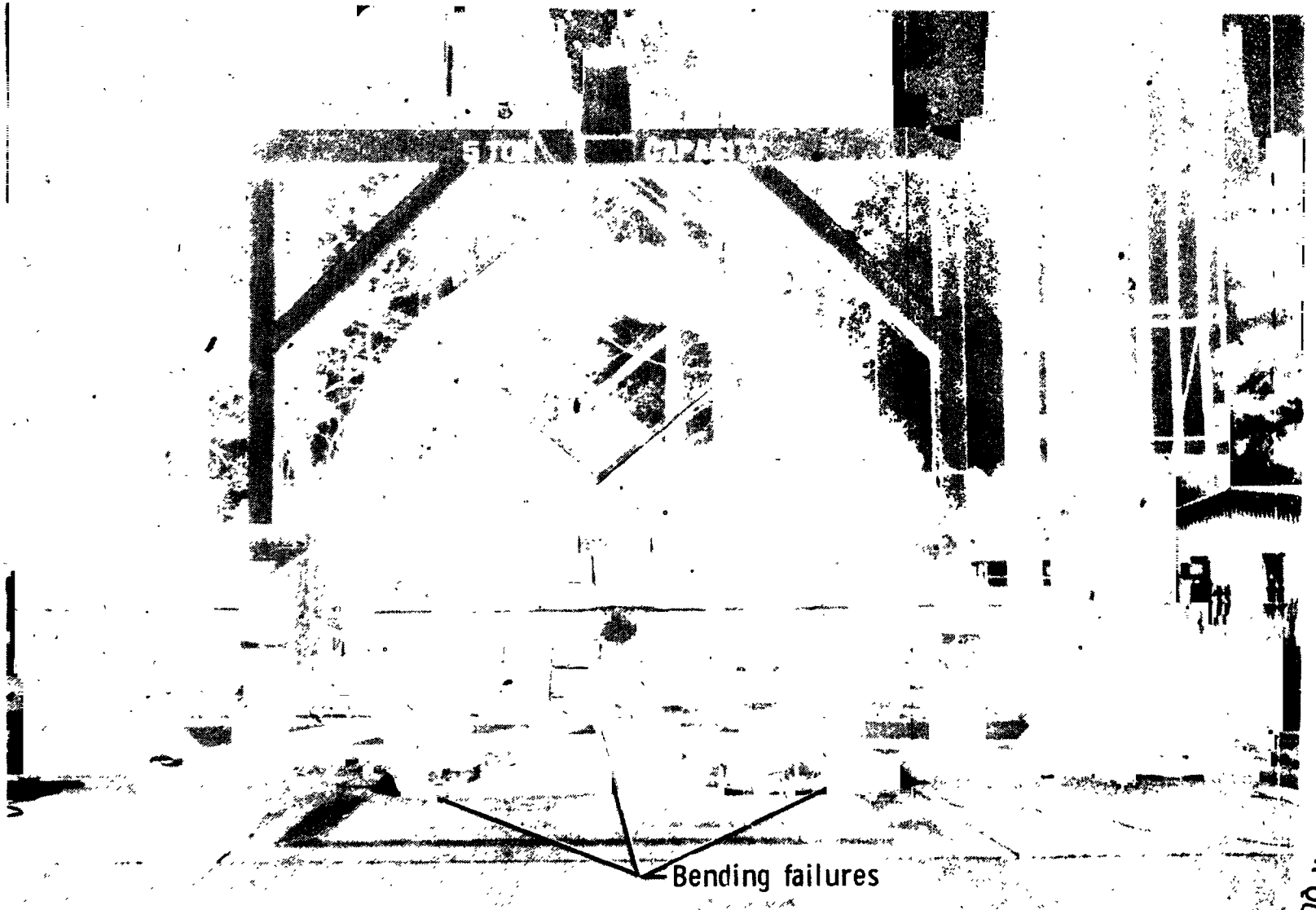

(a) Frontal view of section post-test.

Figure 8.- Post-test photographs of transport section test.

ORIGINAL PAGE IS OF POOR QUALITY

ORIGINAL PAGE IS
OF POOR QUALITY

NASA
L-83-4,186

(b) Frontal view of damage in baggage compartment.

Figure 8.- Continued.

ORIGINAL PAGE IS
OF POOR QUALITY

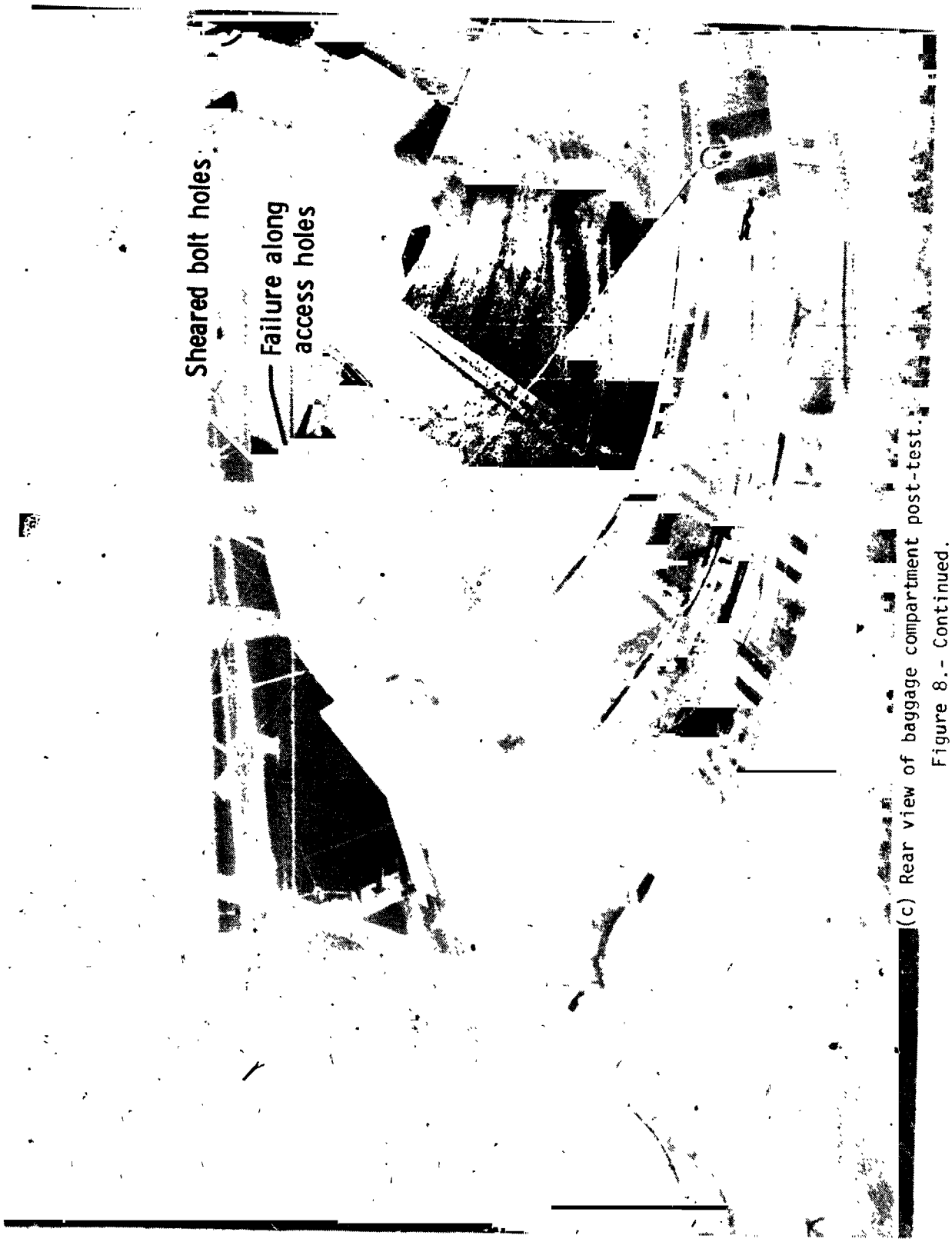

(c) Rear view of baggage compartment post-test.

Figure 8.- Continued.

ORIGINAL PAGE IS
OF POOR QUALITY

(d) Bending failure of frame in lower fuselage.

Figure 8.- Concluded.

ORIGINAL PAGE IS
OF POOR QUALITY

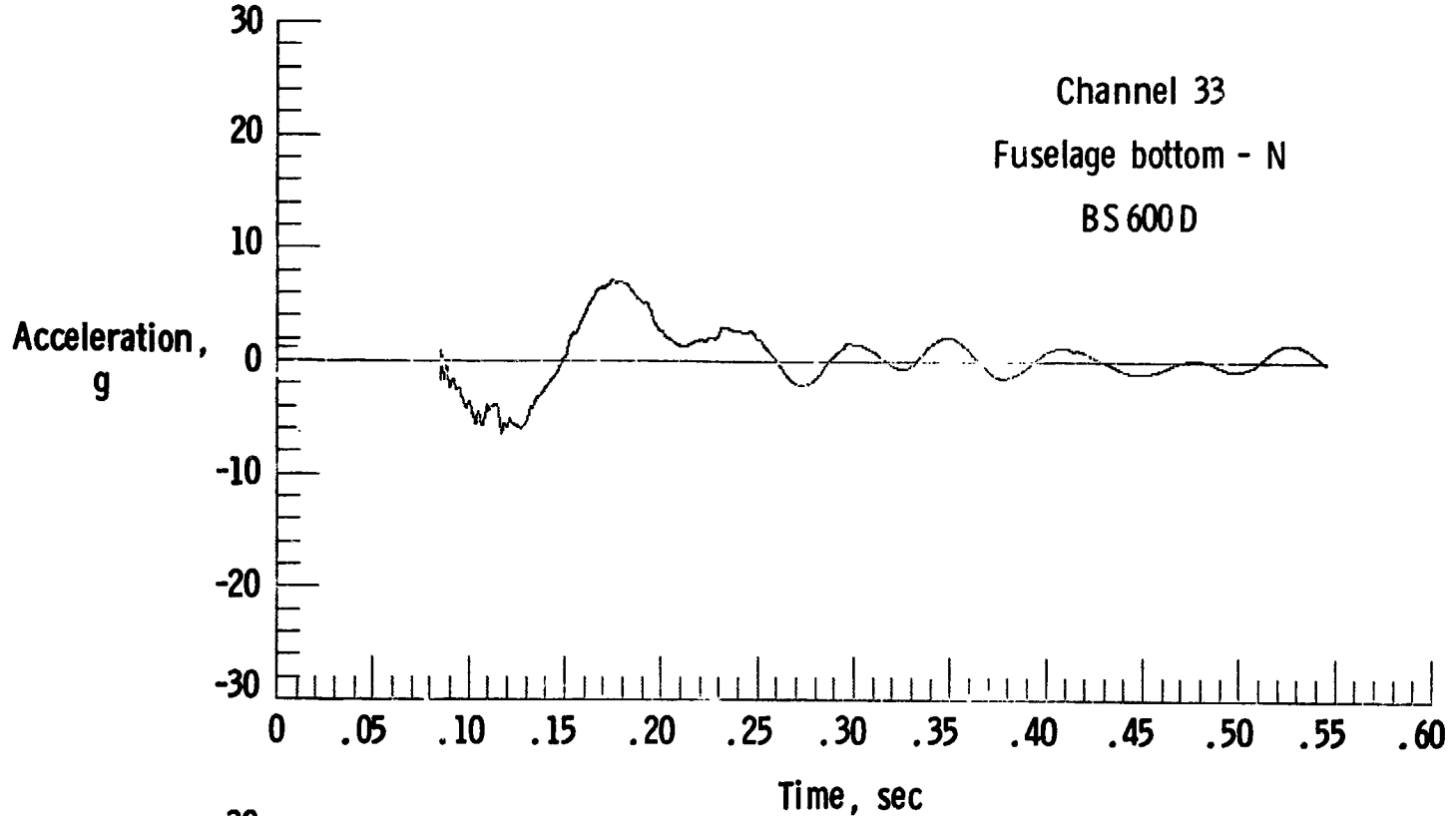

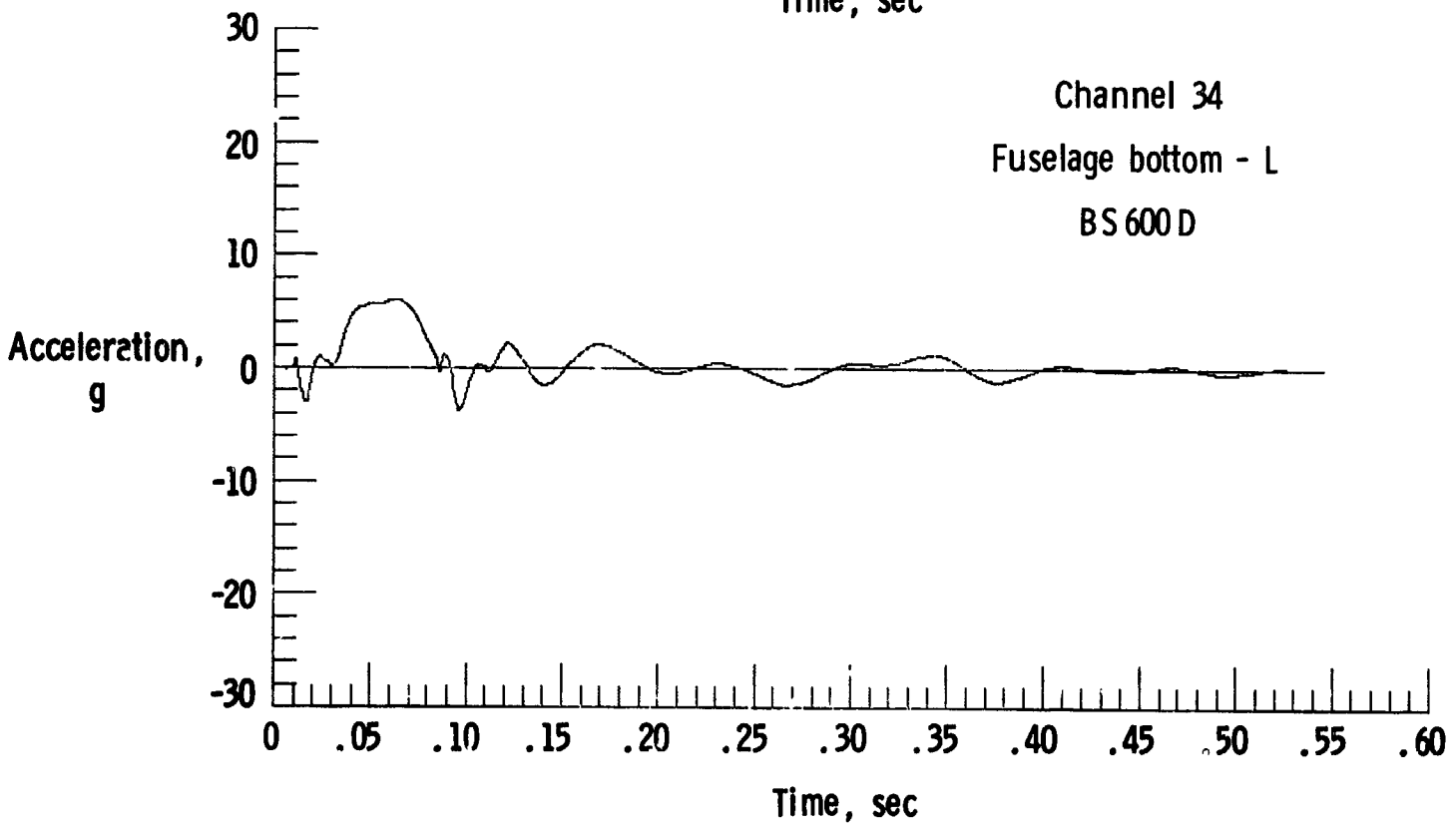

(a) Structural acceleration time histories.

Figure 9.- Acceleration time histories measured on the aircraft structure.

ORIGINAL PAGE IS
OF POOR QUALITY

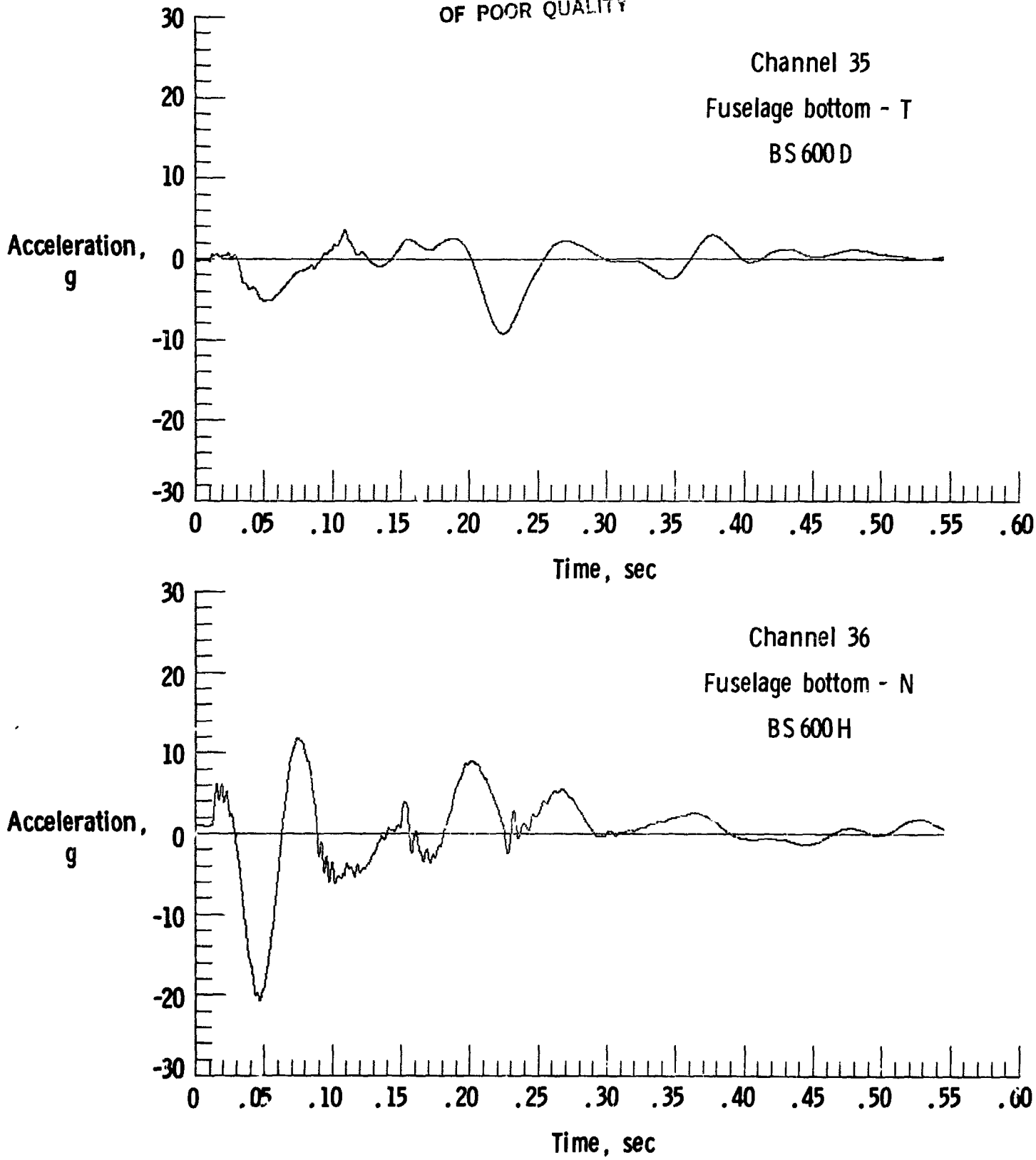

(b) Structural acceleration time histories.
Figure 9.- Continued.

ORIGINAL PAGE IS
OF POOR QUALITY

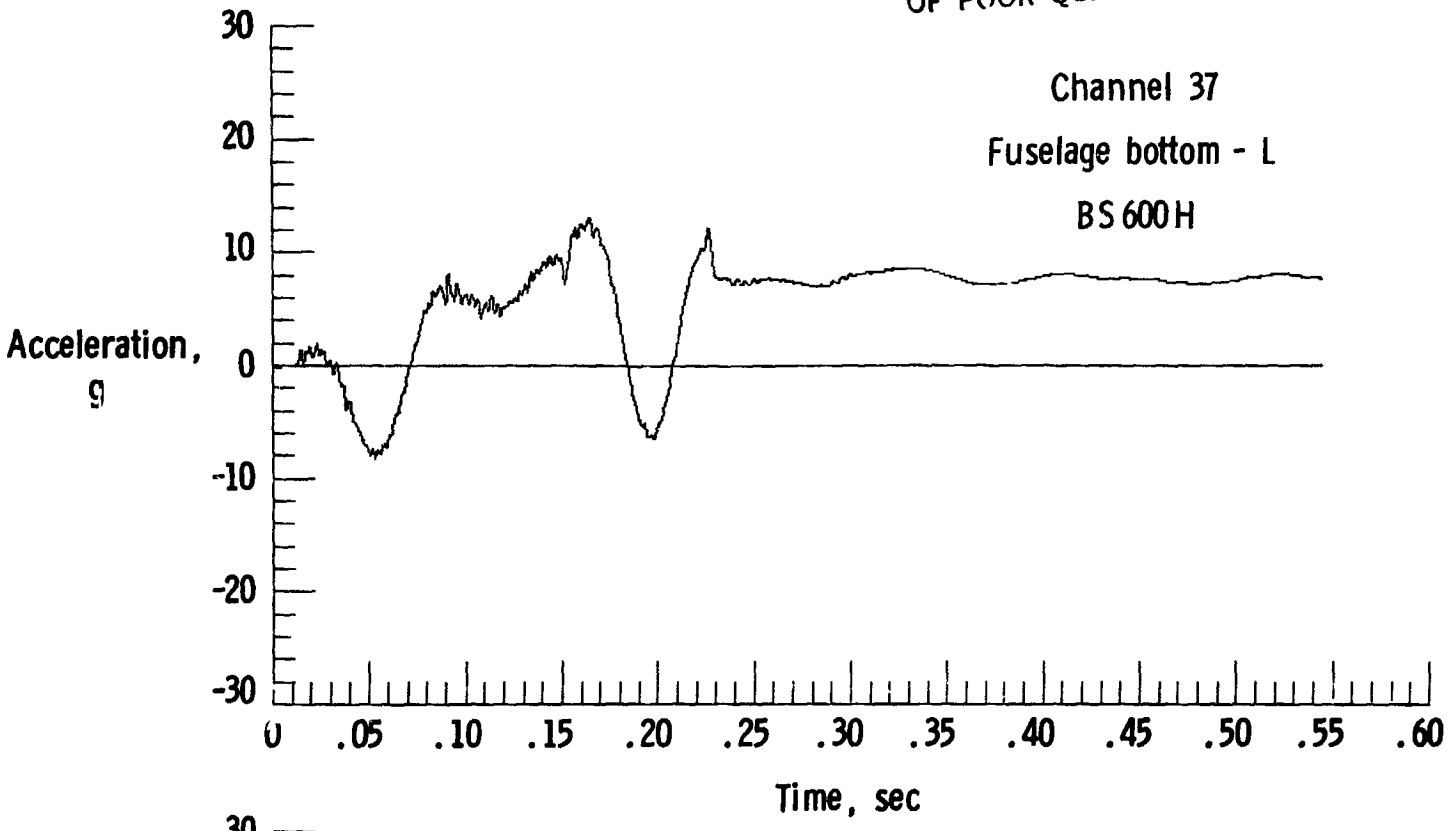

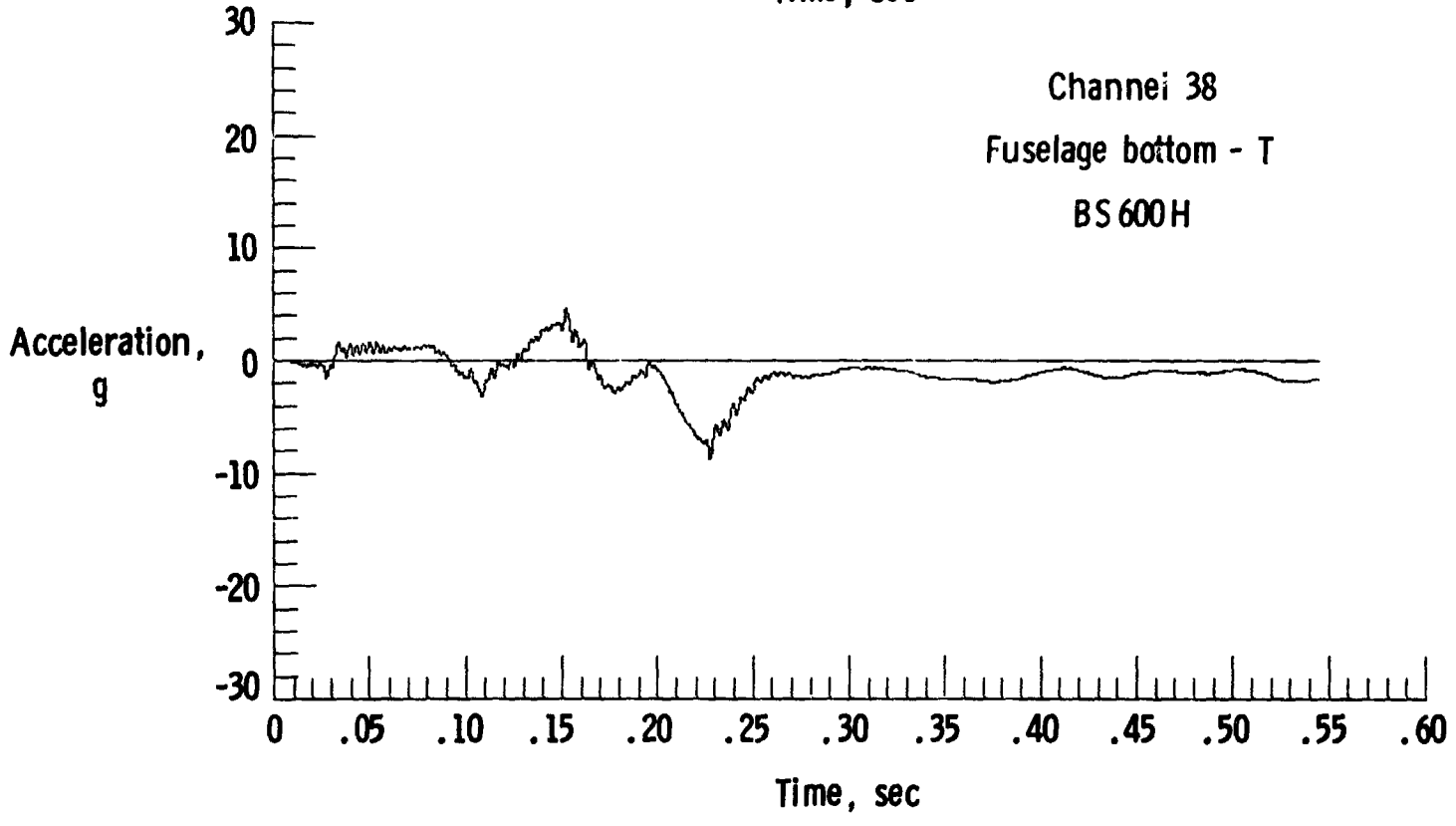

(c) Structural acceleration time histories.
Figure 9.- Continued.

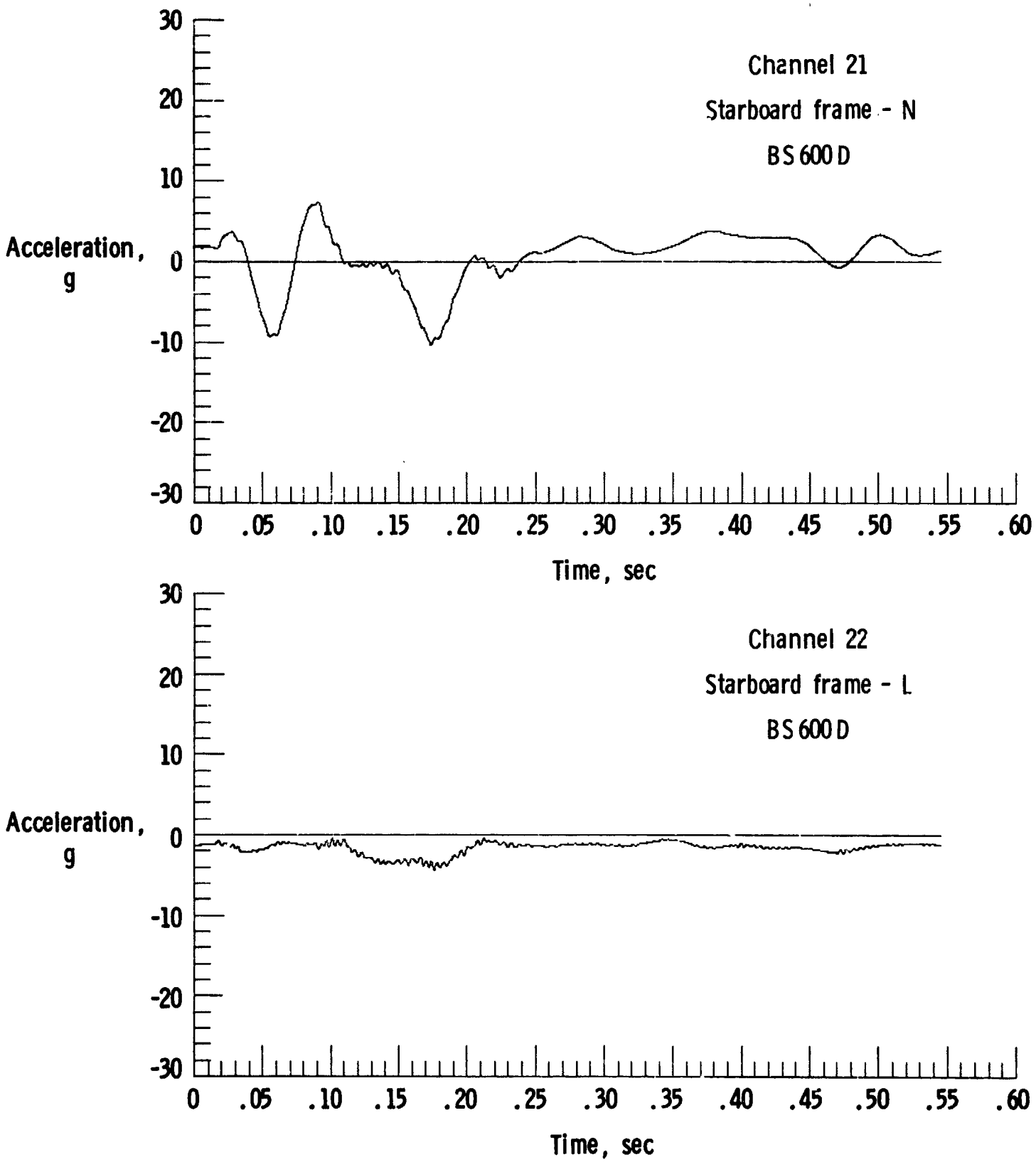

(d) Structural acceleration time histories.
Figure 9.- Continued.

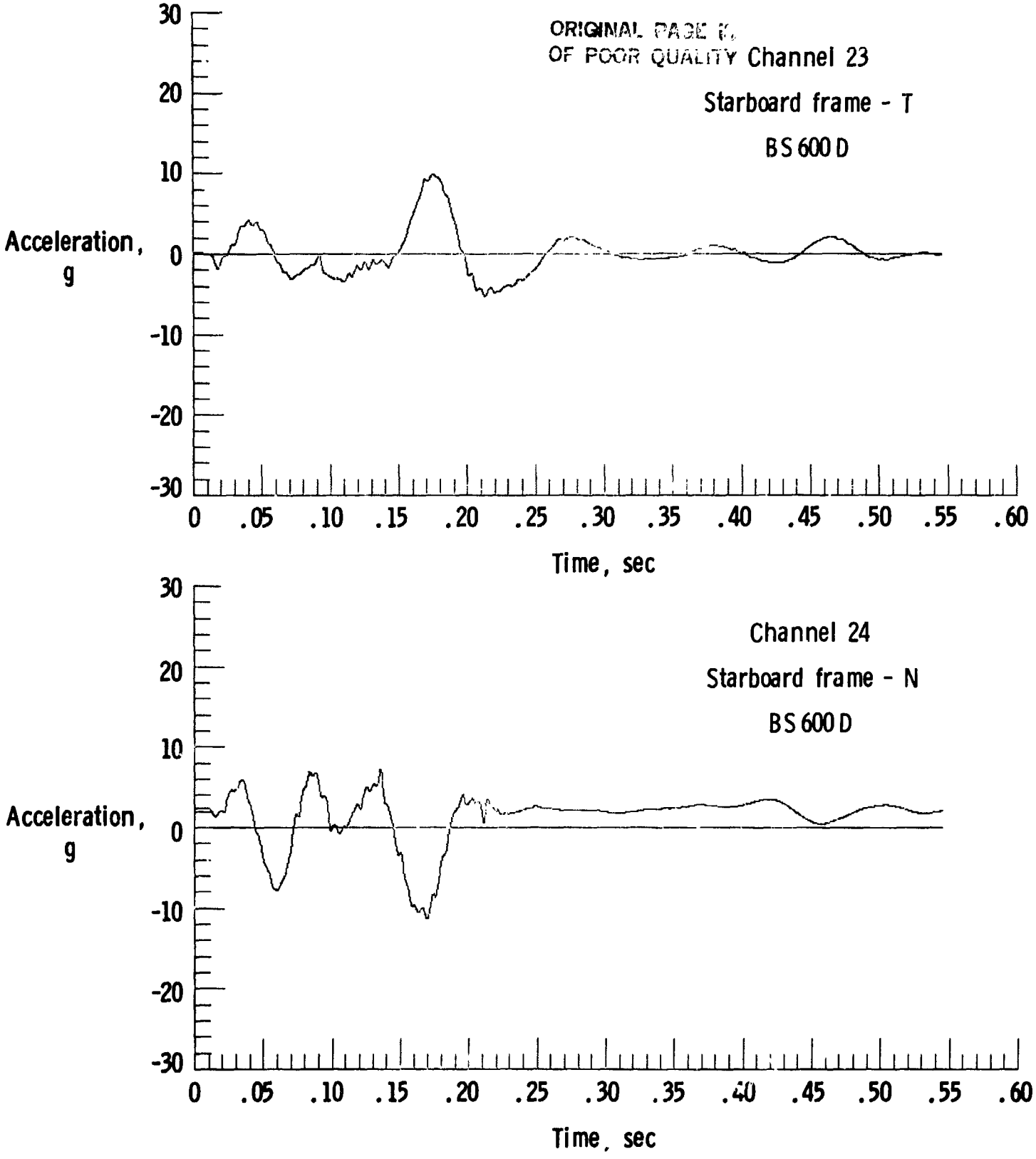

(e) Structural acceleration time histories.
Figure 9.- Continued.

ORIGINAL PAGE IS
OF POOR QUALITY

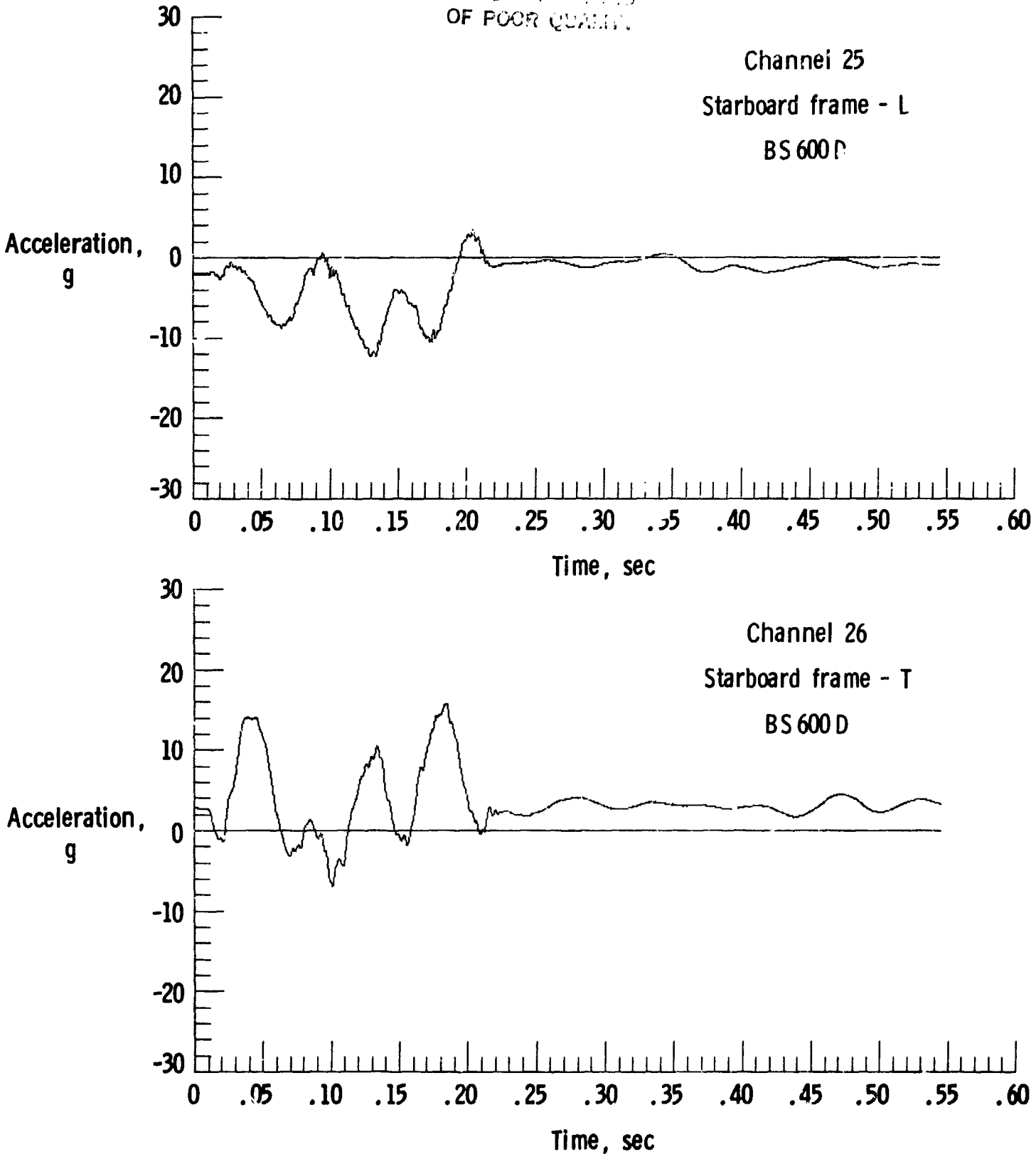

(f) Structural acceleration time histories.
Figure 9.- Continued.

ORIGINAL PAGE IS
OF POOR QUALITY

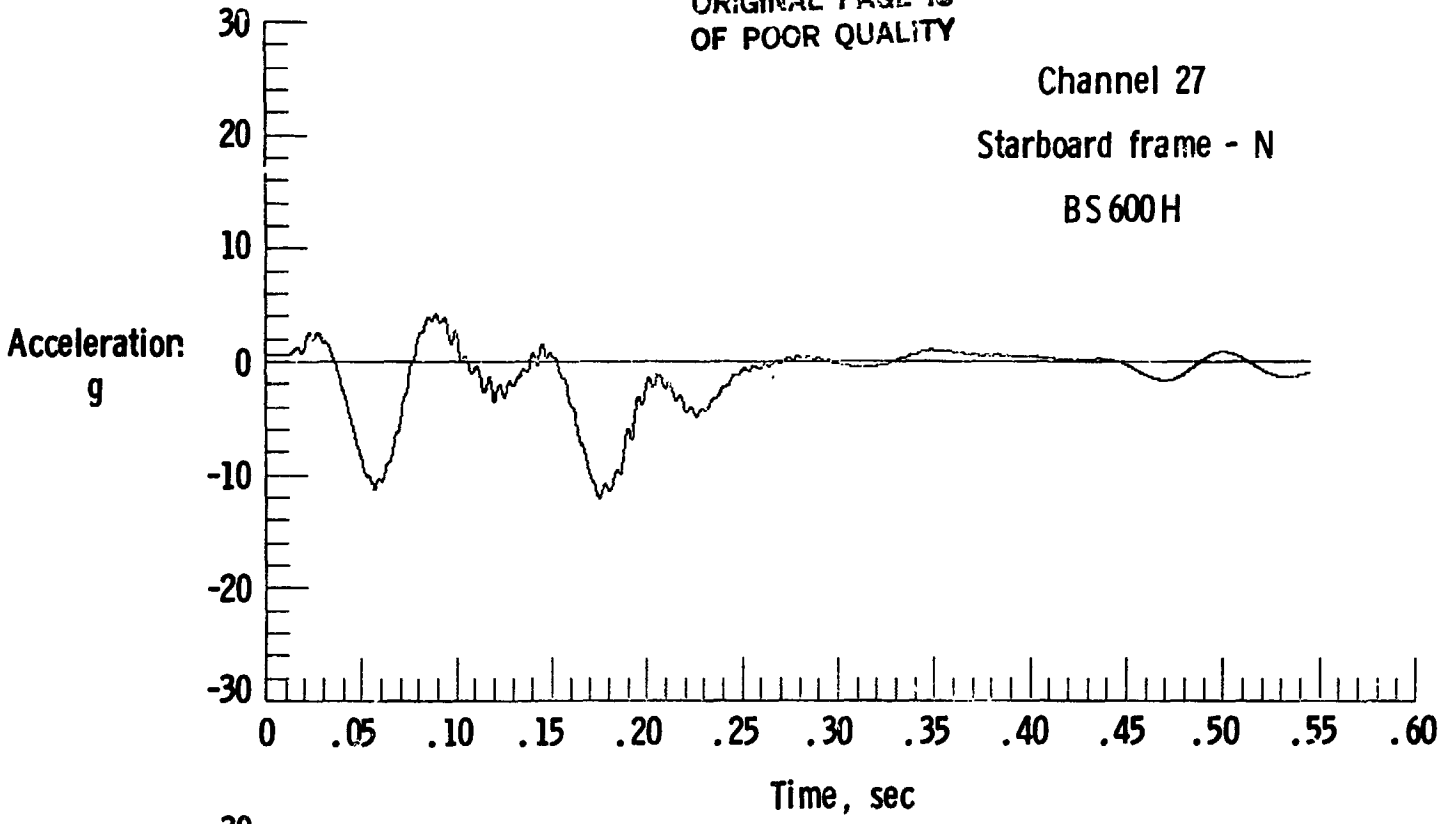

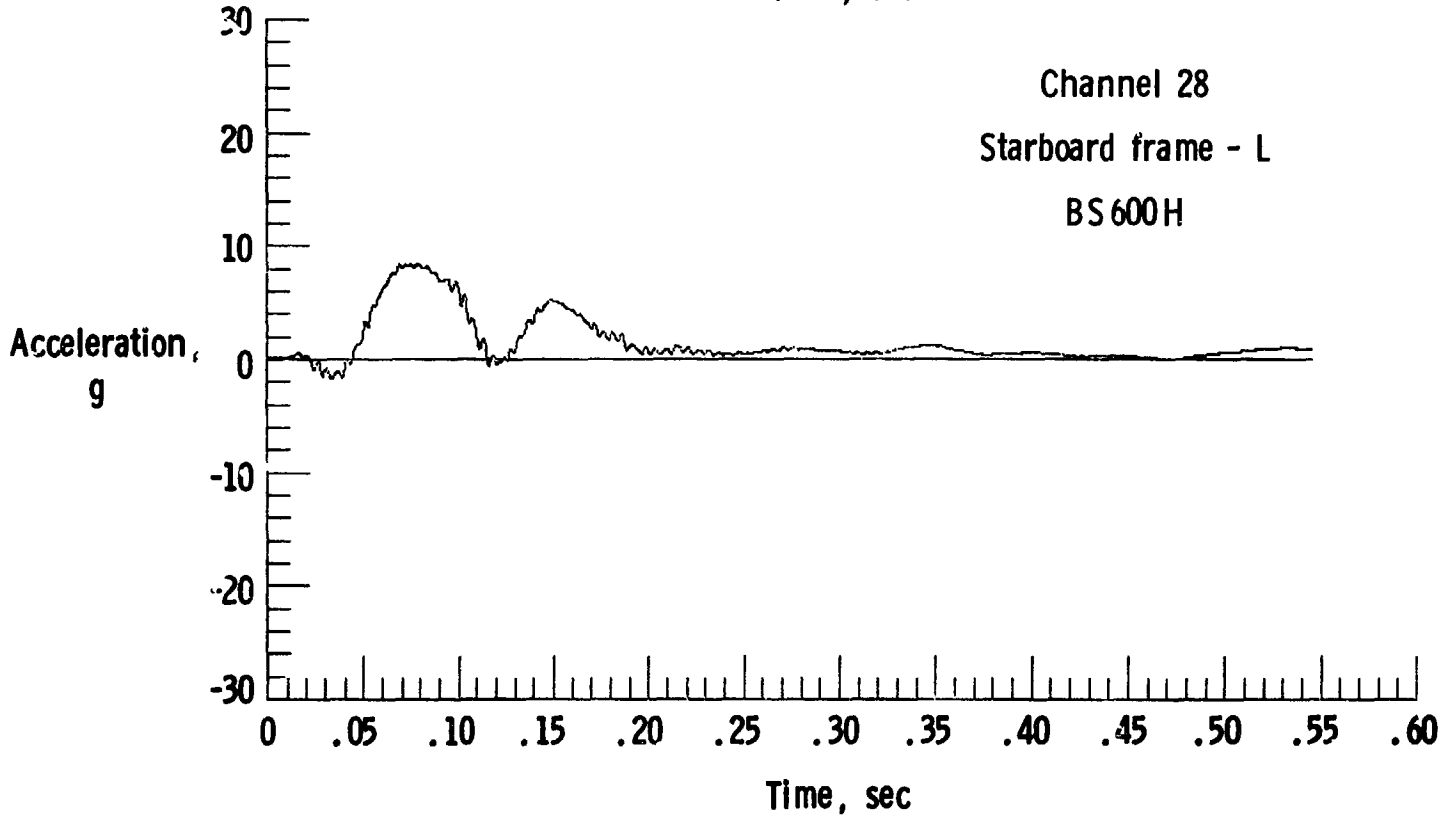

(g) Structural acceleration time histories.
Figure 9.- Continued.

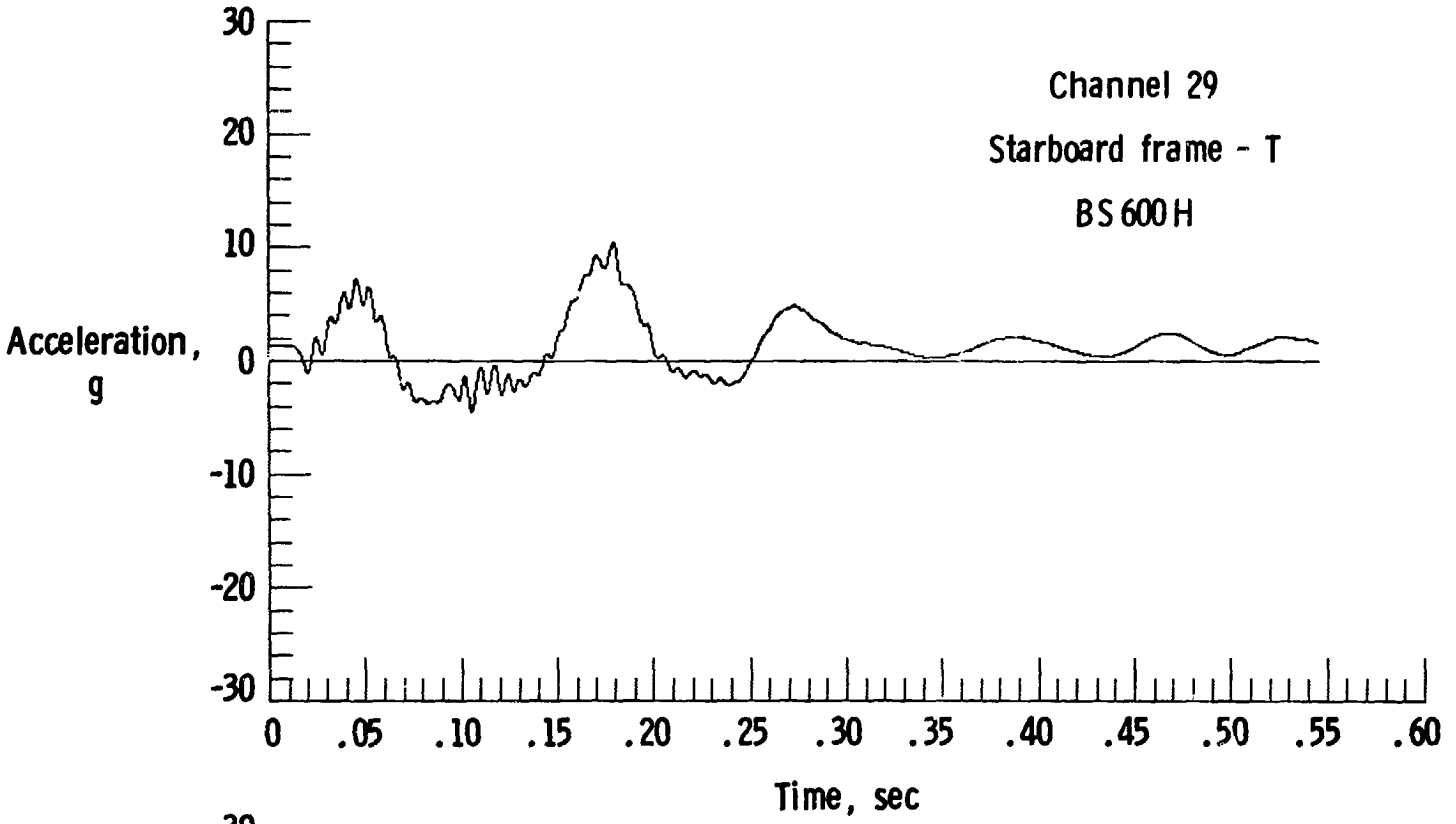

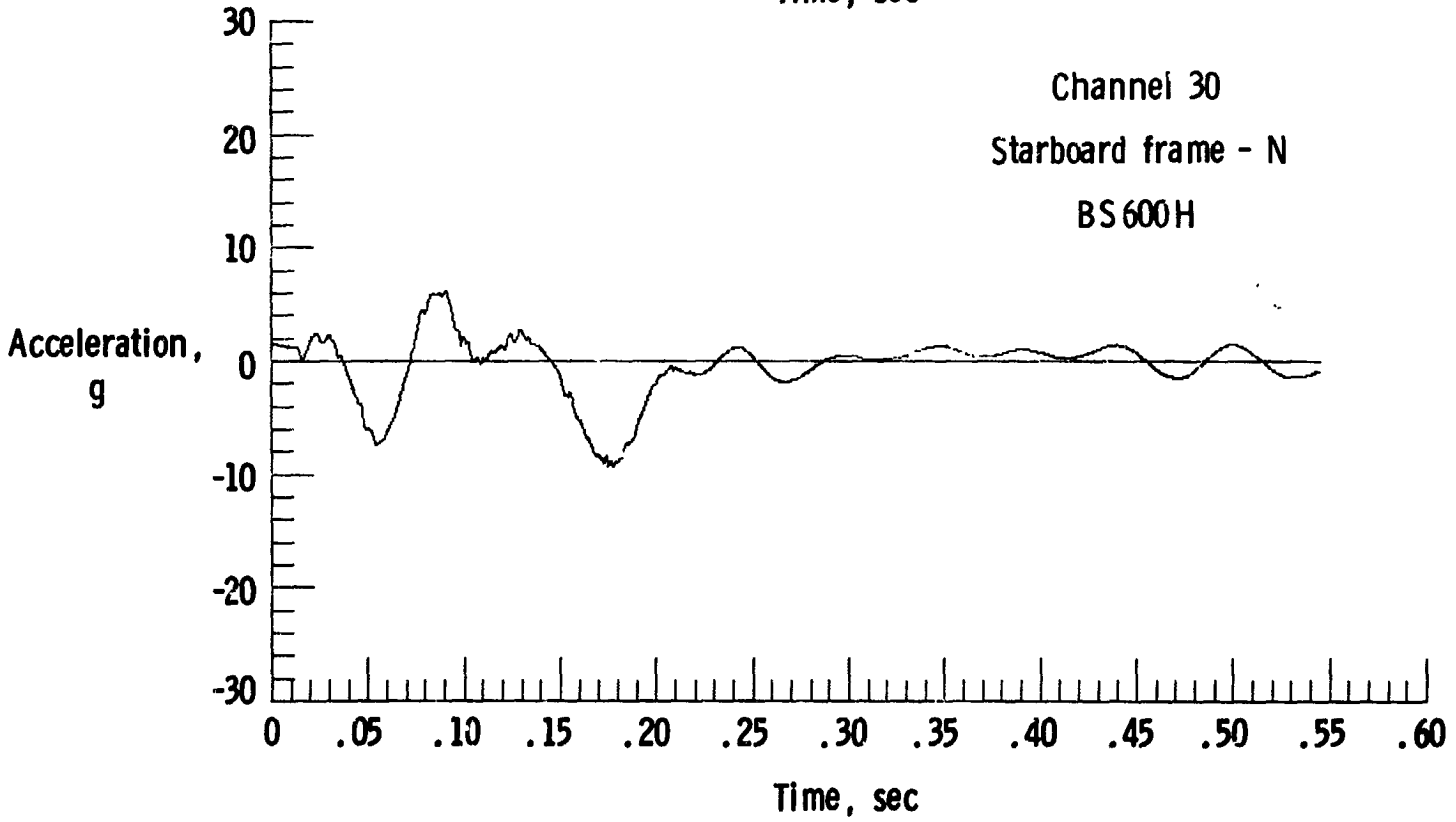

(h) Structural acceleration time histories.
Figure 9.- Continued.

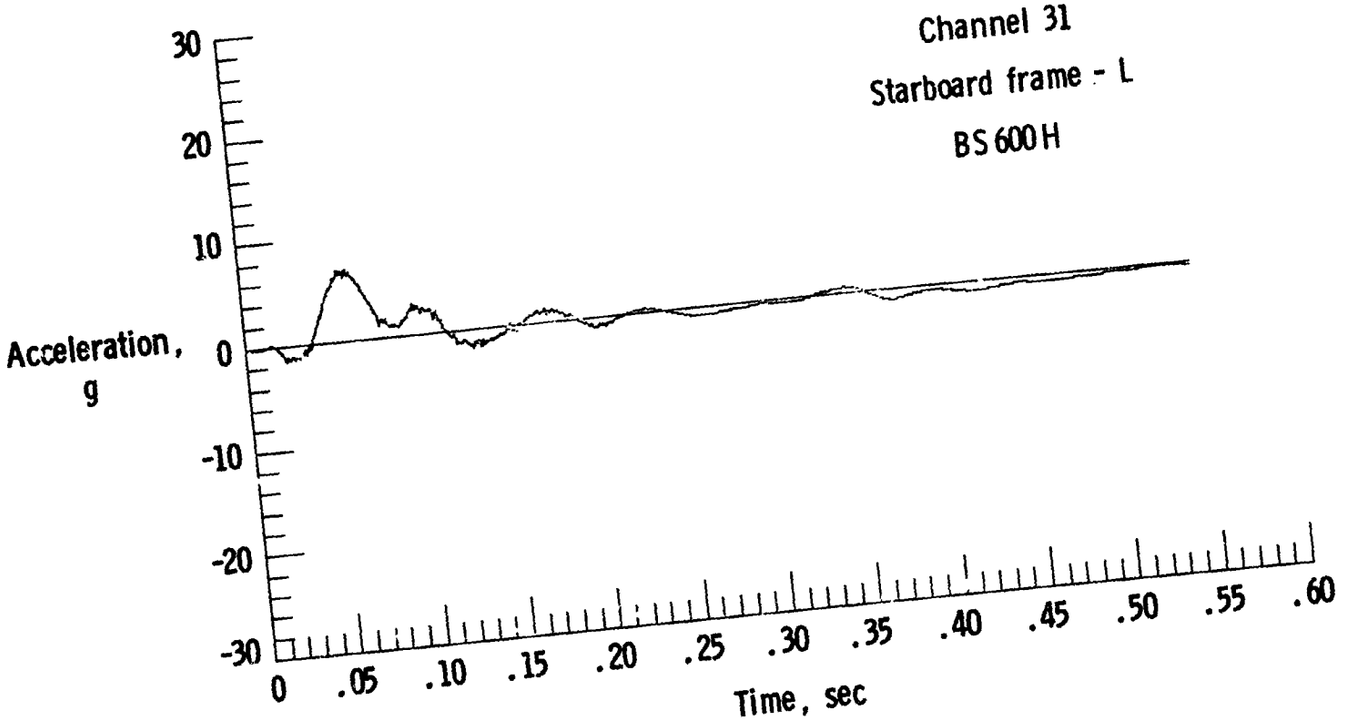

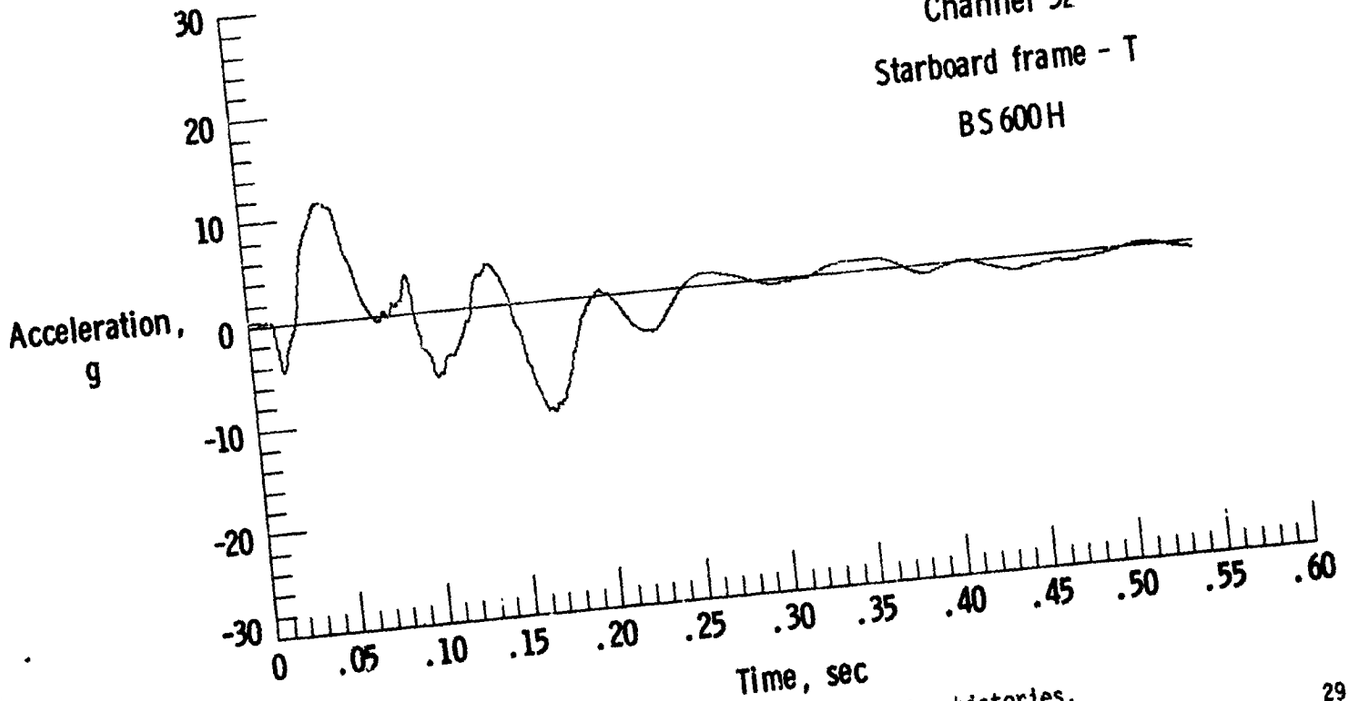

(i) Structural acceleration time histories.
Figure 9.- Continued.

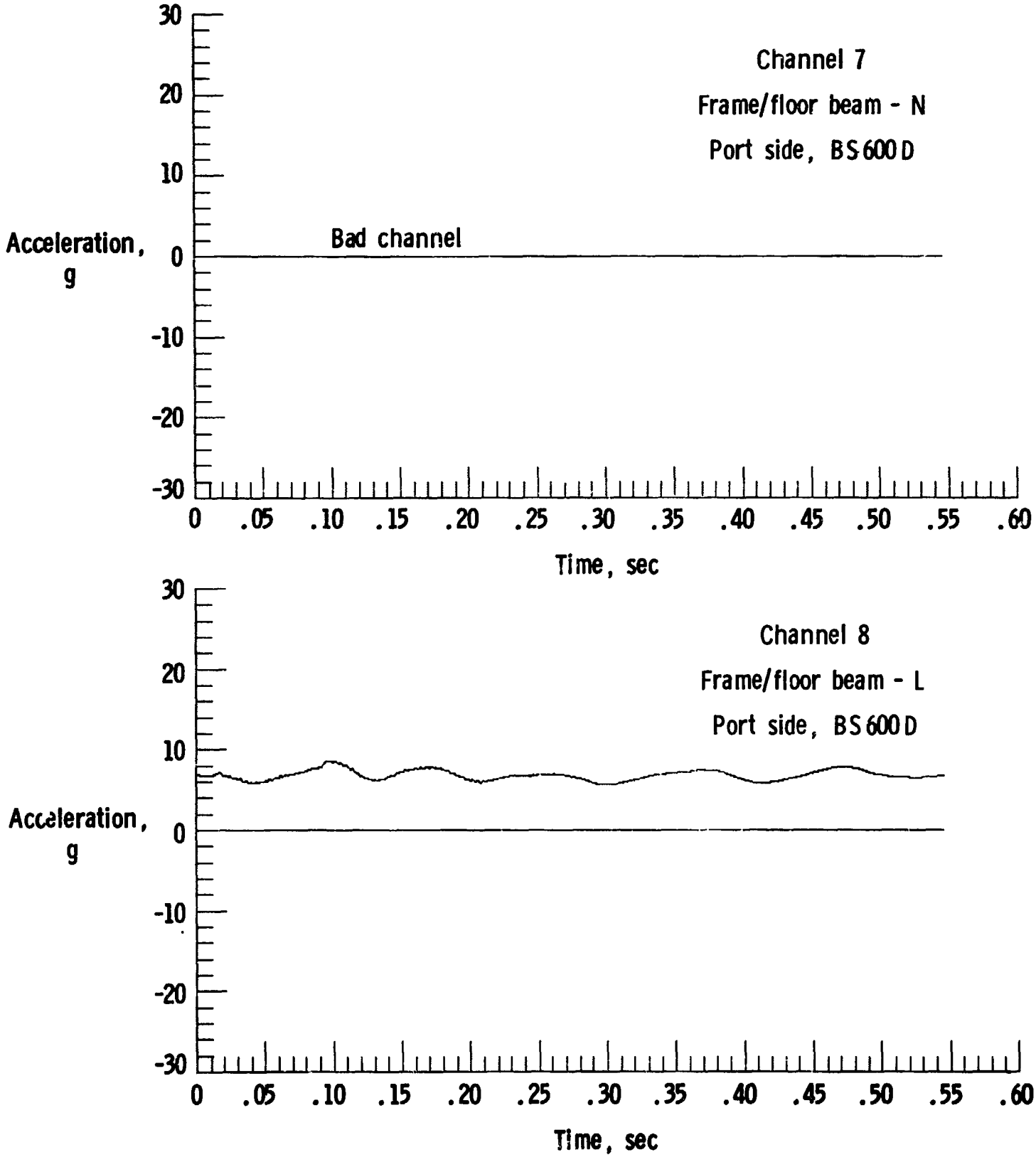

(j) Structural acceleration time histories.
Figure 9.- Continued.

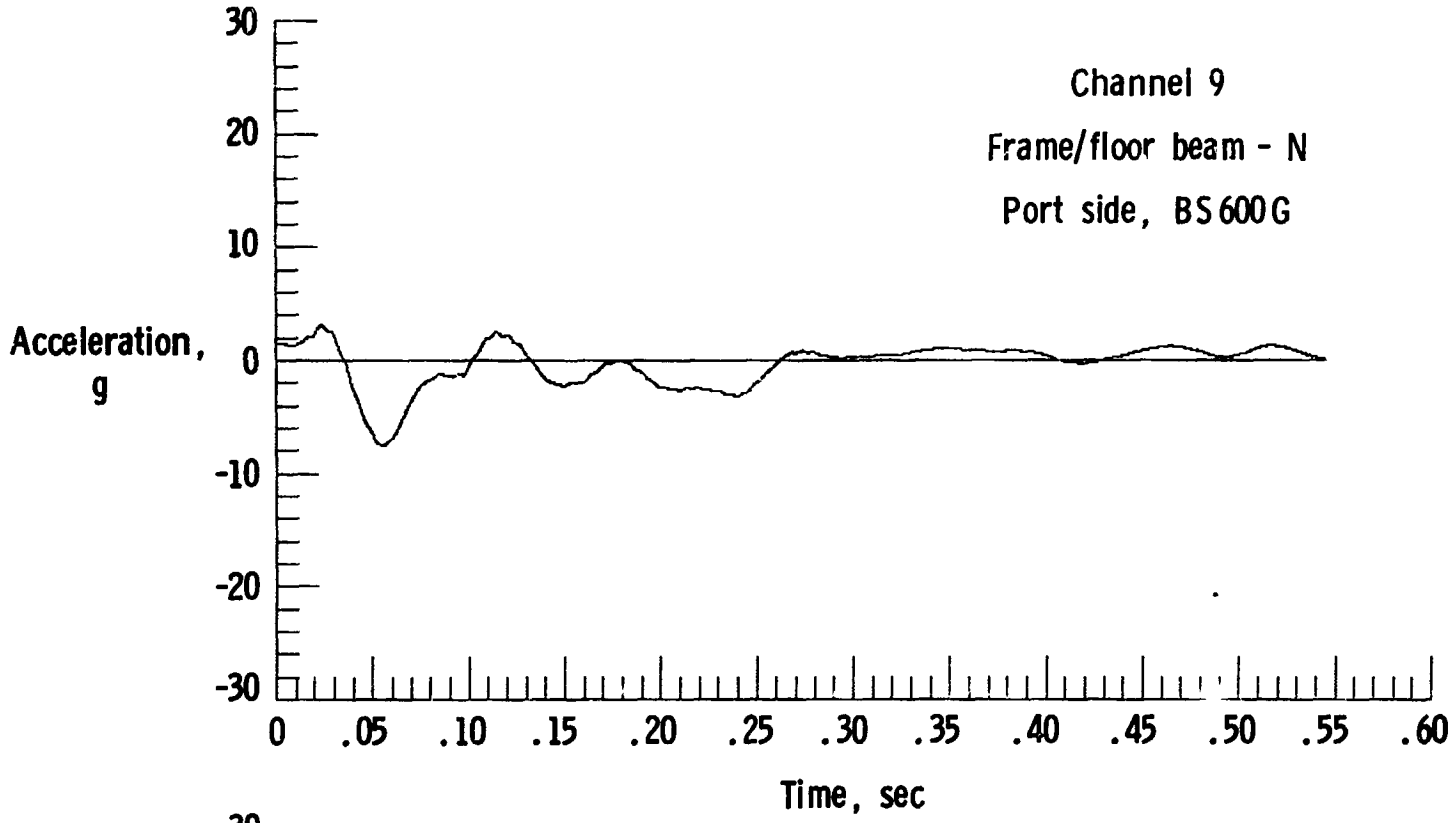

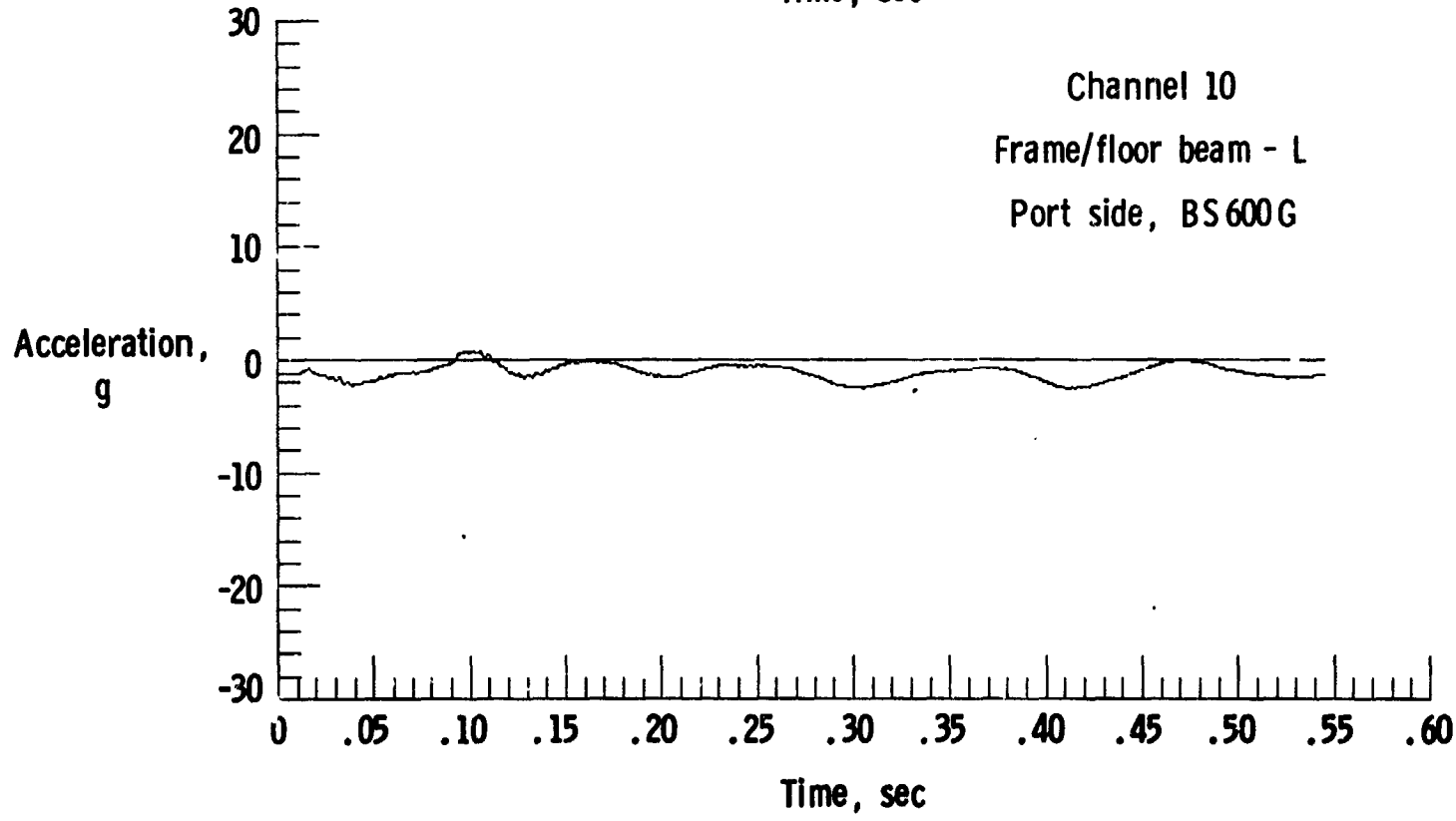

(k) Structural acceleration time histories.

Figure 9.- Continued.

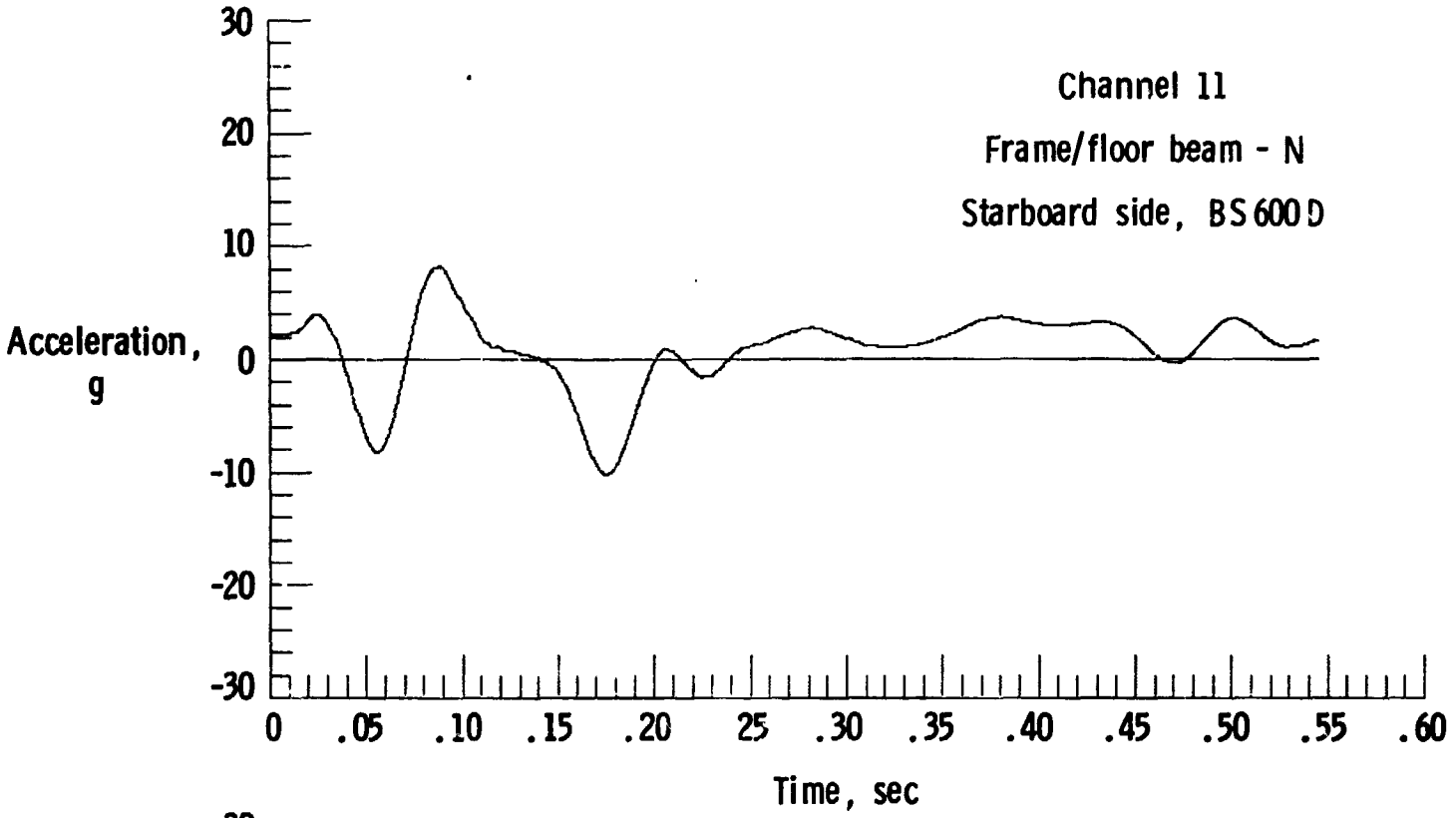

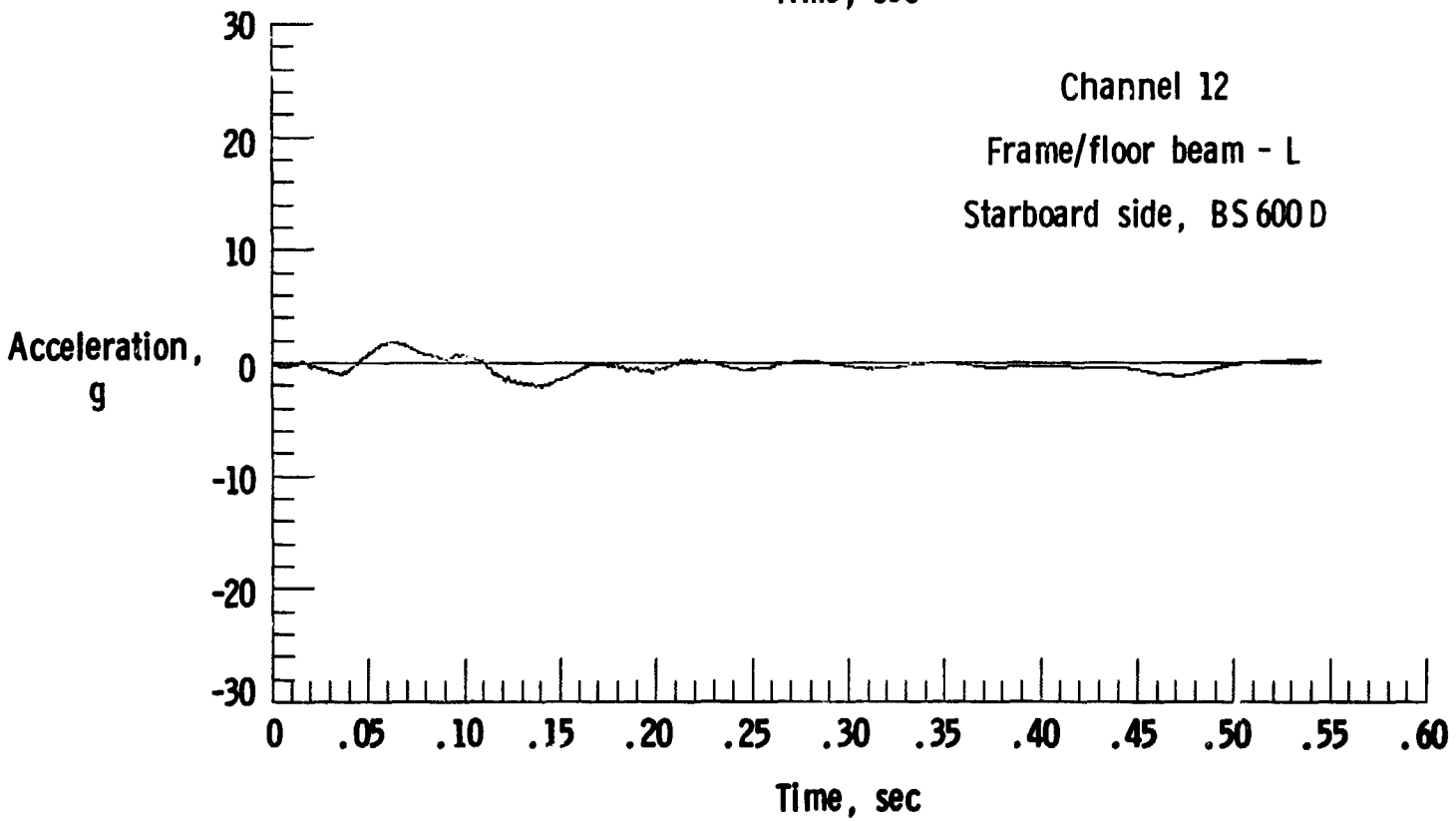

(1) Structural acceleration time histories.
Figure 9.- Continued.

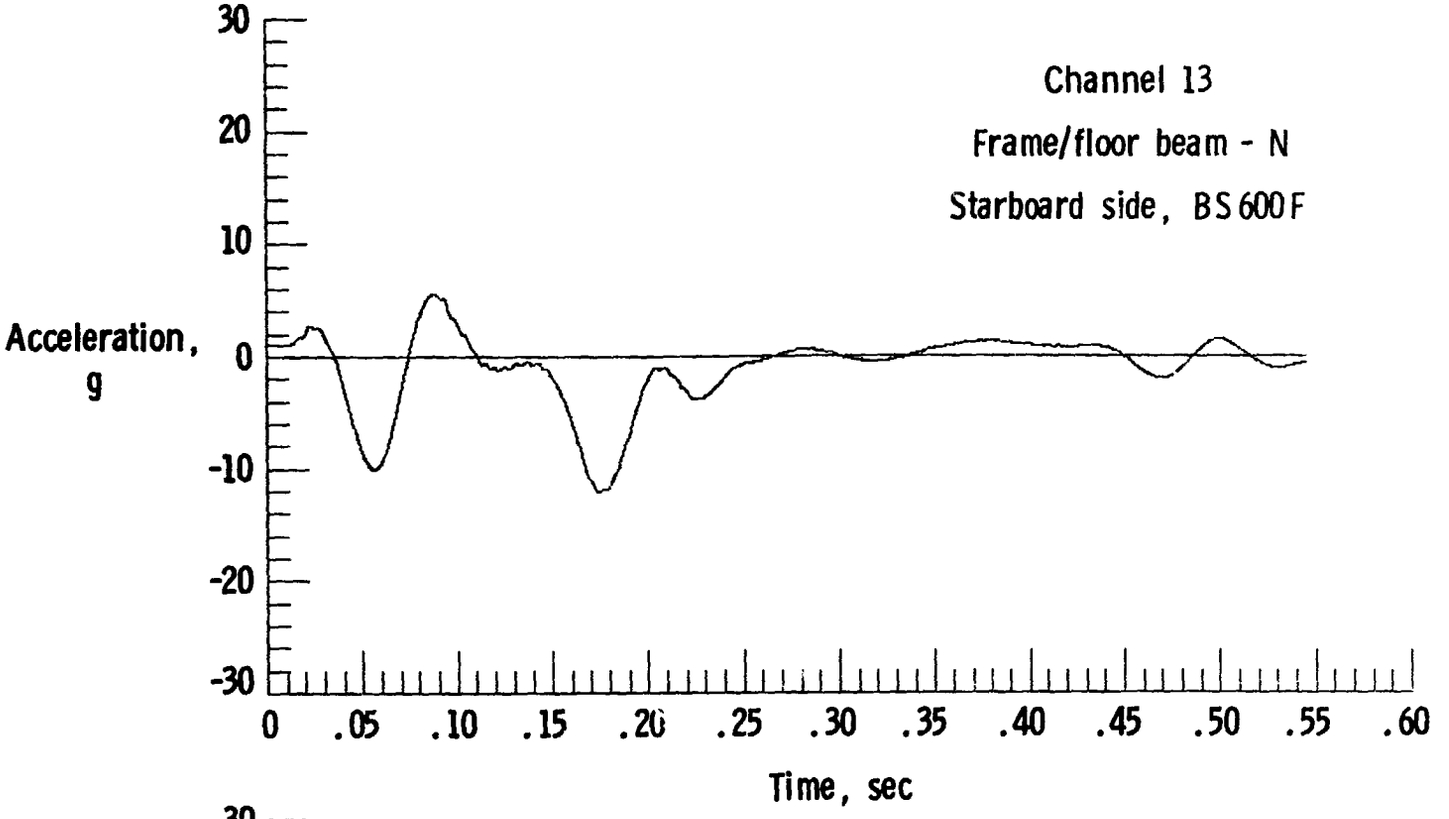

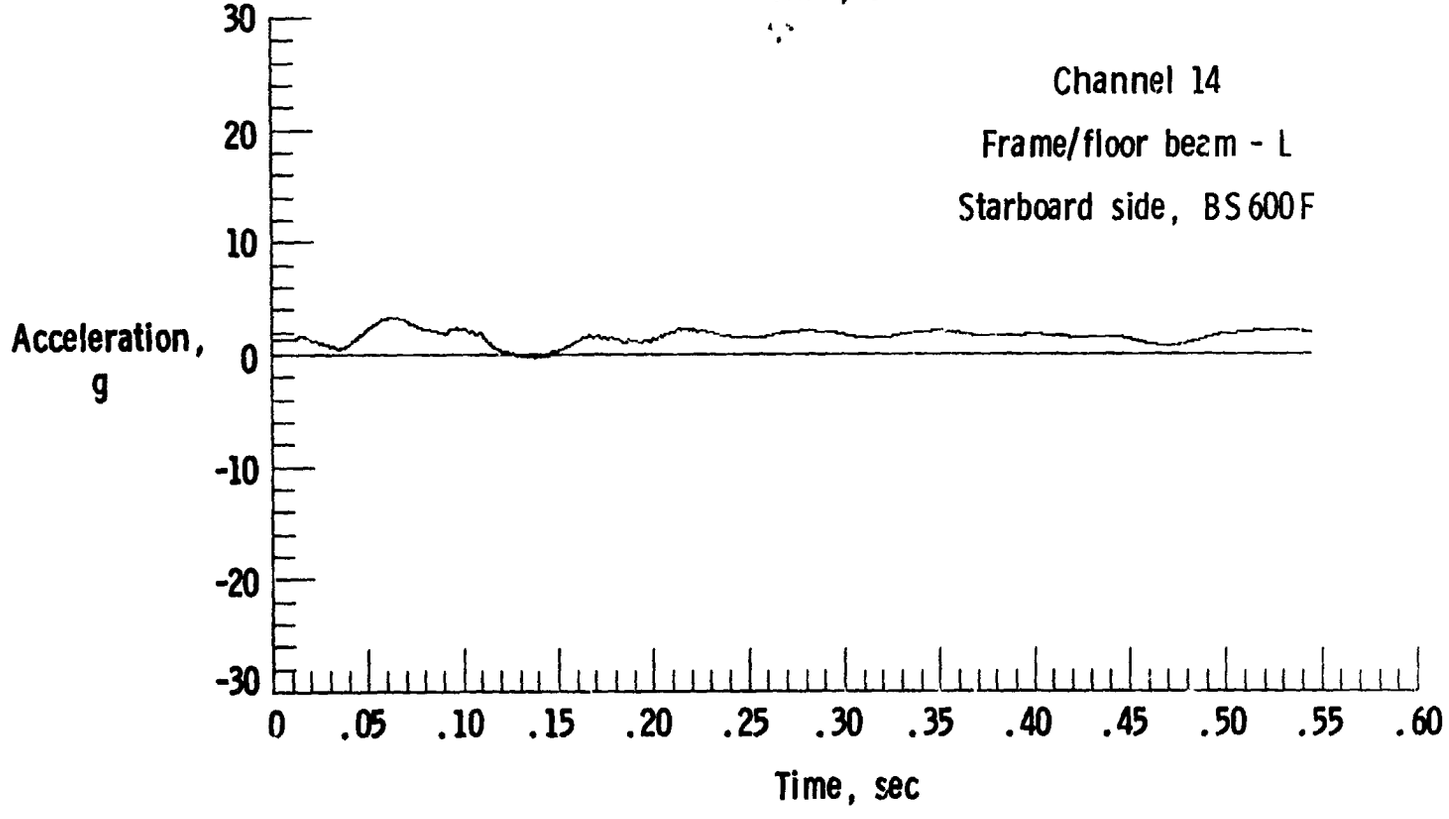

(m) Structural acceleration time histories.
Figure 9.- Continued.

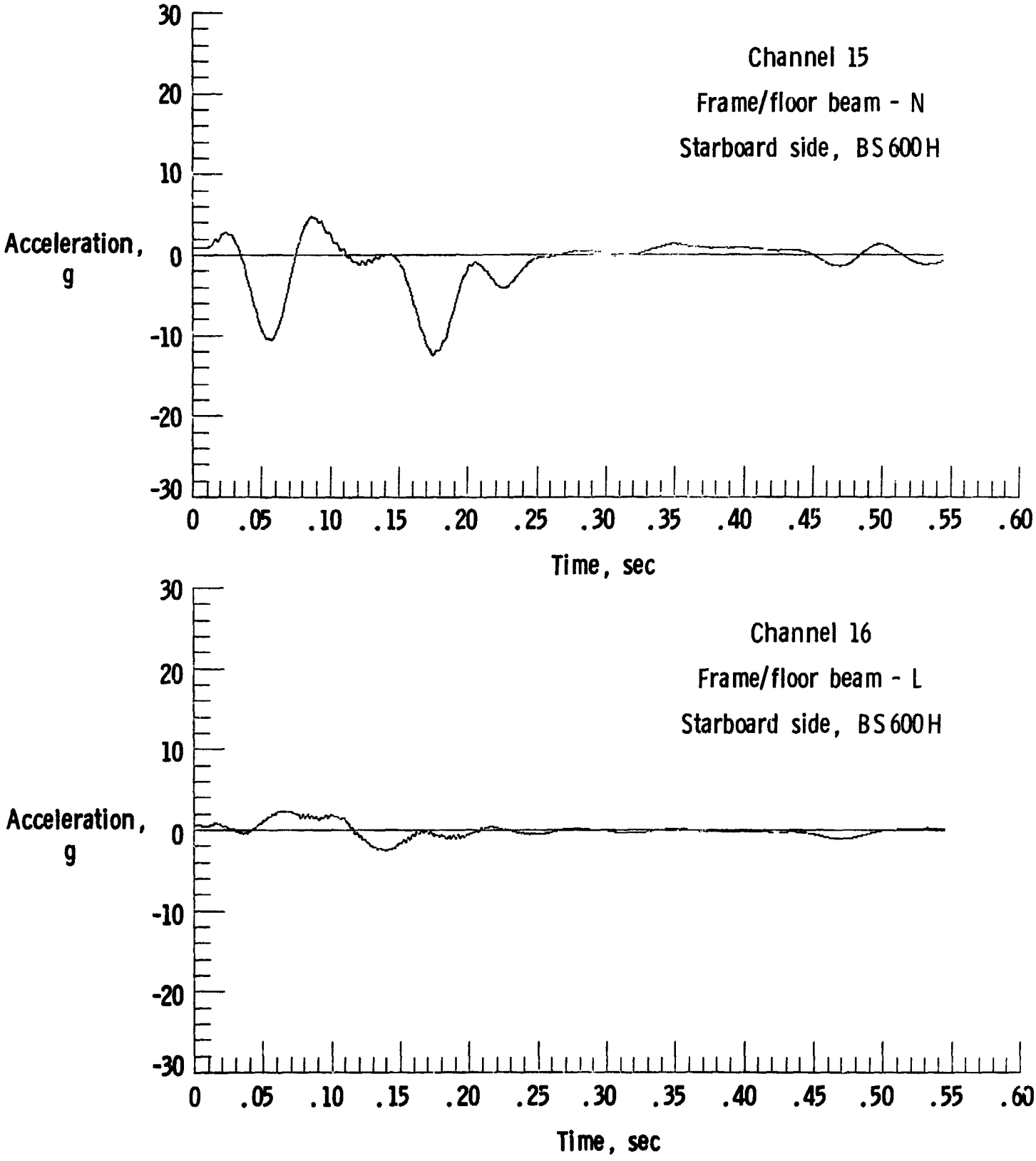

(n) Structural acceleration time histories.
Figure 9.- Continued.

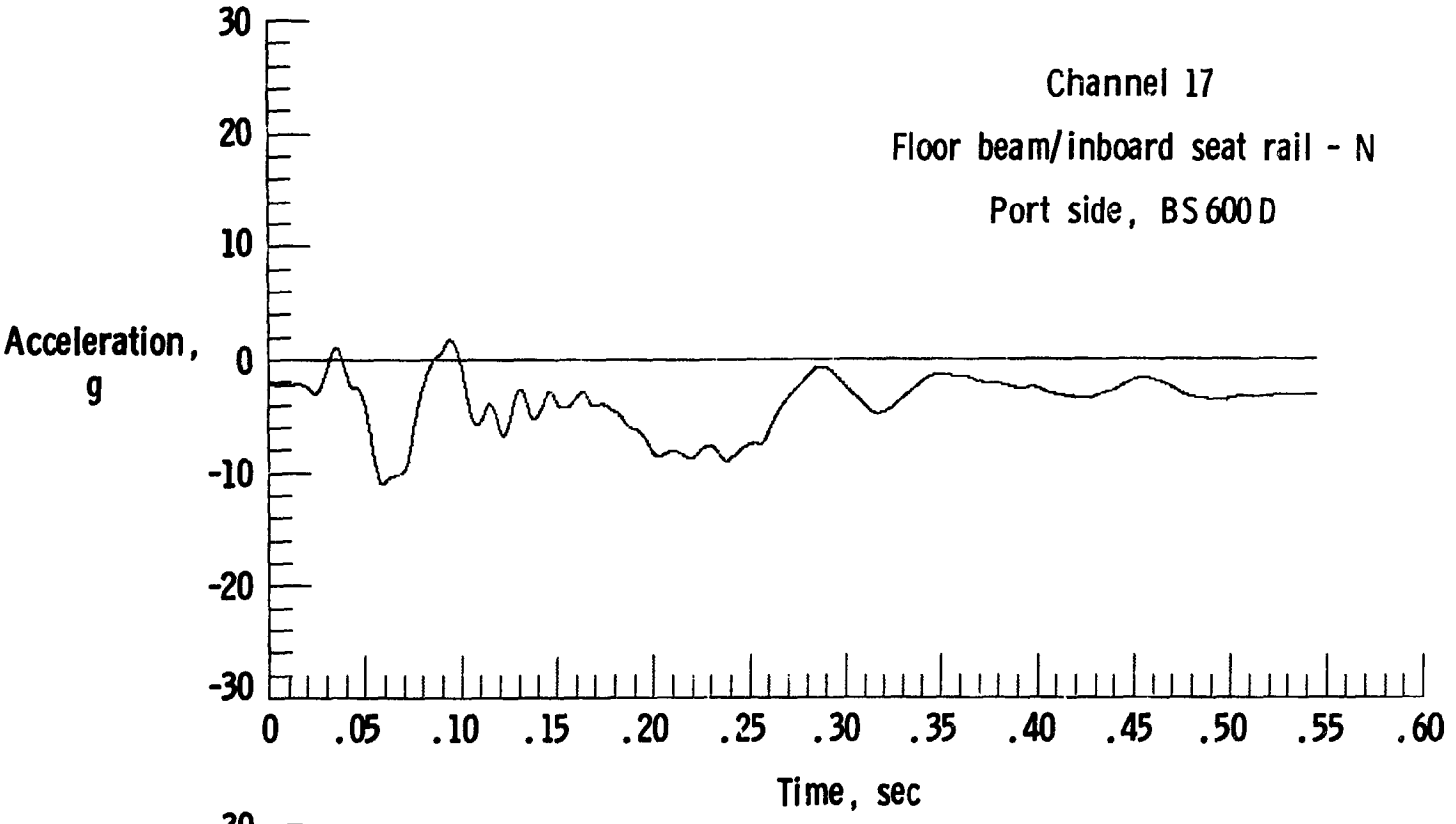

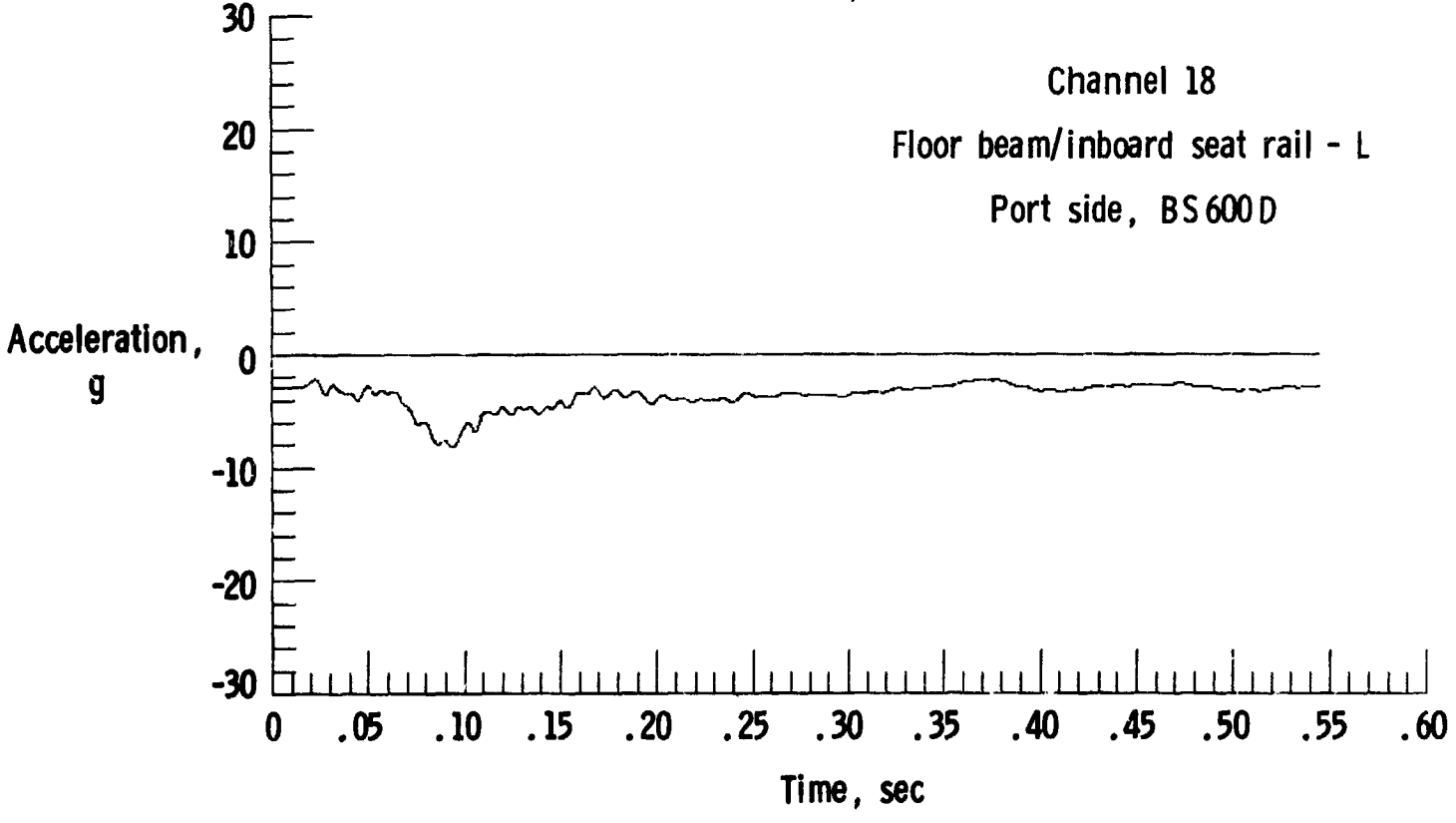

(o) Structural acceleration time histories.

Figure 9.- Continued.

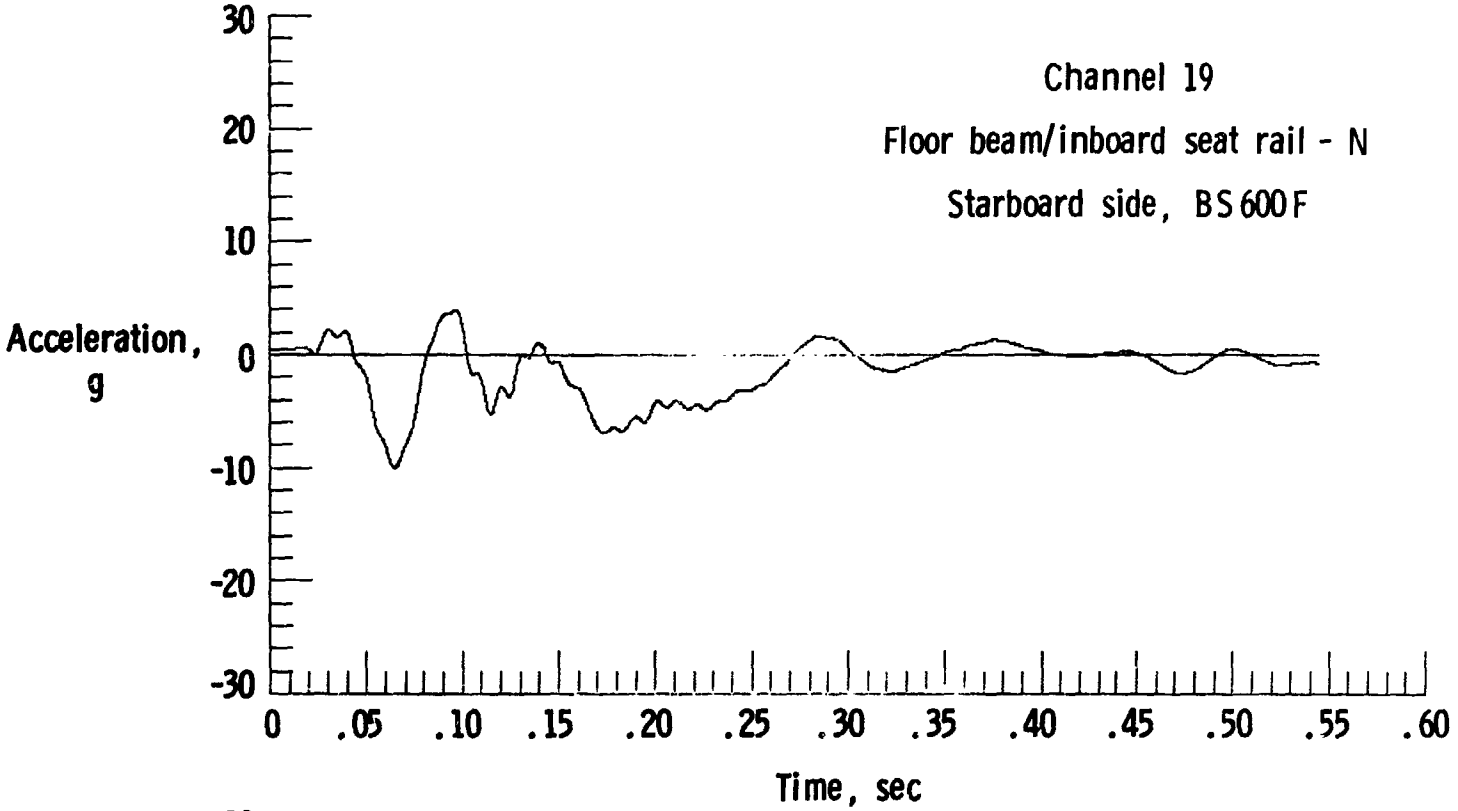

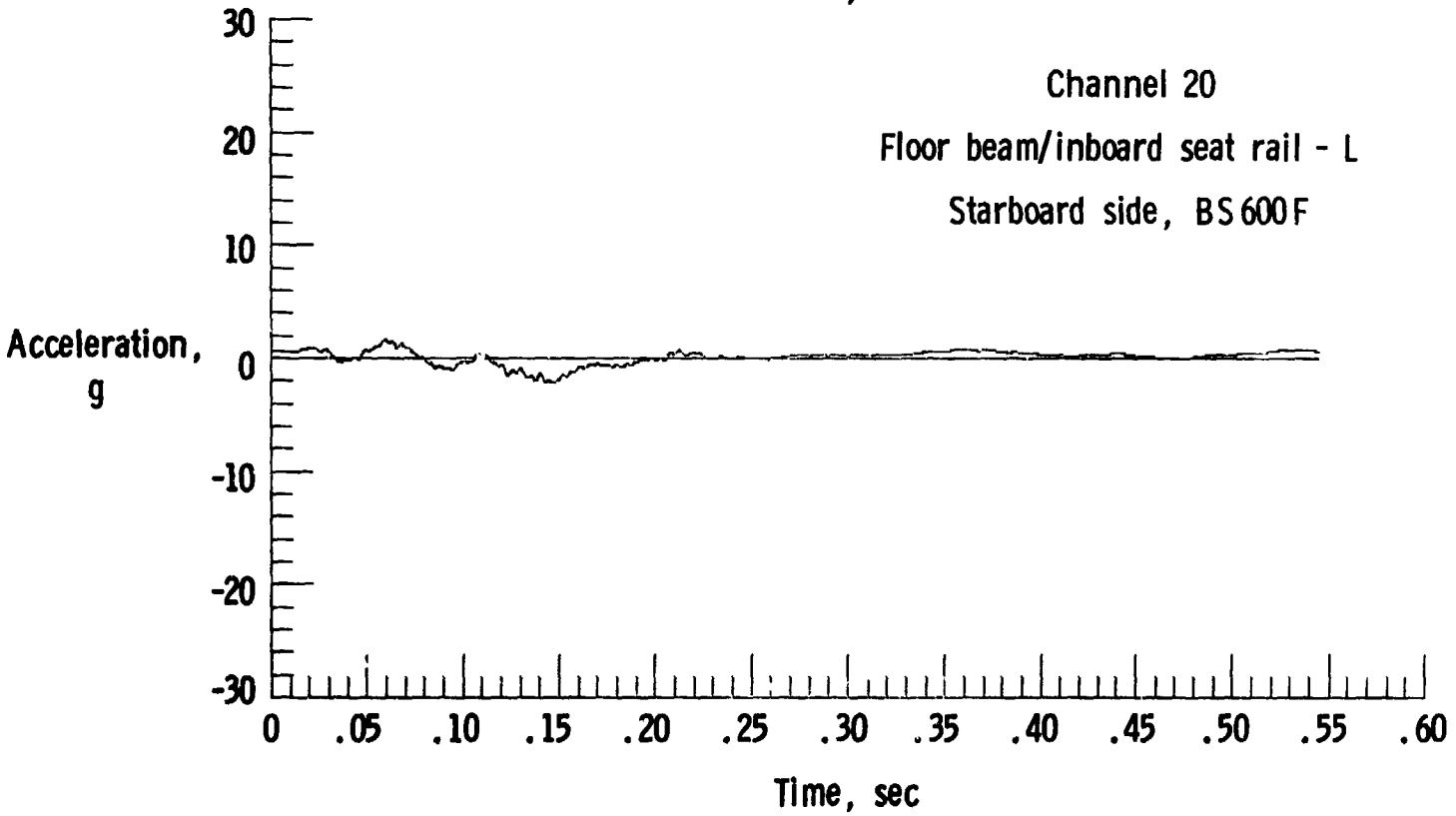

(p) Structural acceleration time histories.
Figure 9.- Continued.

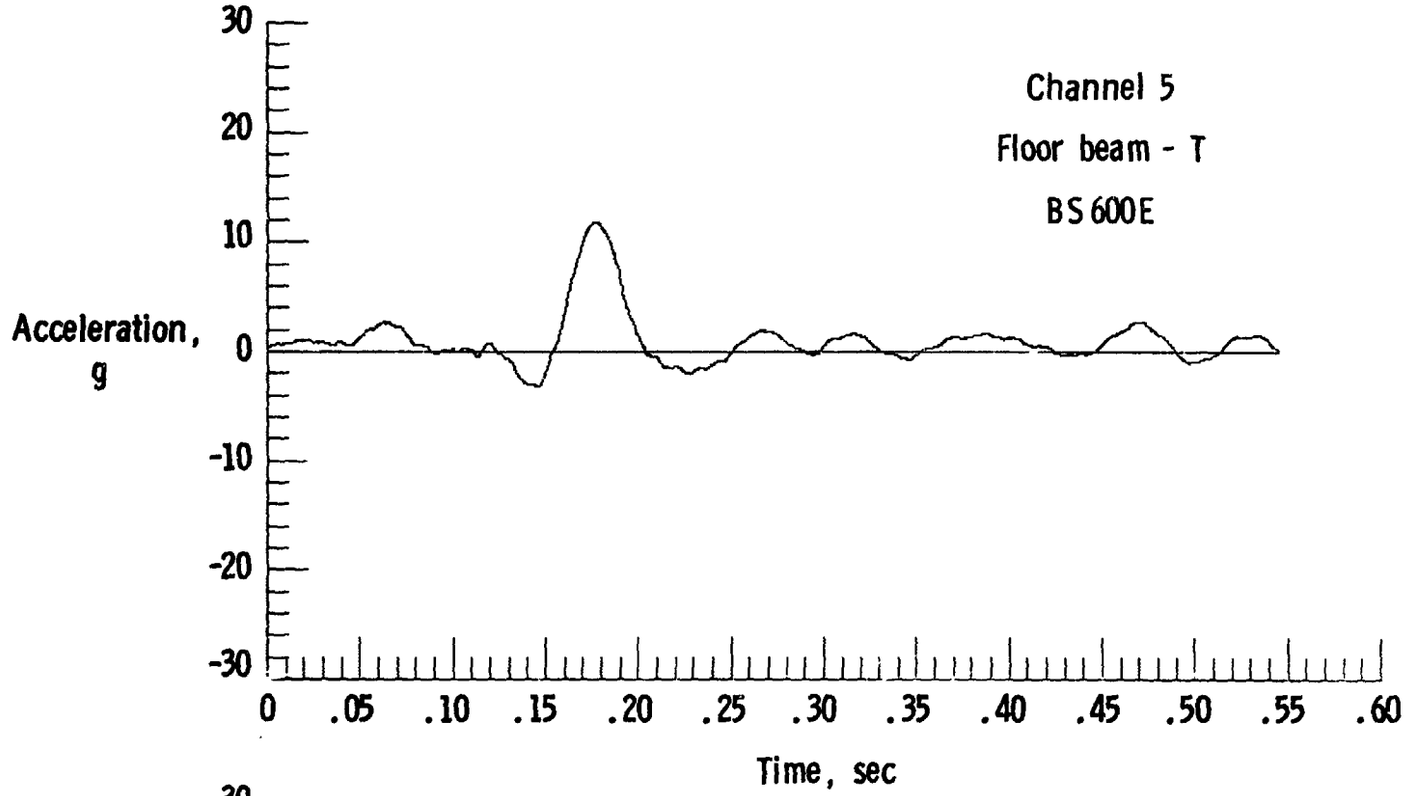

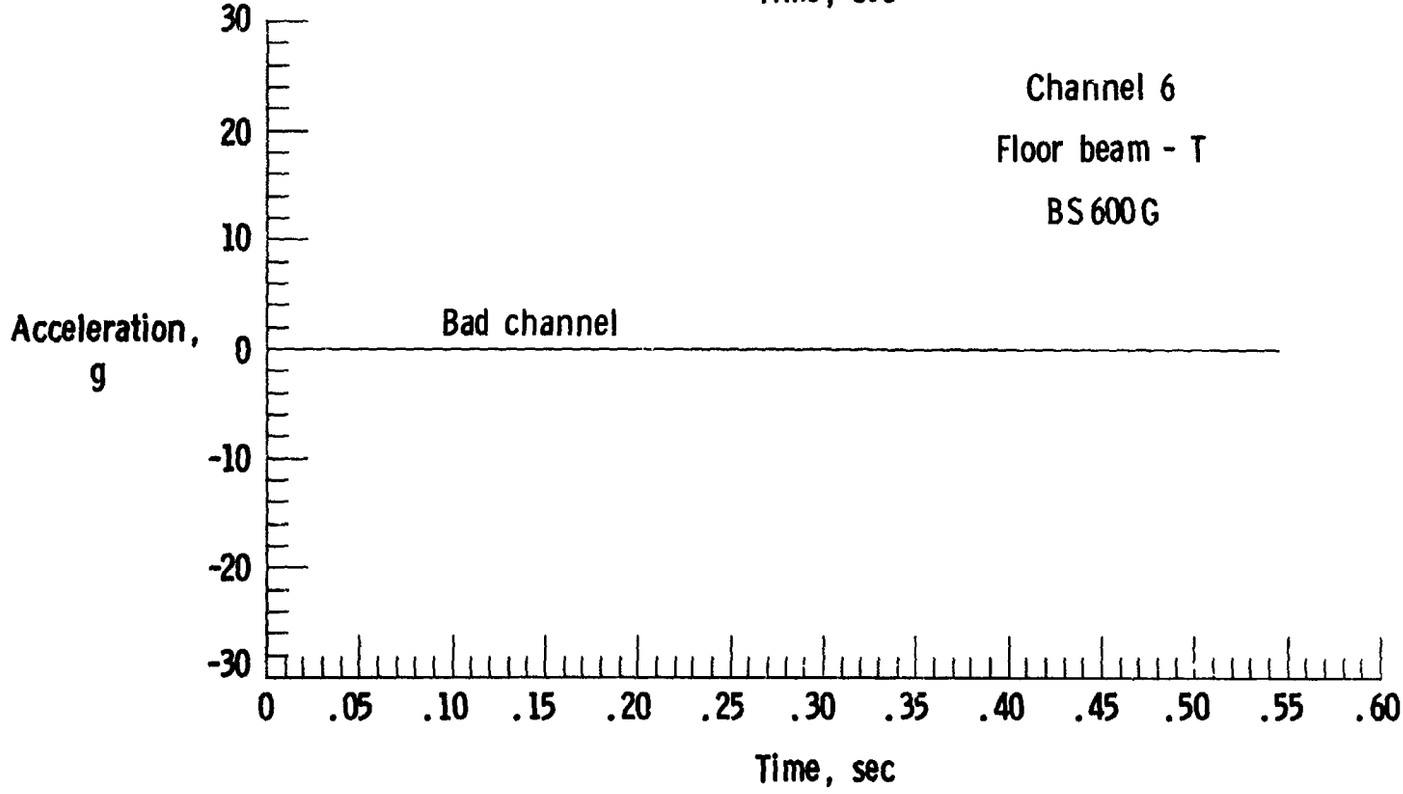

(q) Structural acceleration time histories.

Figure 9.- Continued.

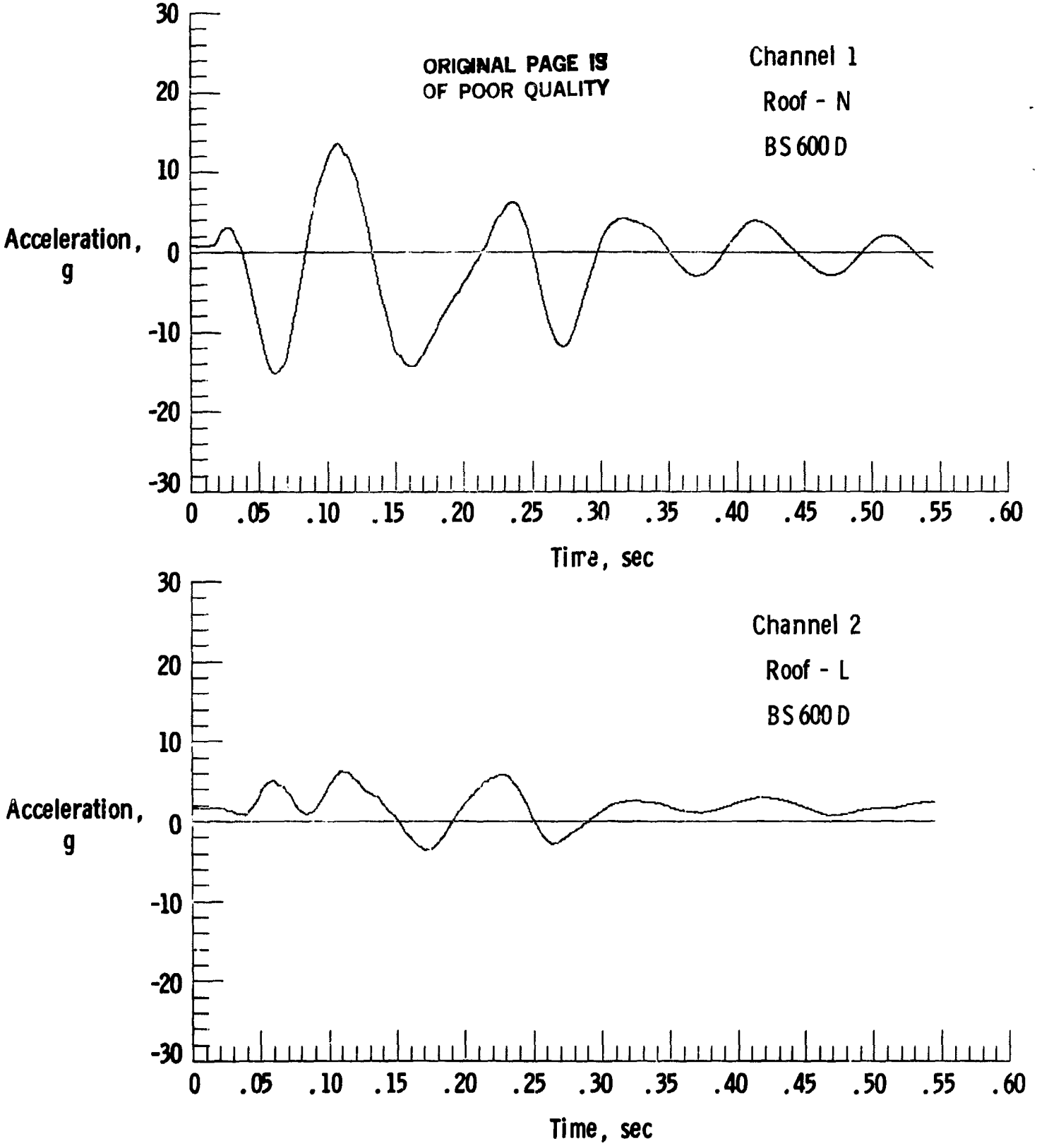

(r) Structural acceleration time histories.
Figure 9.- Continued.

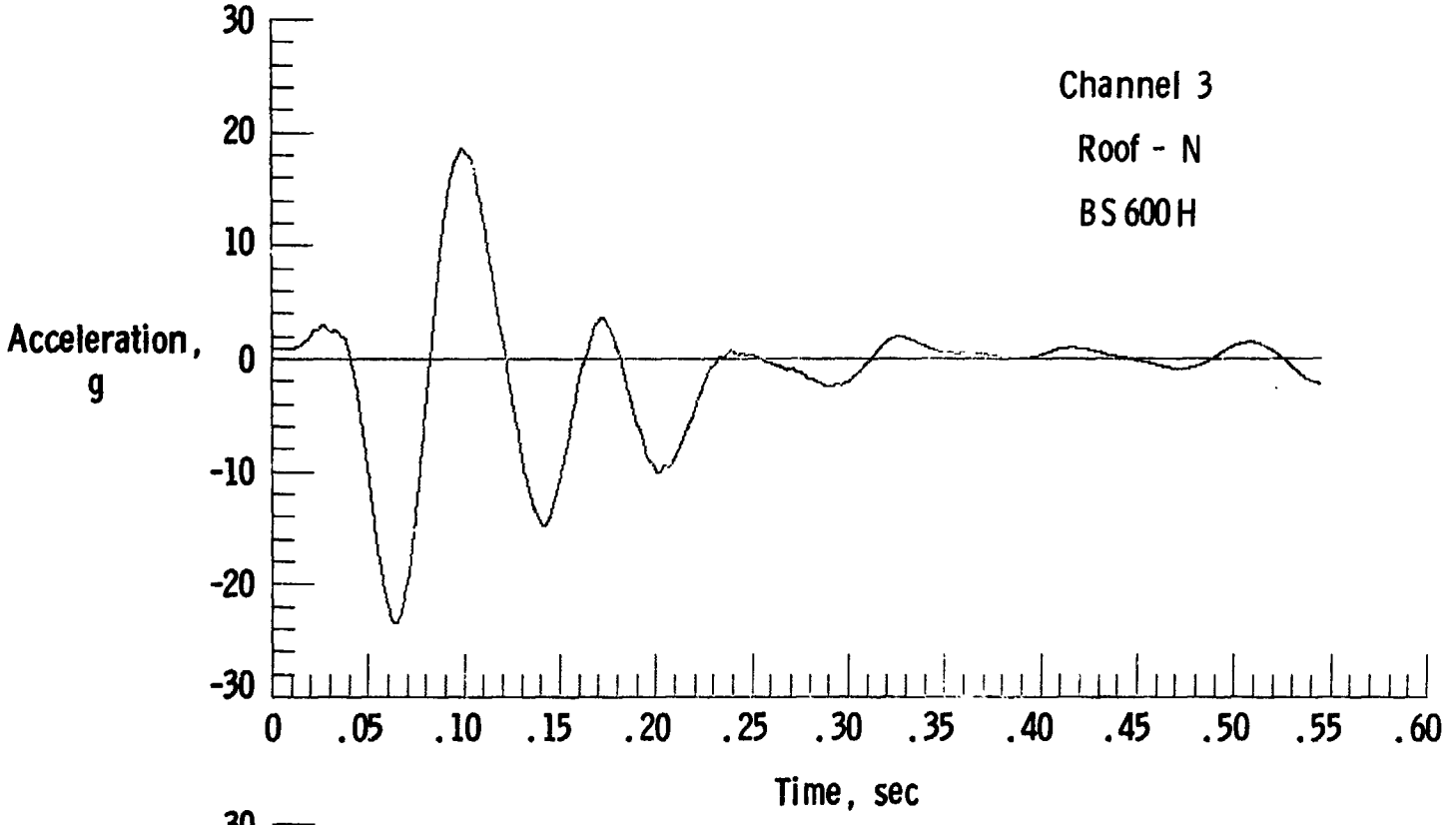

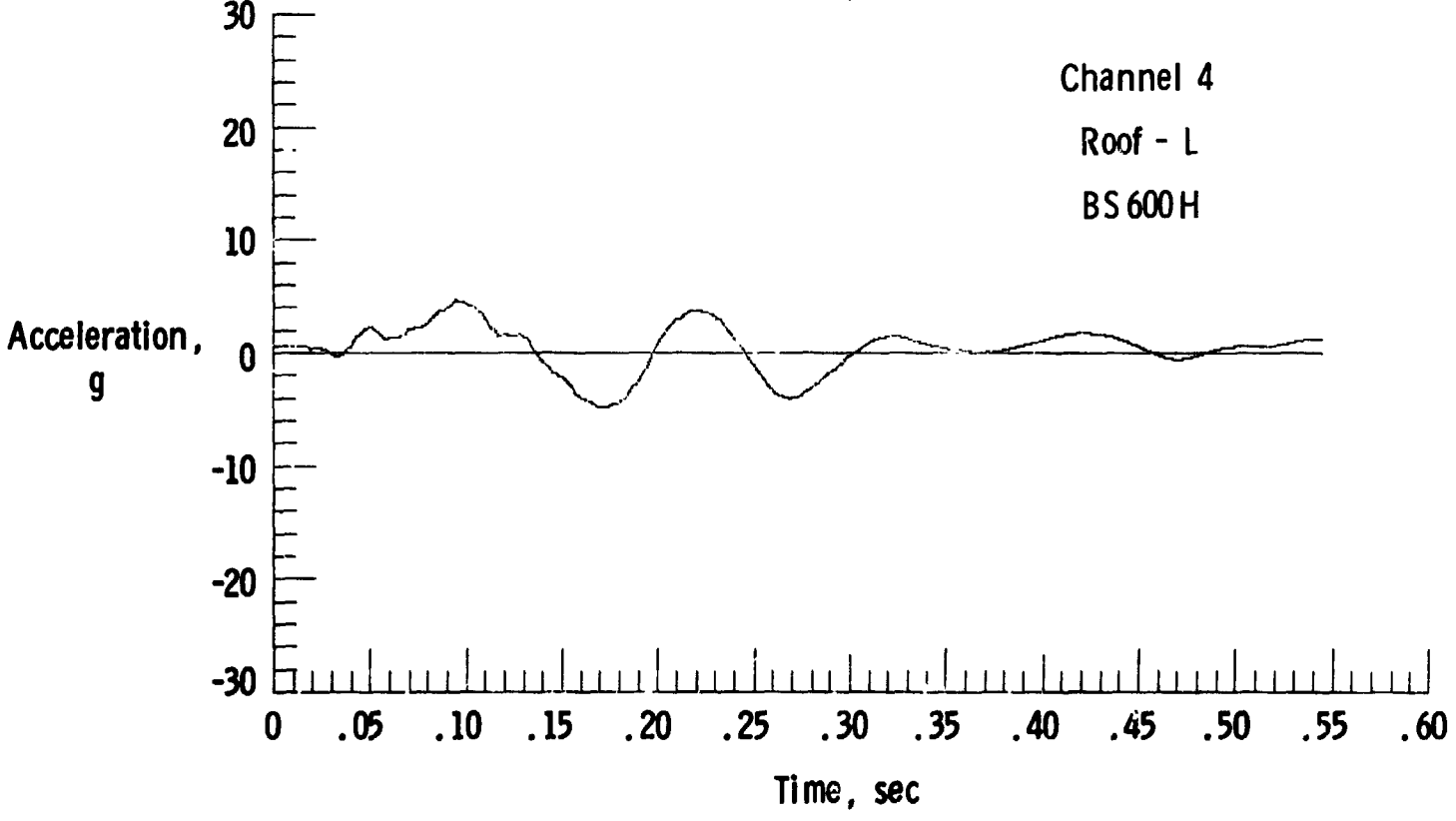

(s) Structural acceleration time histories.
Figure 9.- Concluded.

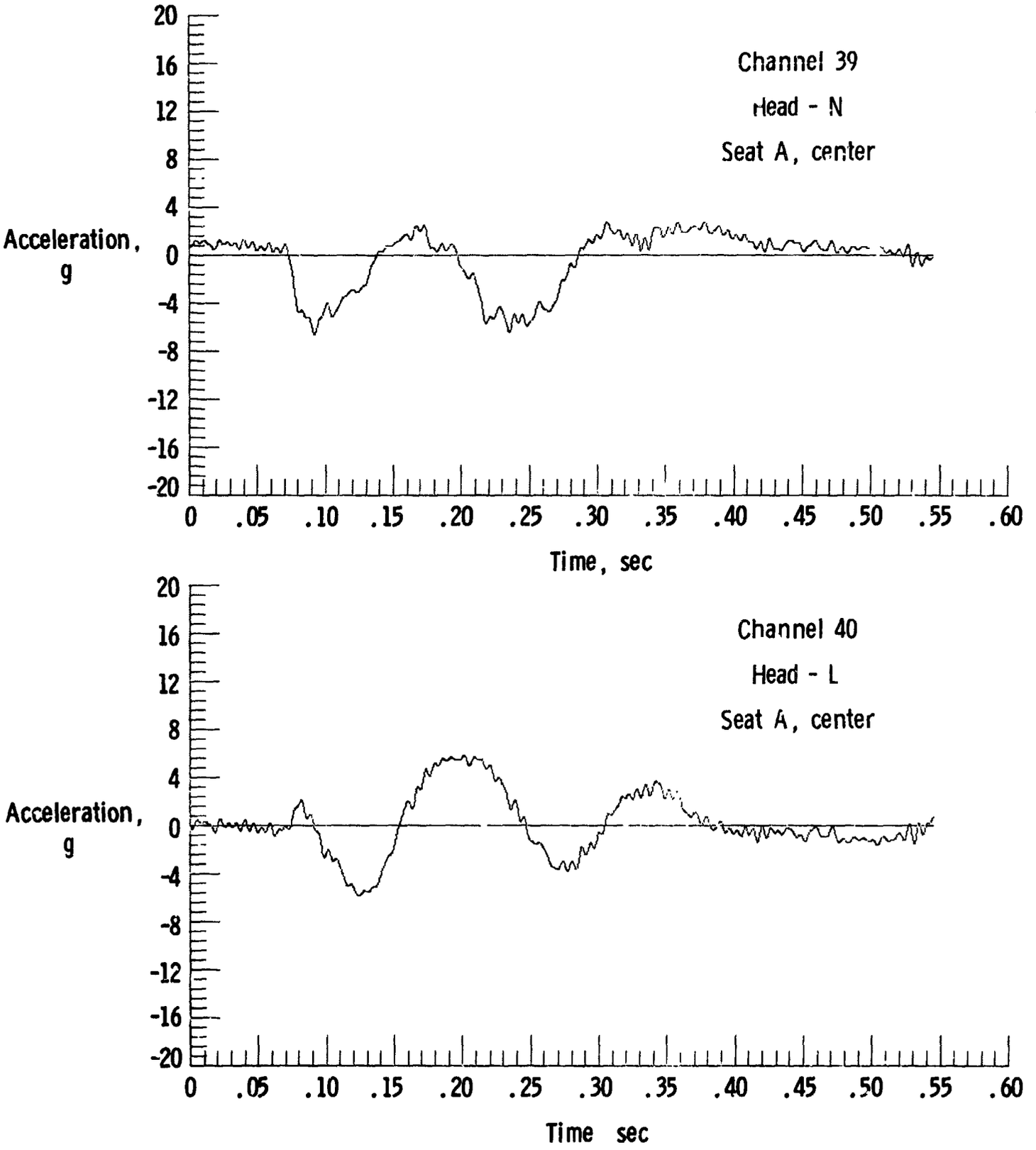

(a) Occupant accelerations.

Figure 10.- Acceleration time histories measured in anthropomorphic dummies.

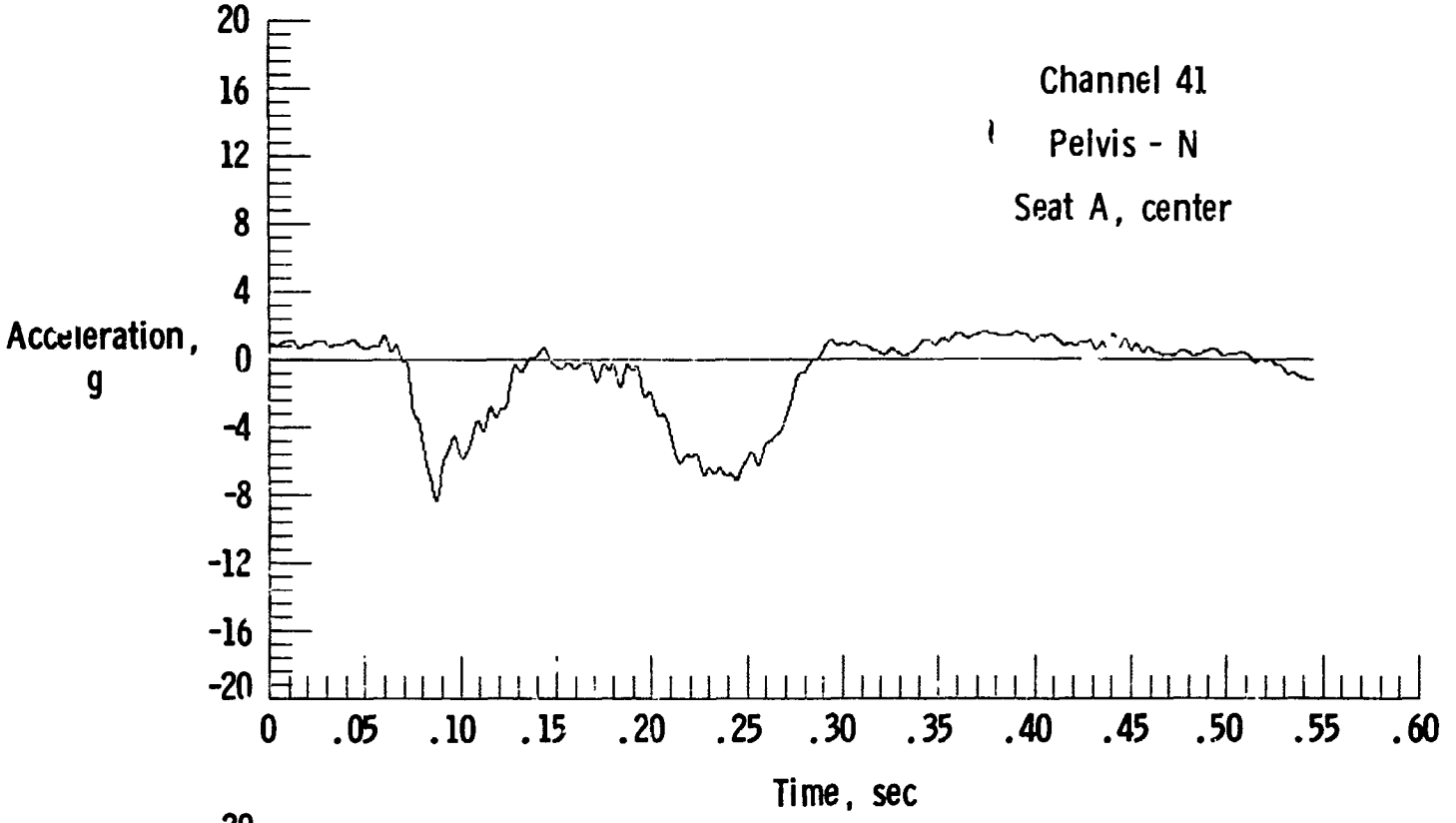

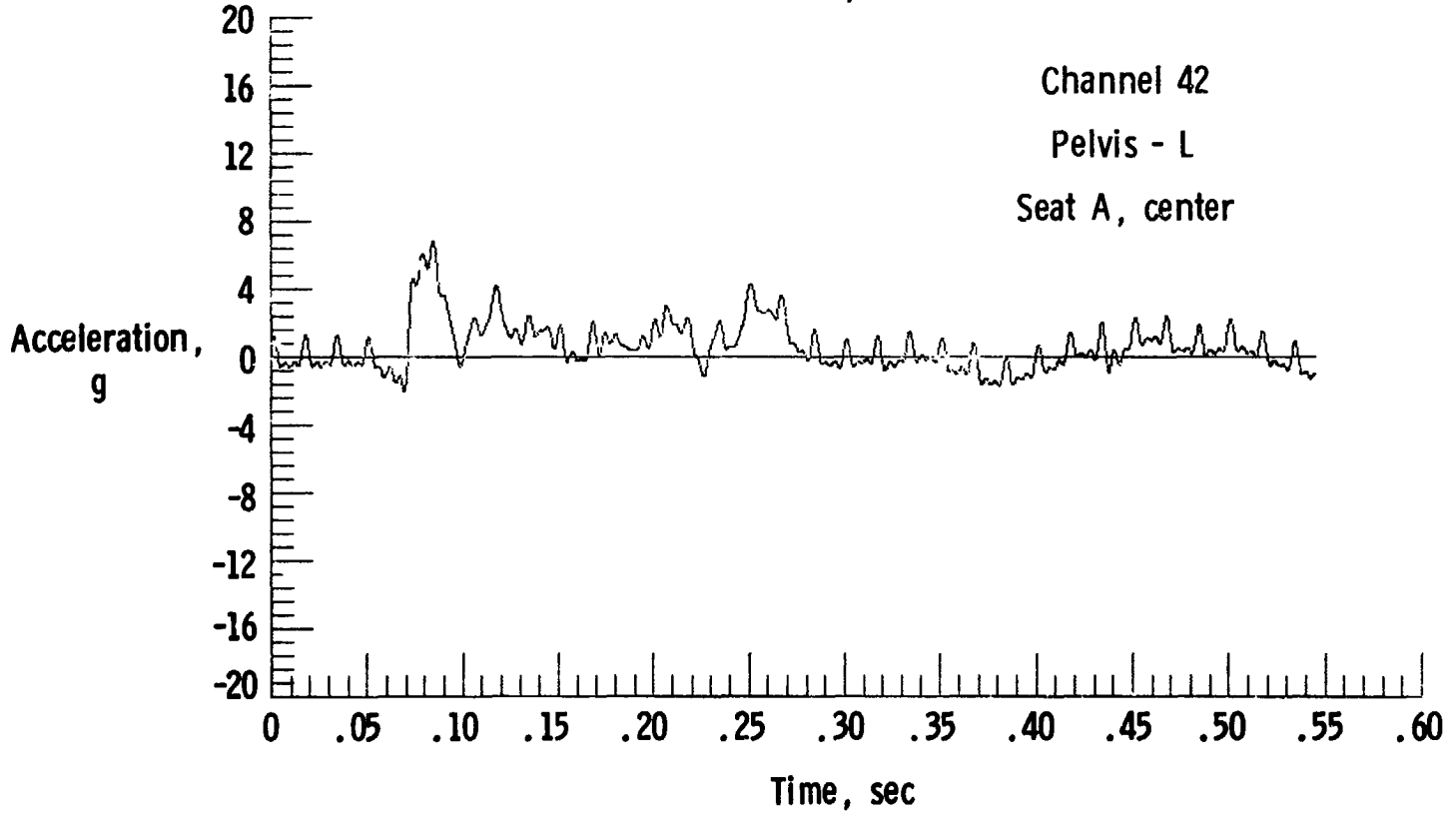

(b) Occupant accelerations.
Figure 10.- Continued.

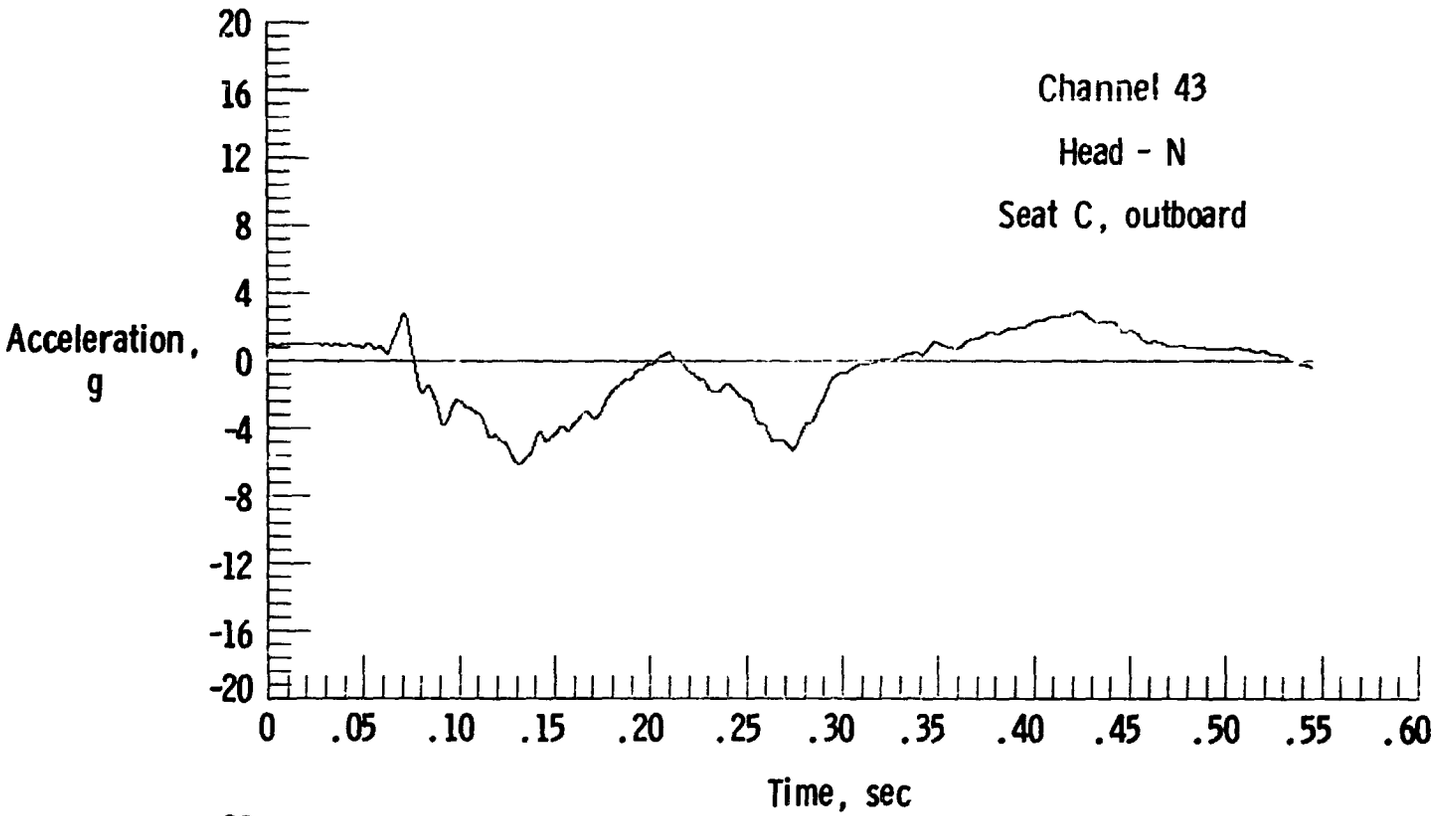

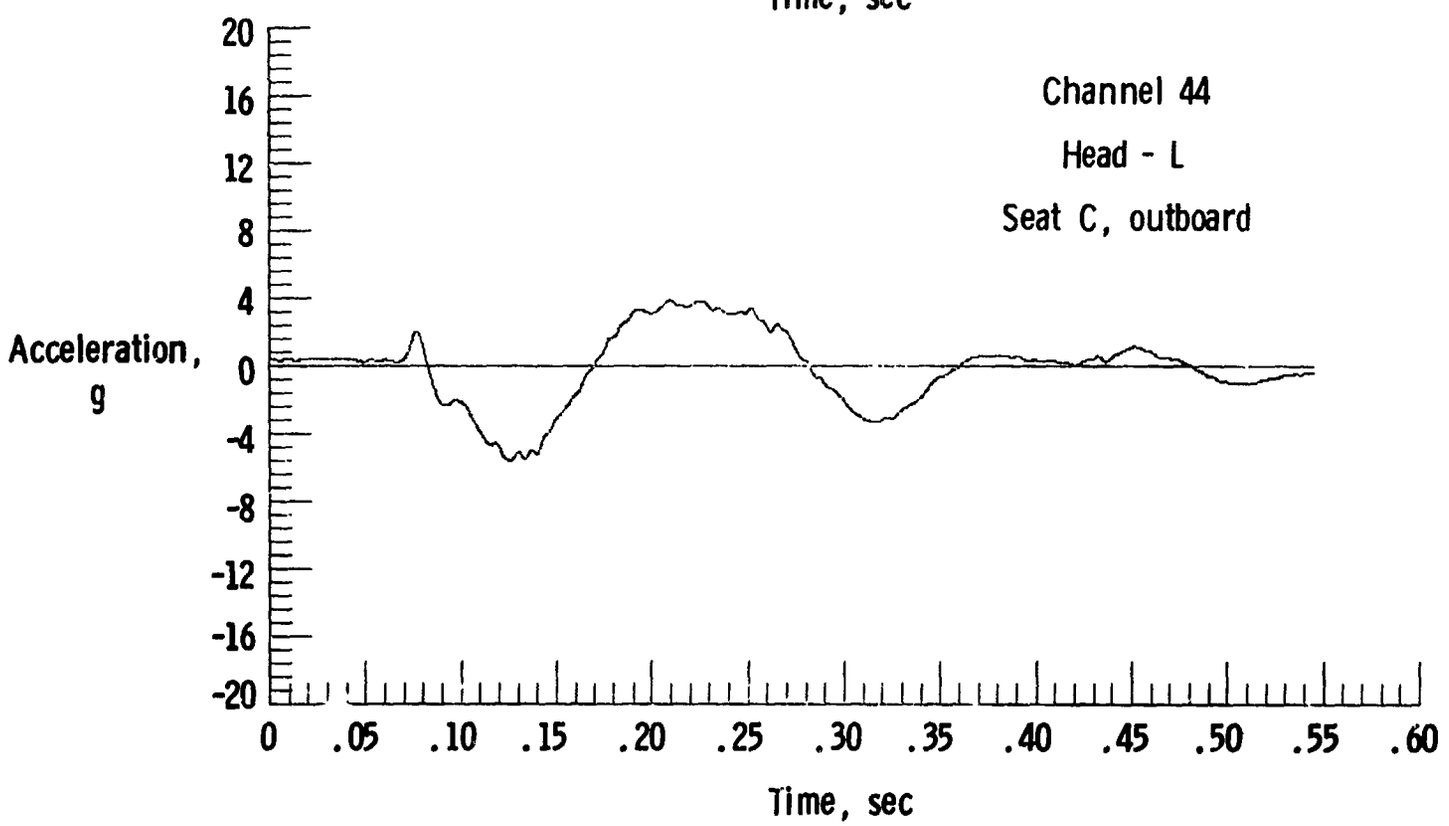

(c) Occupant accelerations.
Figure 10.- Continued.

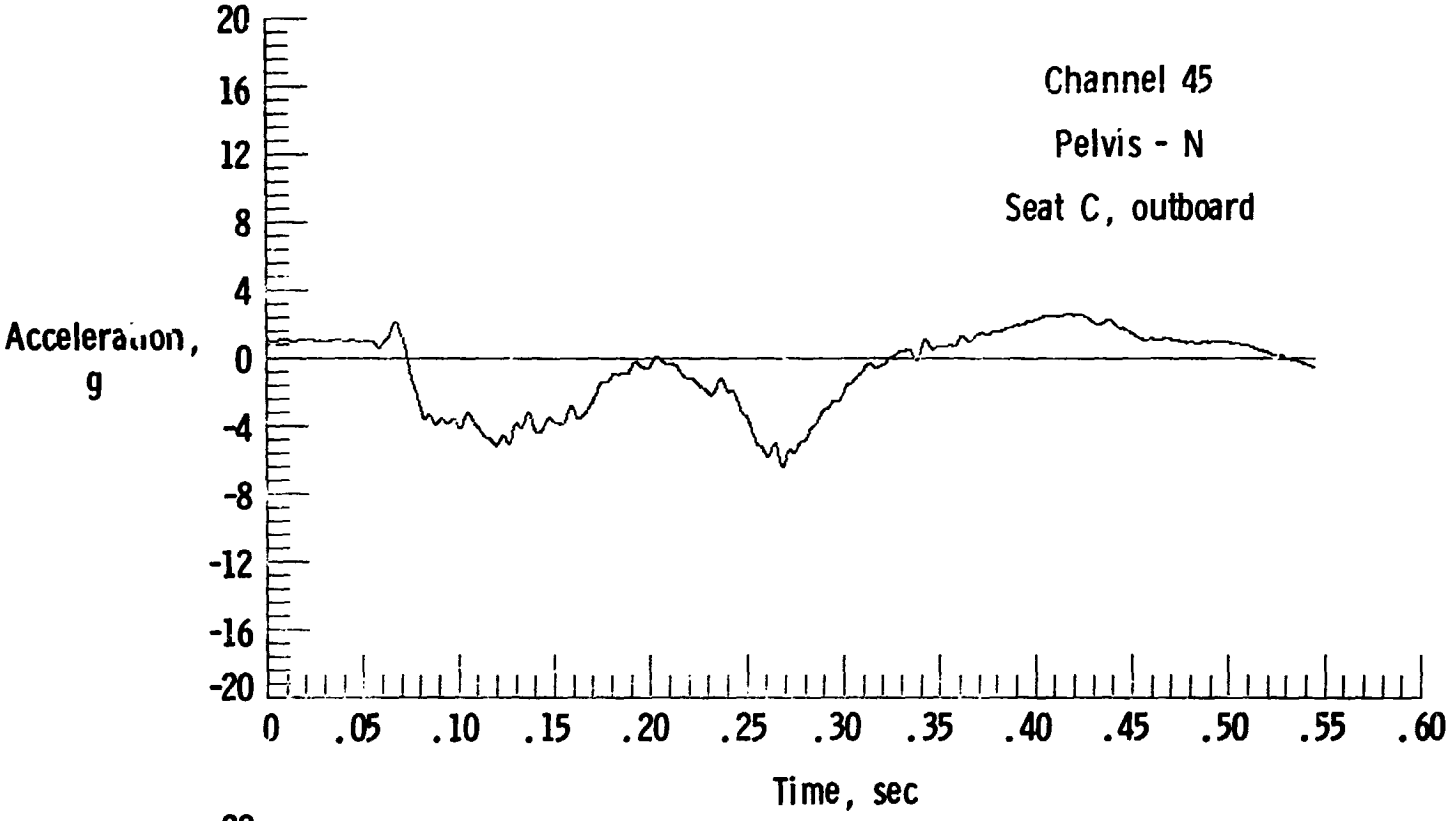

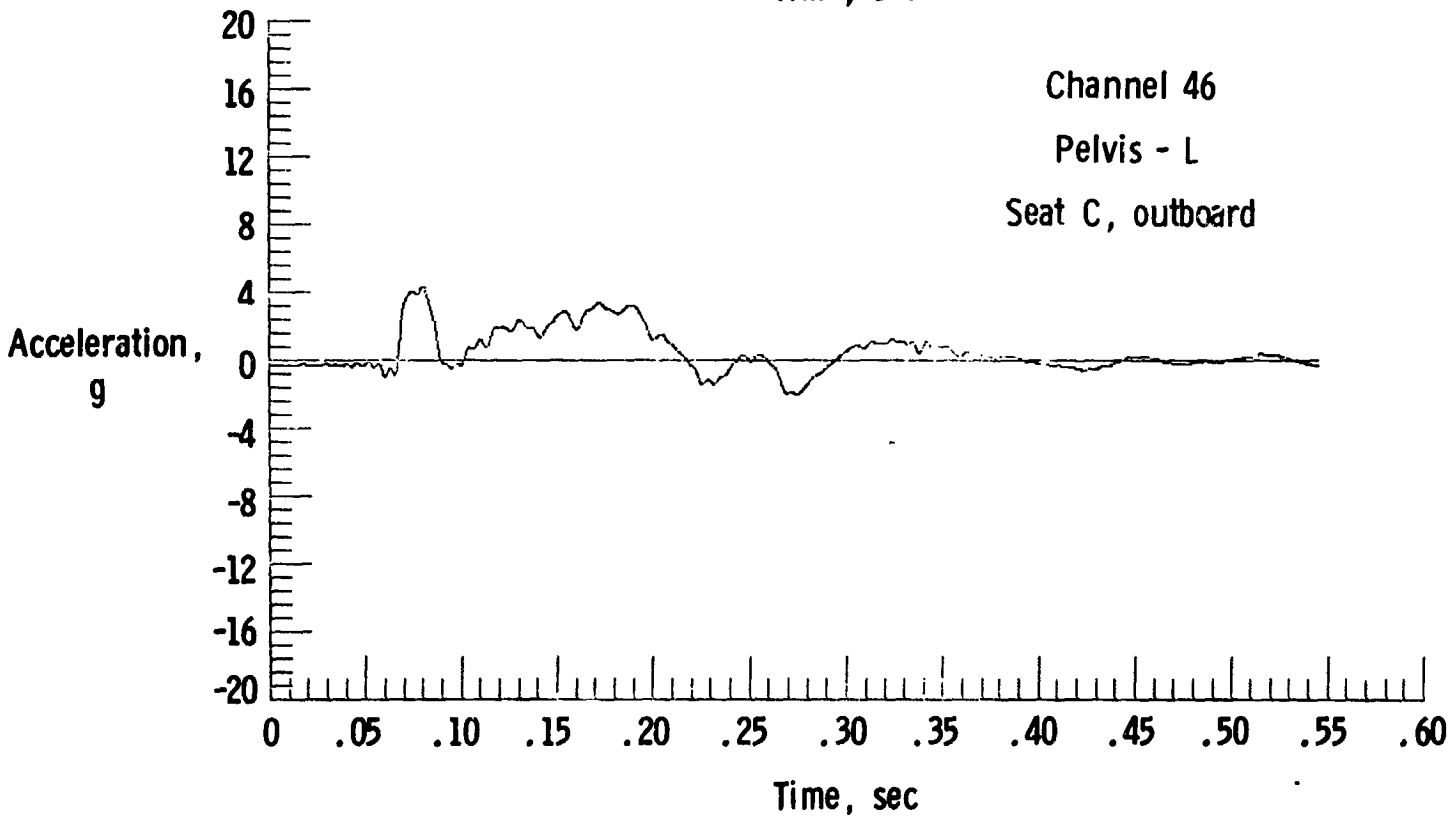

(d) Occupant accelerations.

Figure 10.- Continued.

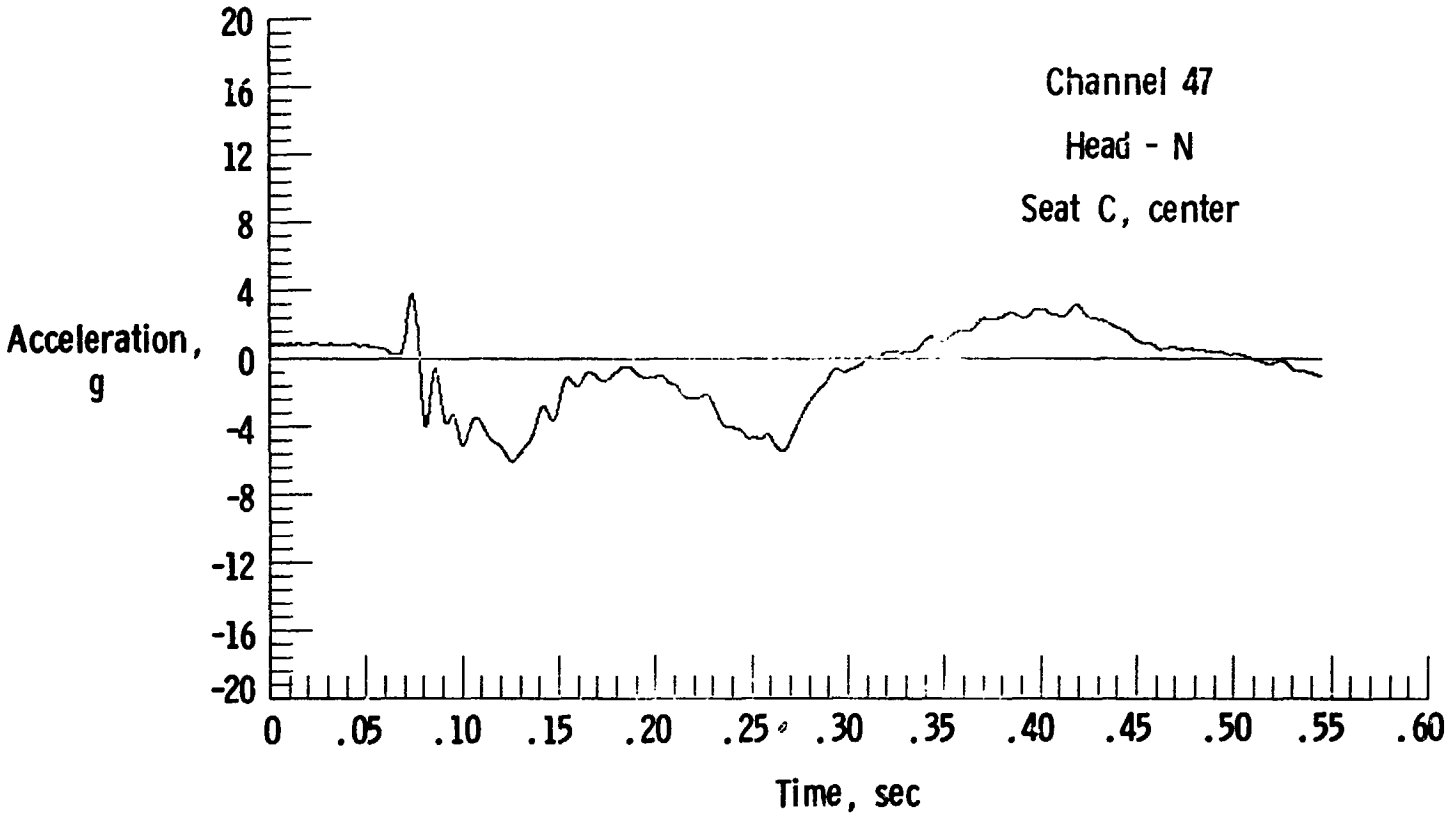

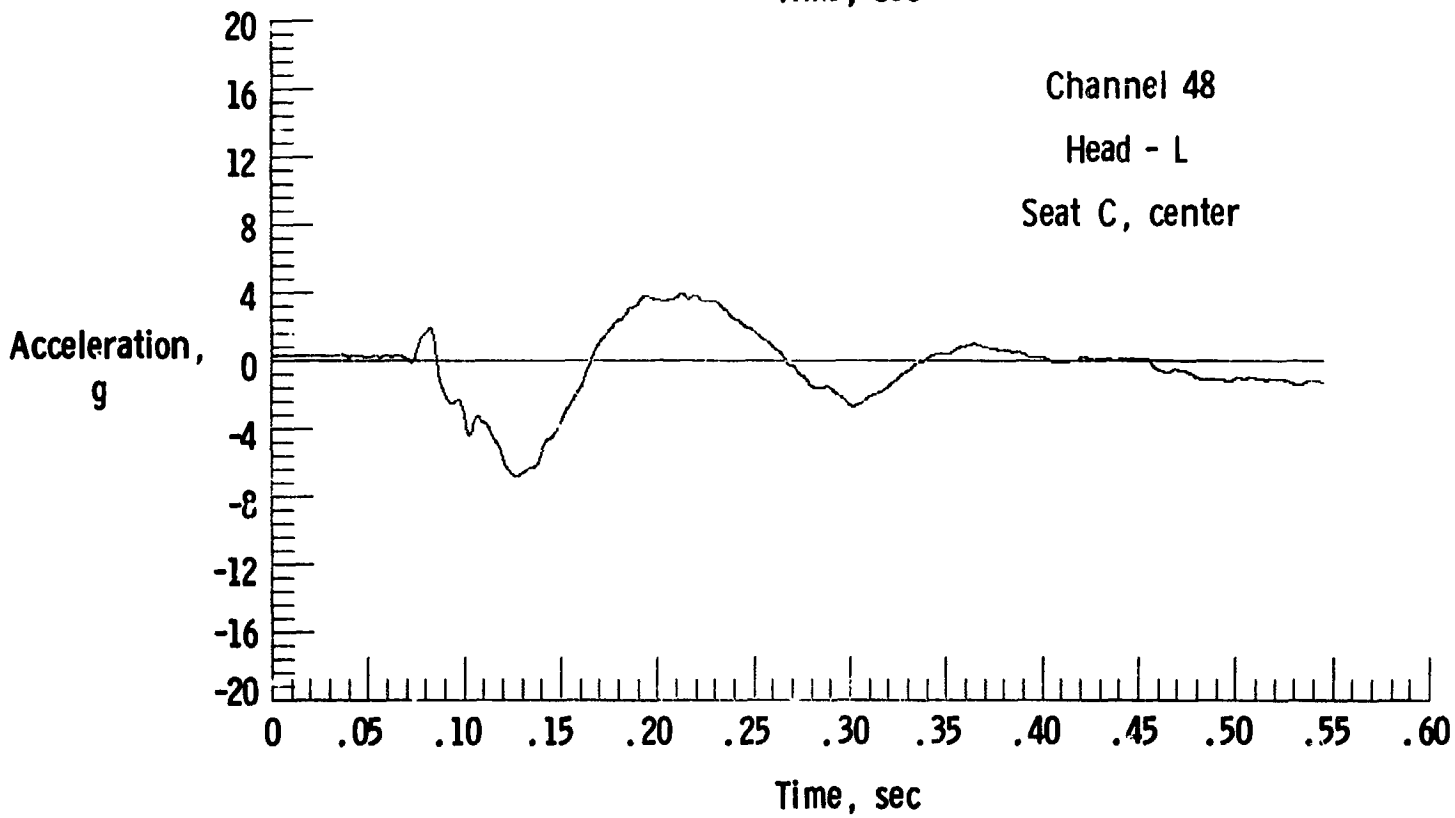

(e) Occupant accelerations.
Figure 10.- Continued.

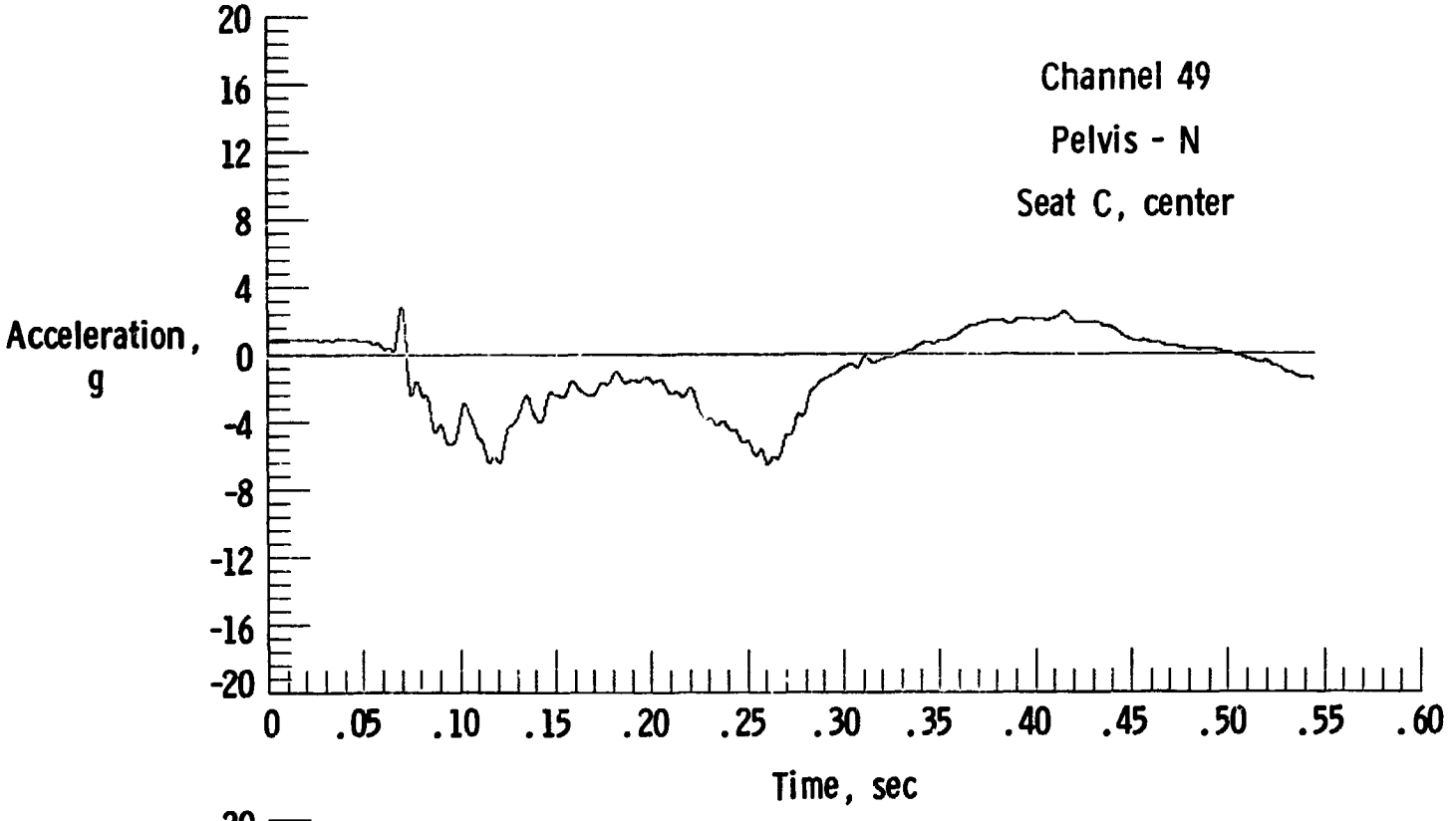

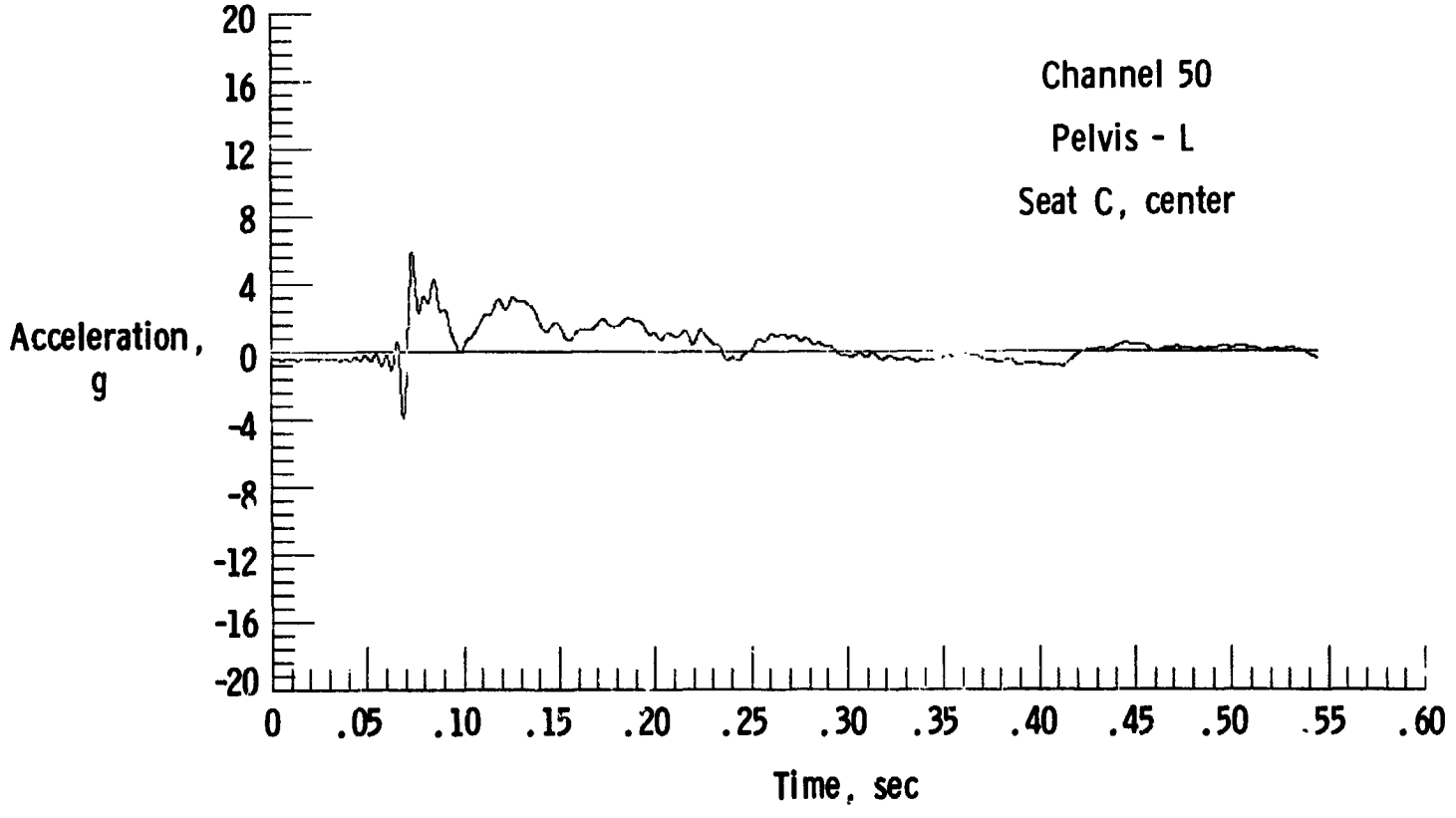

(f) Occupant accelerations.
Figure 10.- Continued.

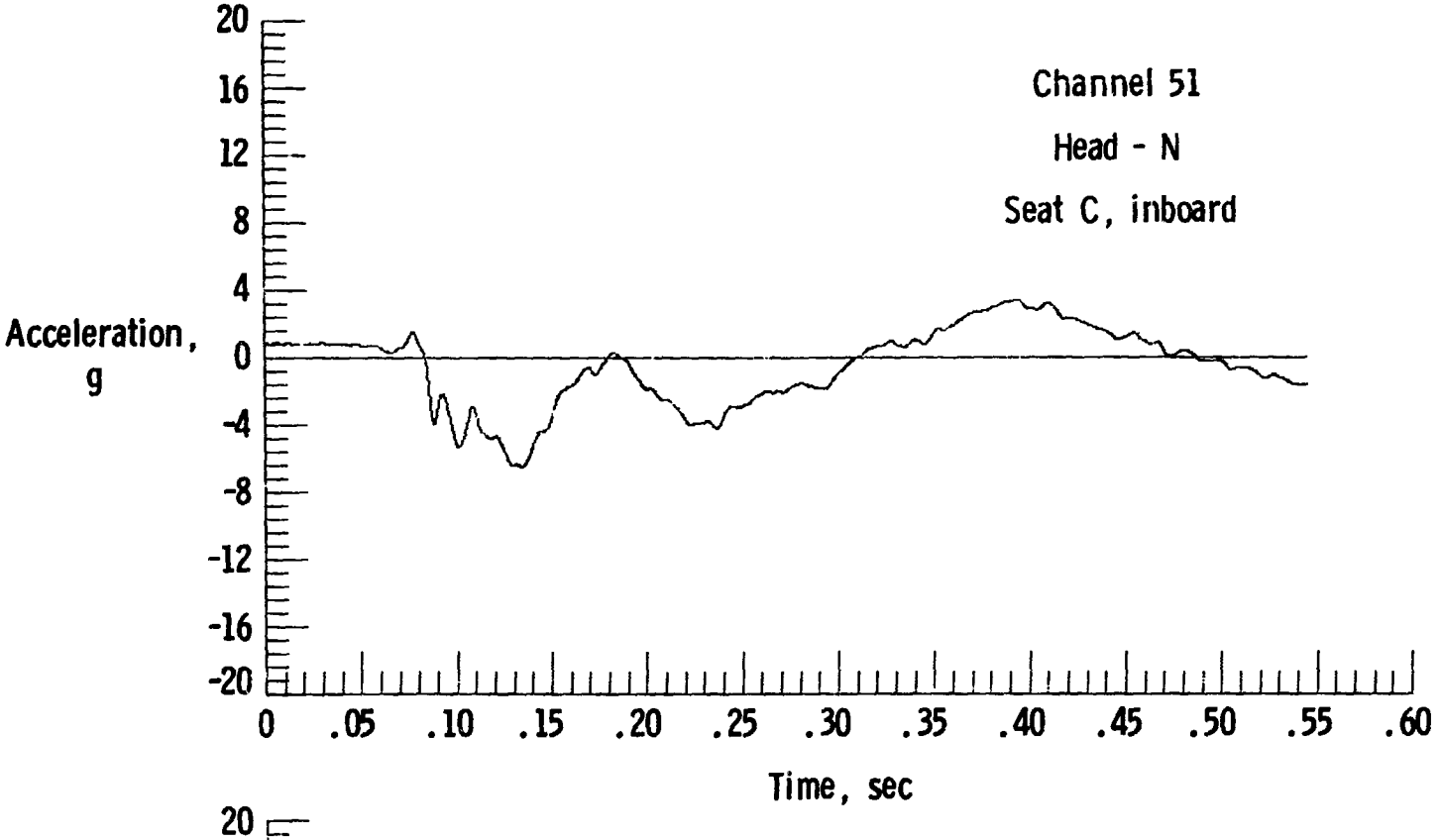

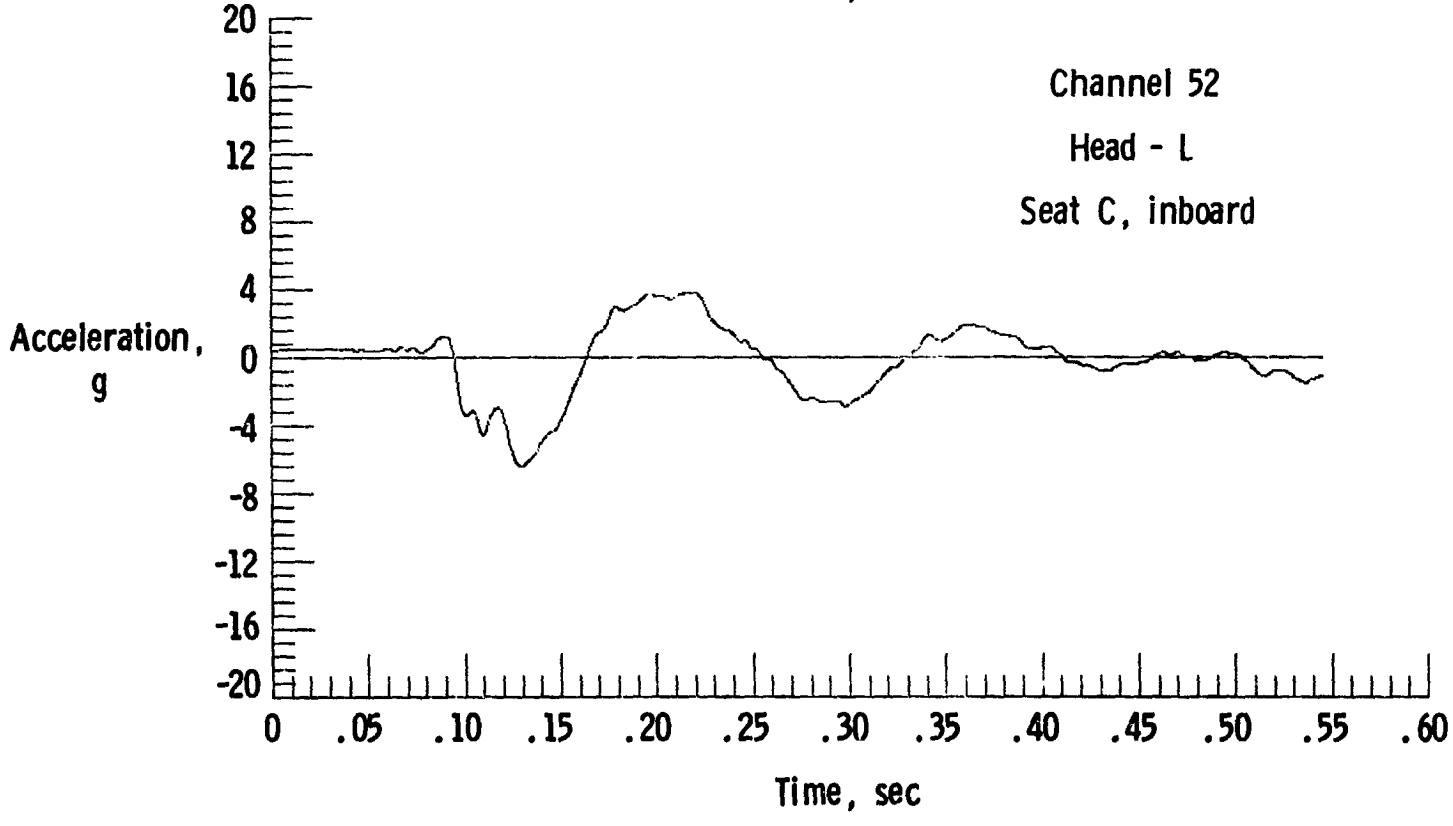

(g) Occupant accelerations.
Figure 10.- Continued.

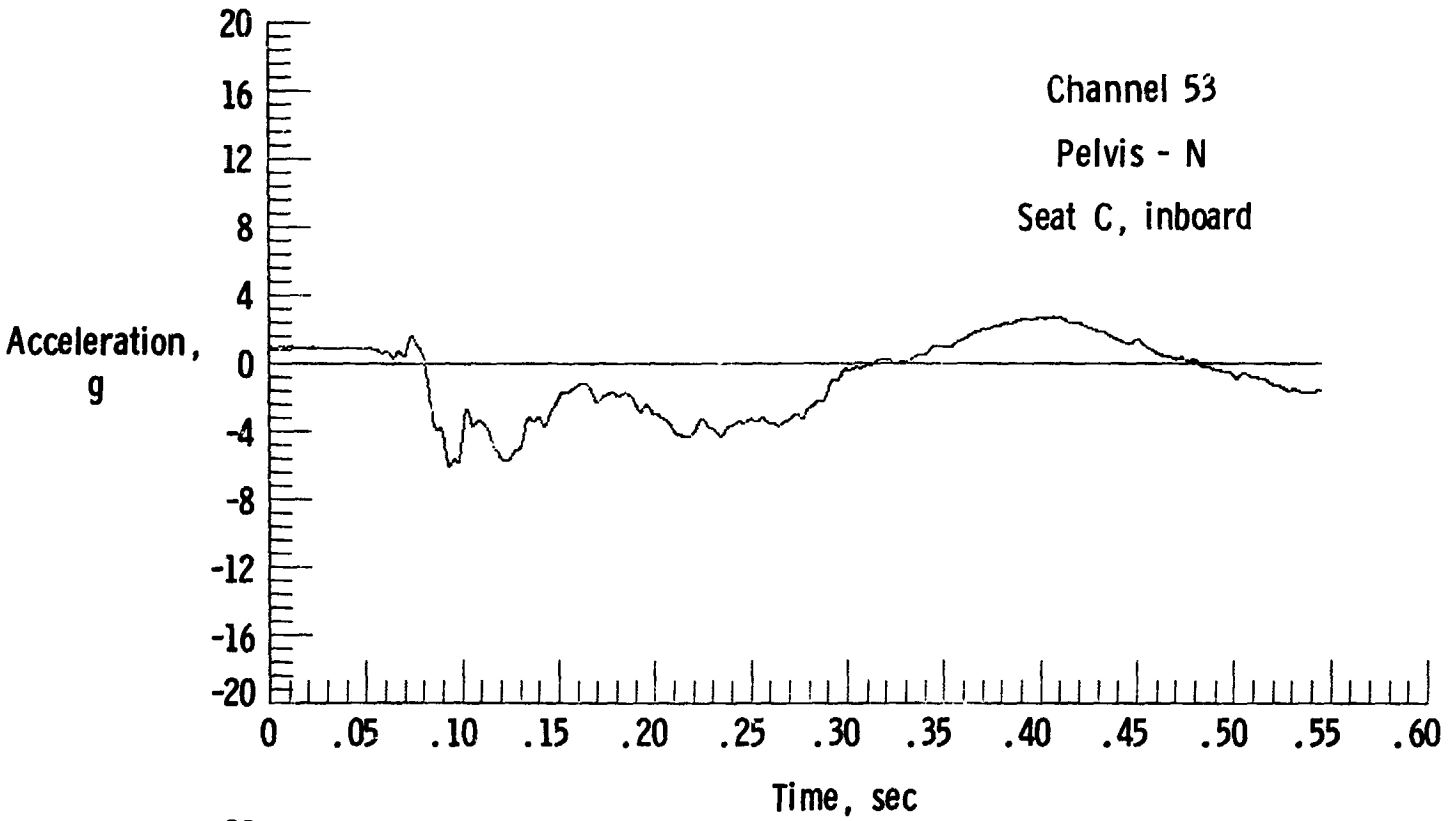

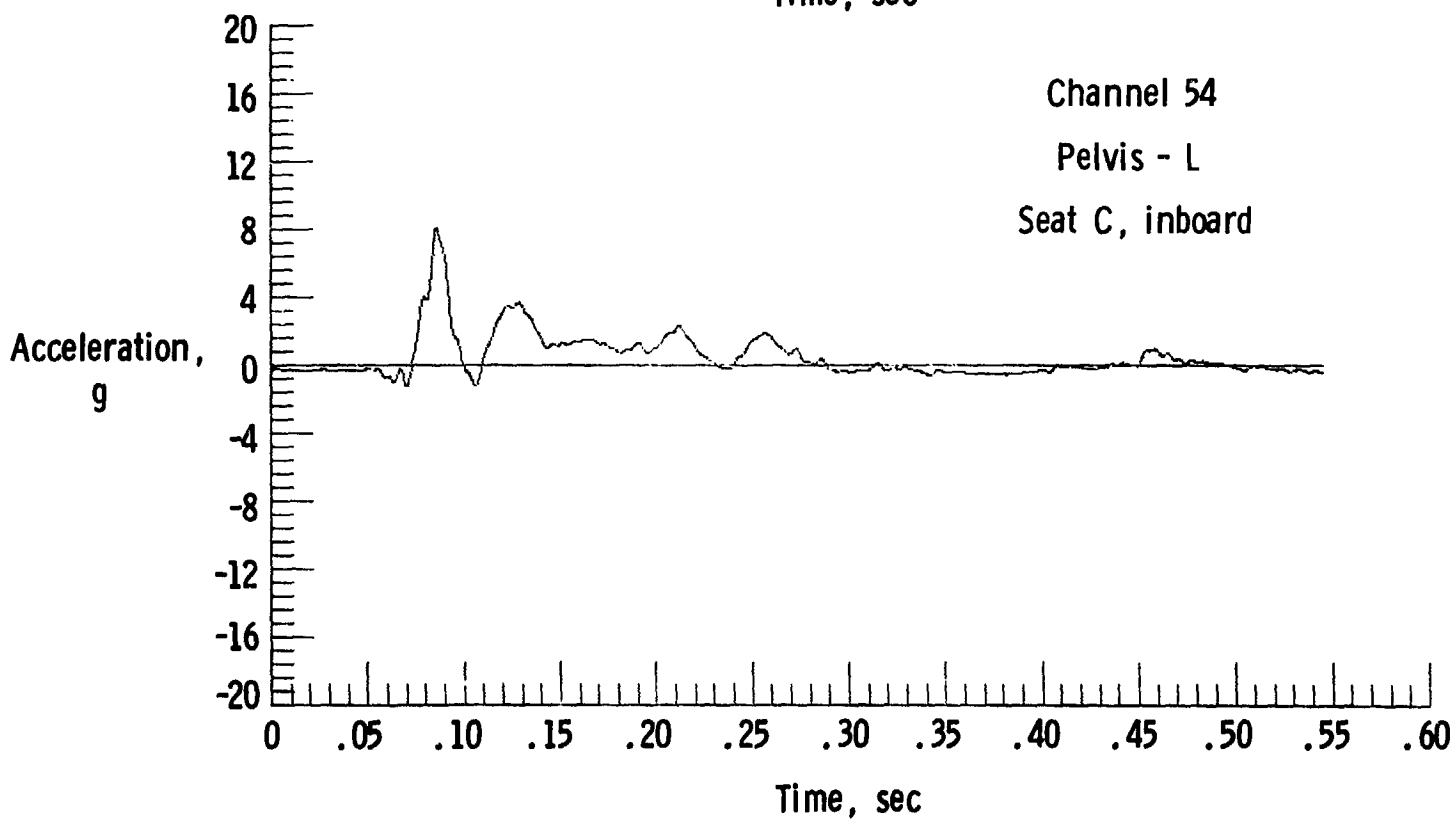

(h) Occupant accelerations.
Figure 10.- Continued.

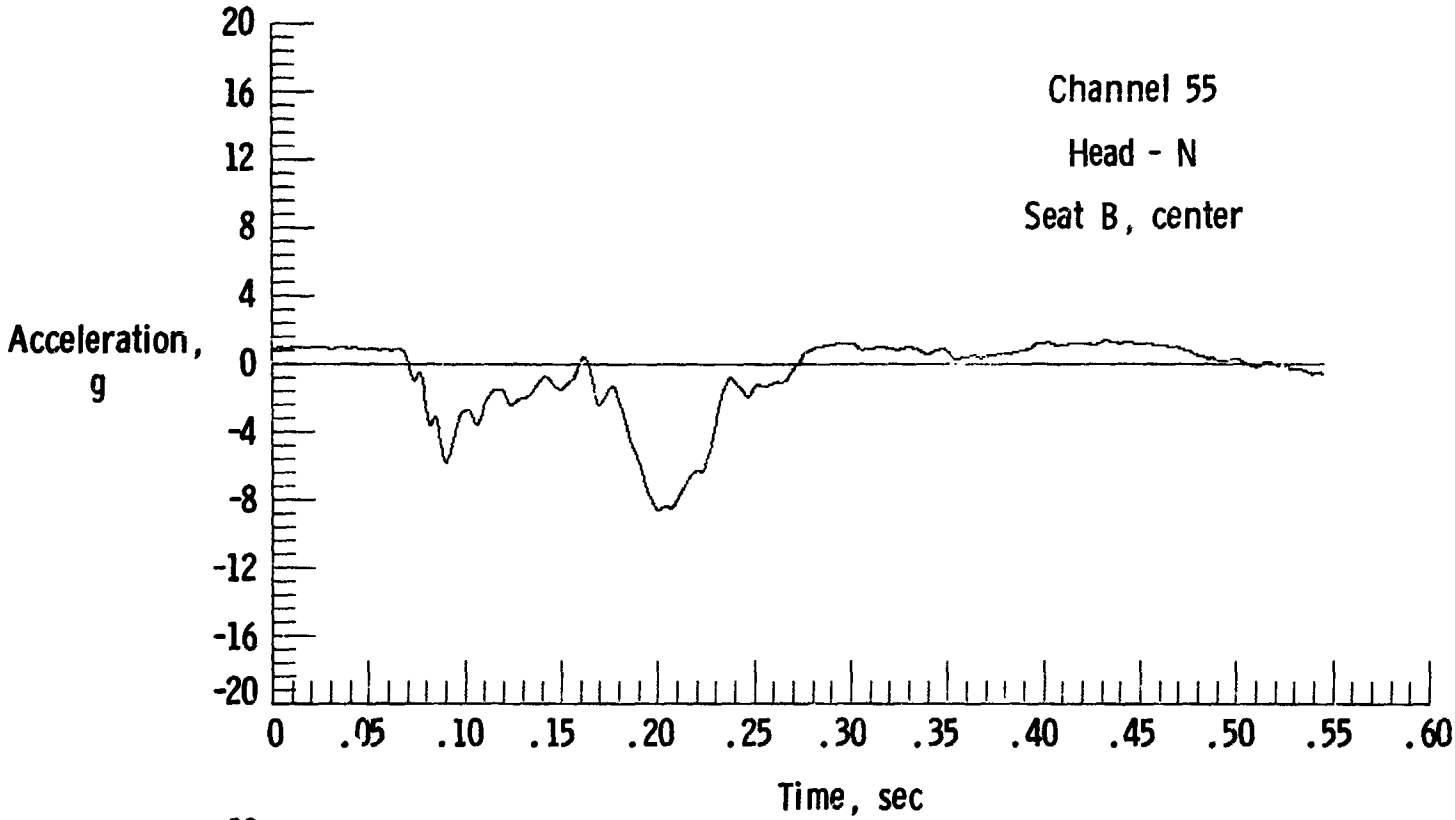

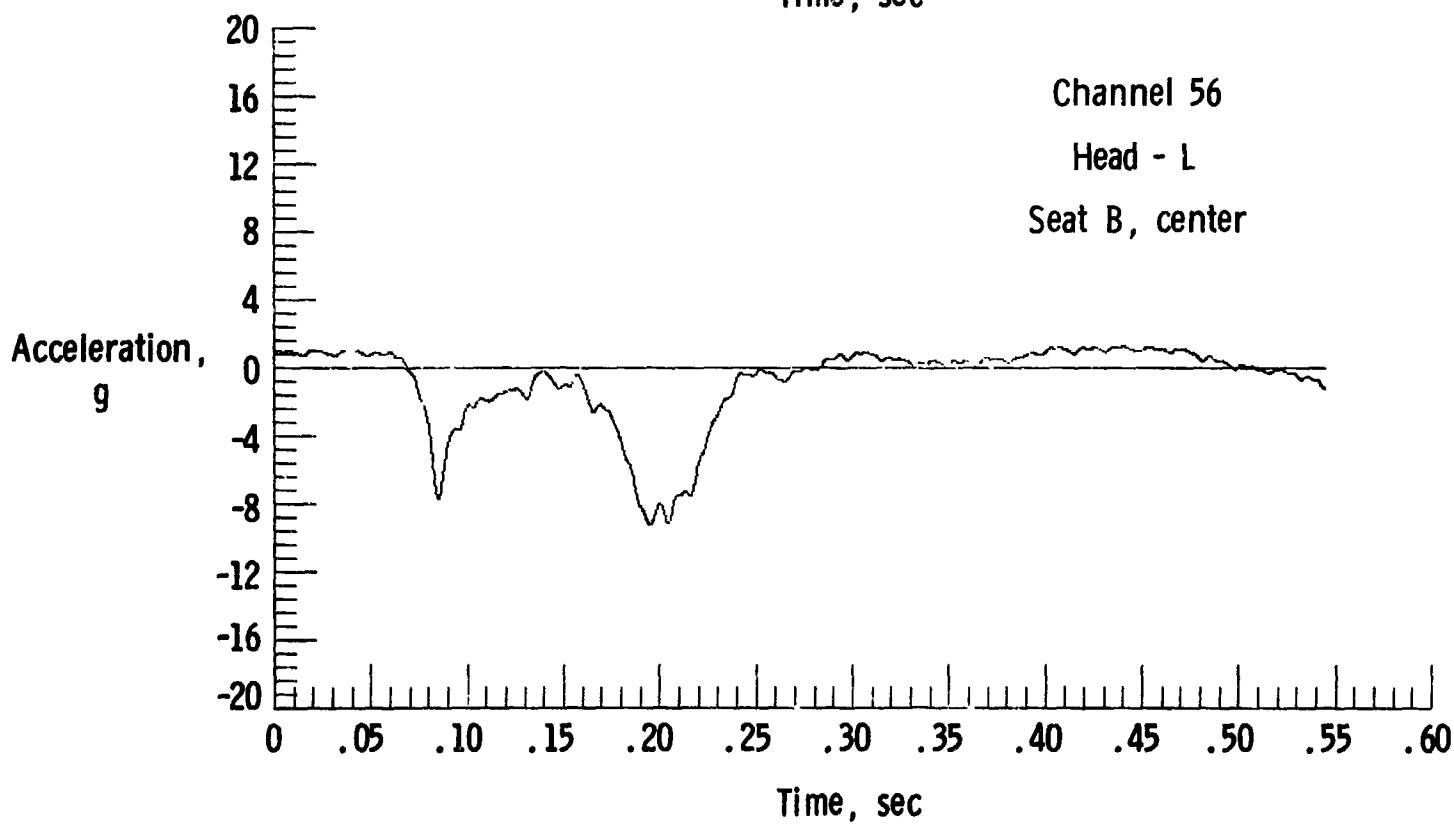

(i) Occupant accelerations.
Figure 10.- Continued.

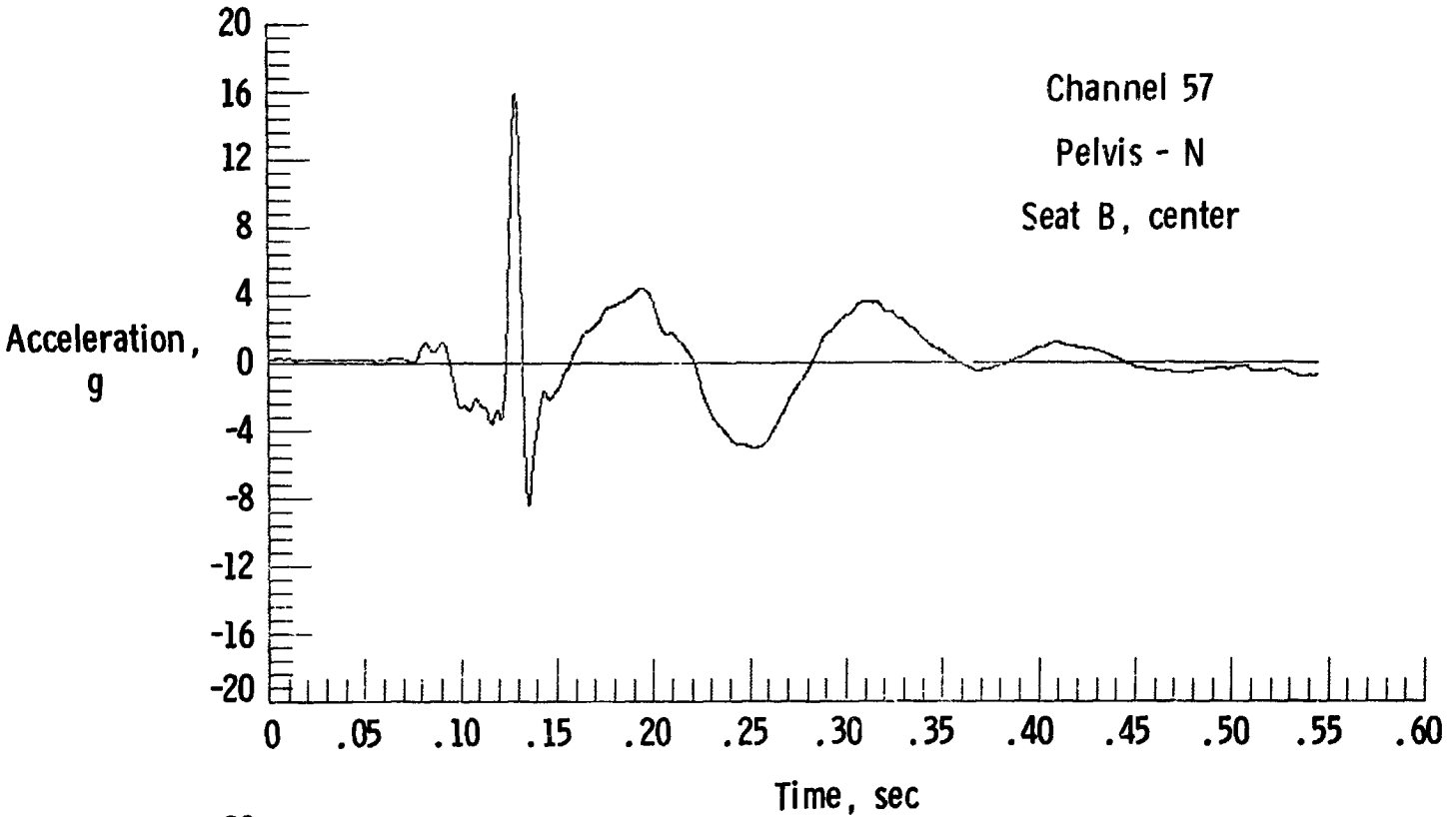

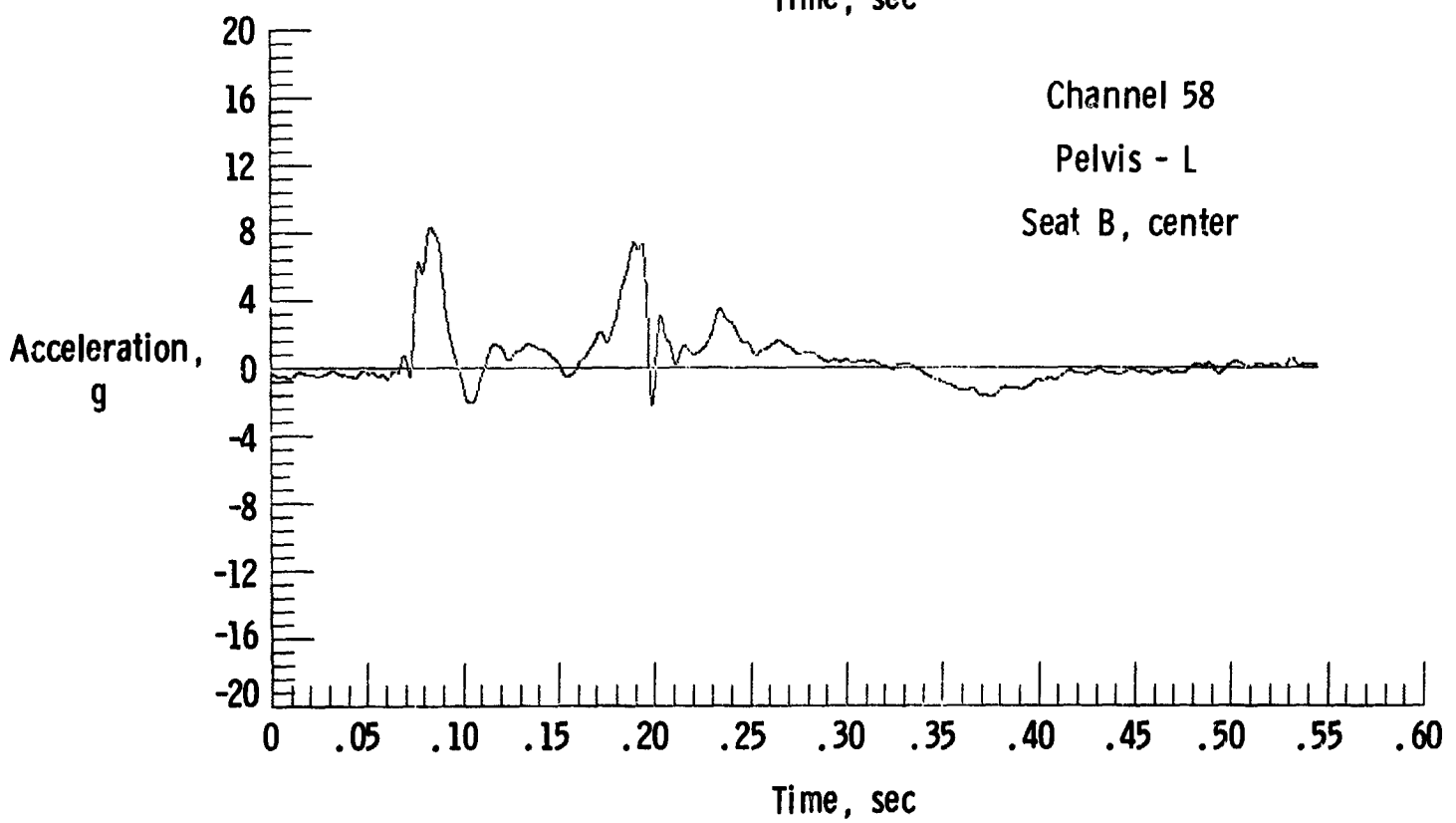

(j) Occupant accelerations.
Figure 10.- Continued.

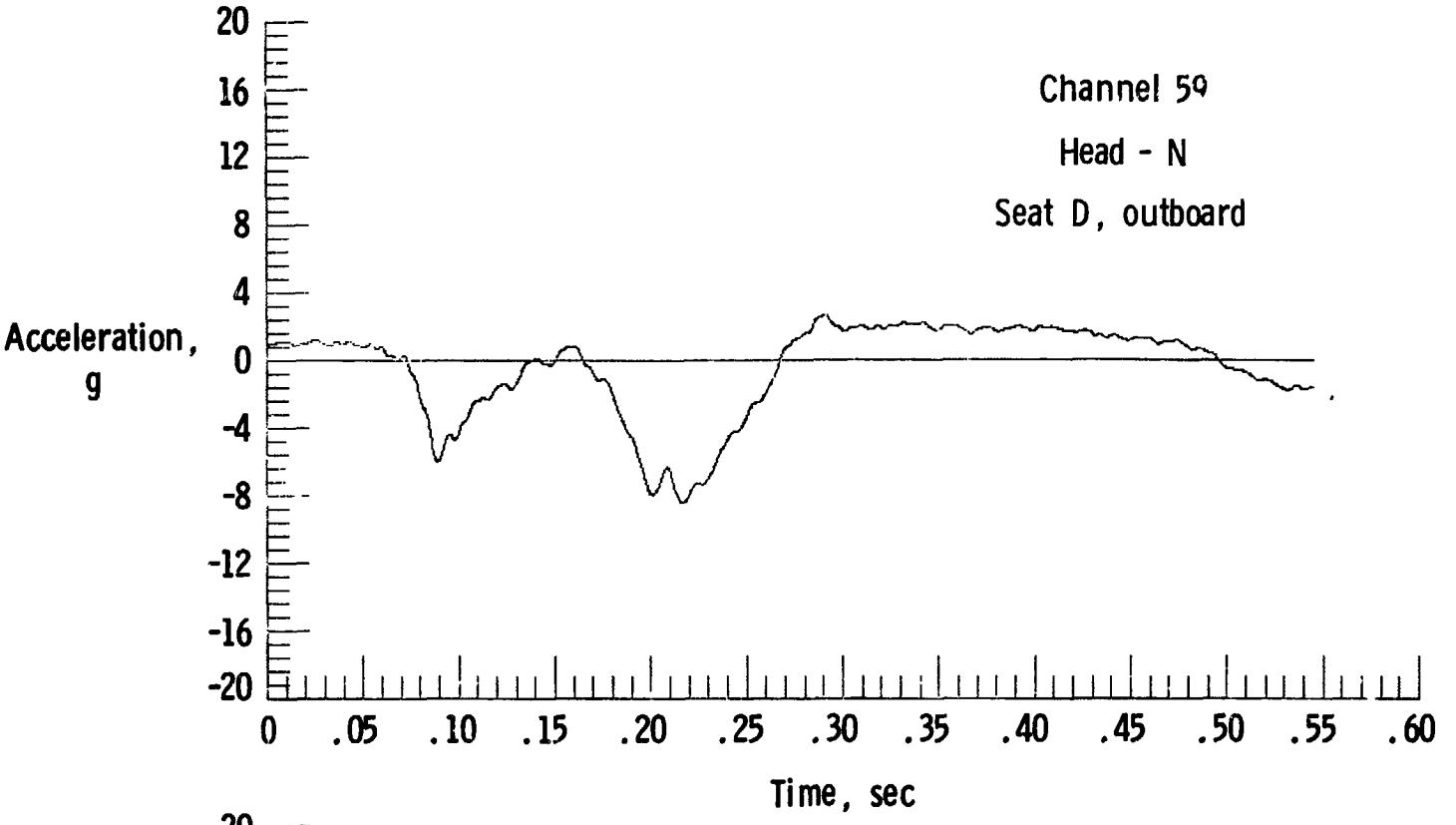

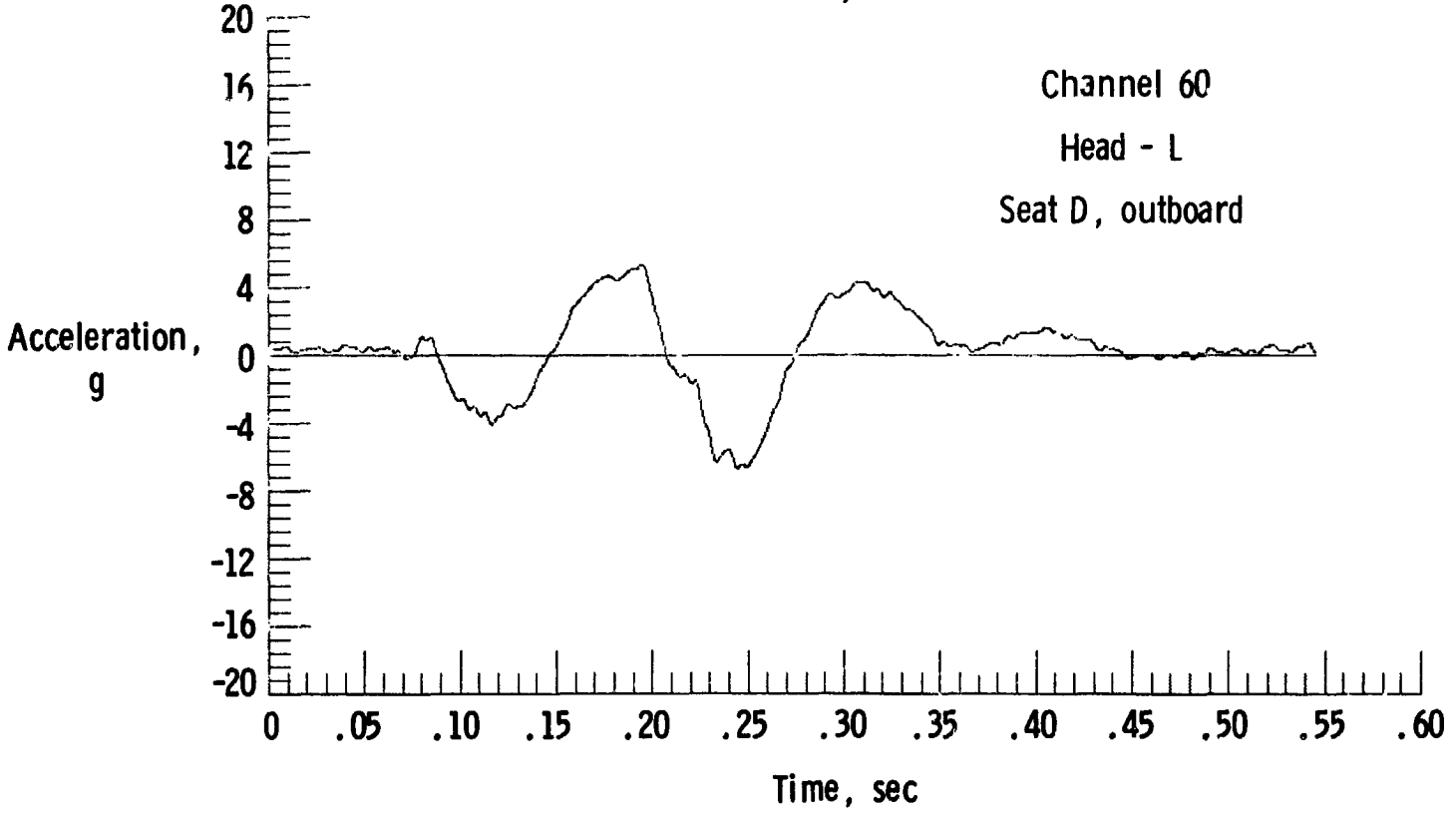

(k) Occupant accelerations.
Figure 10.- Continued.

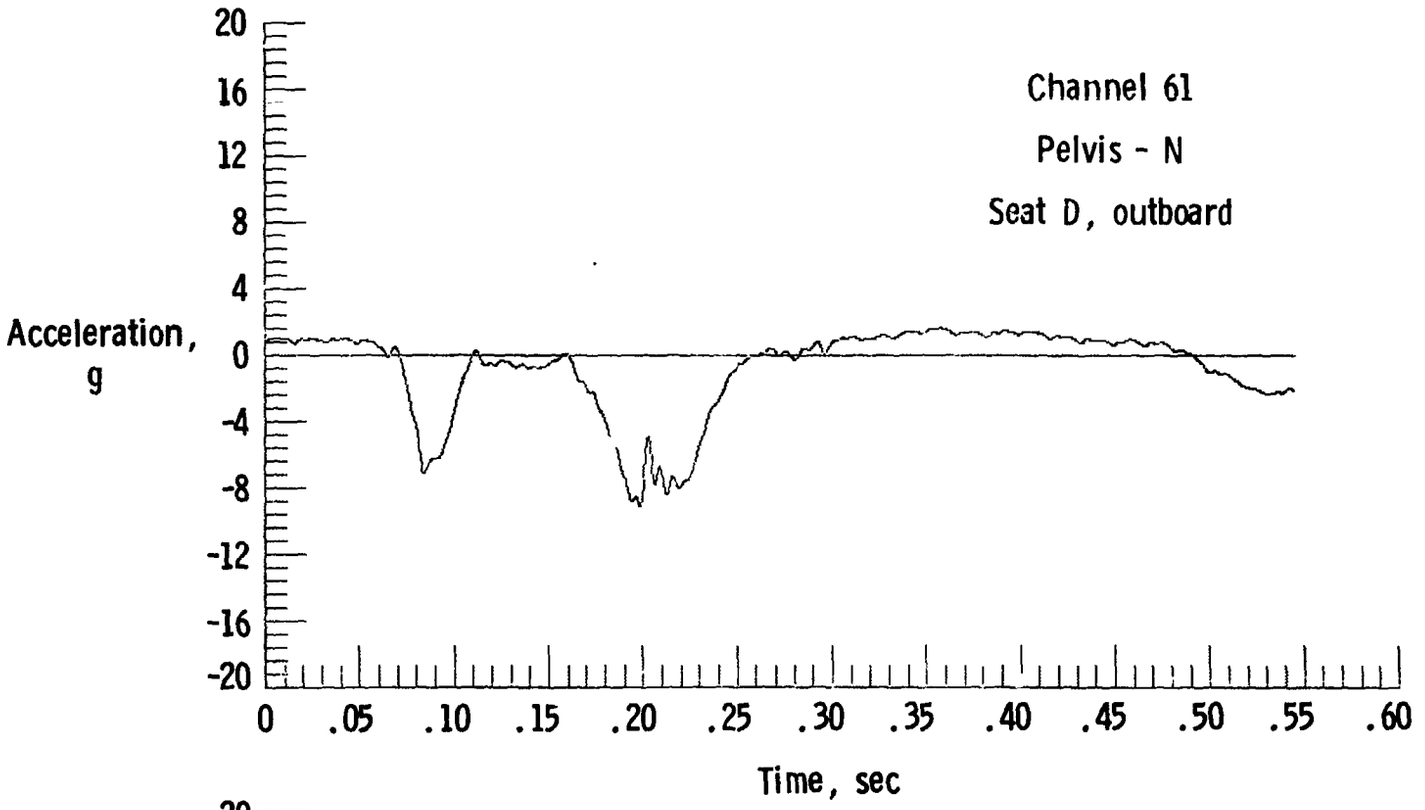

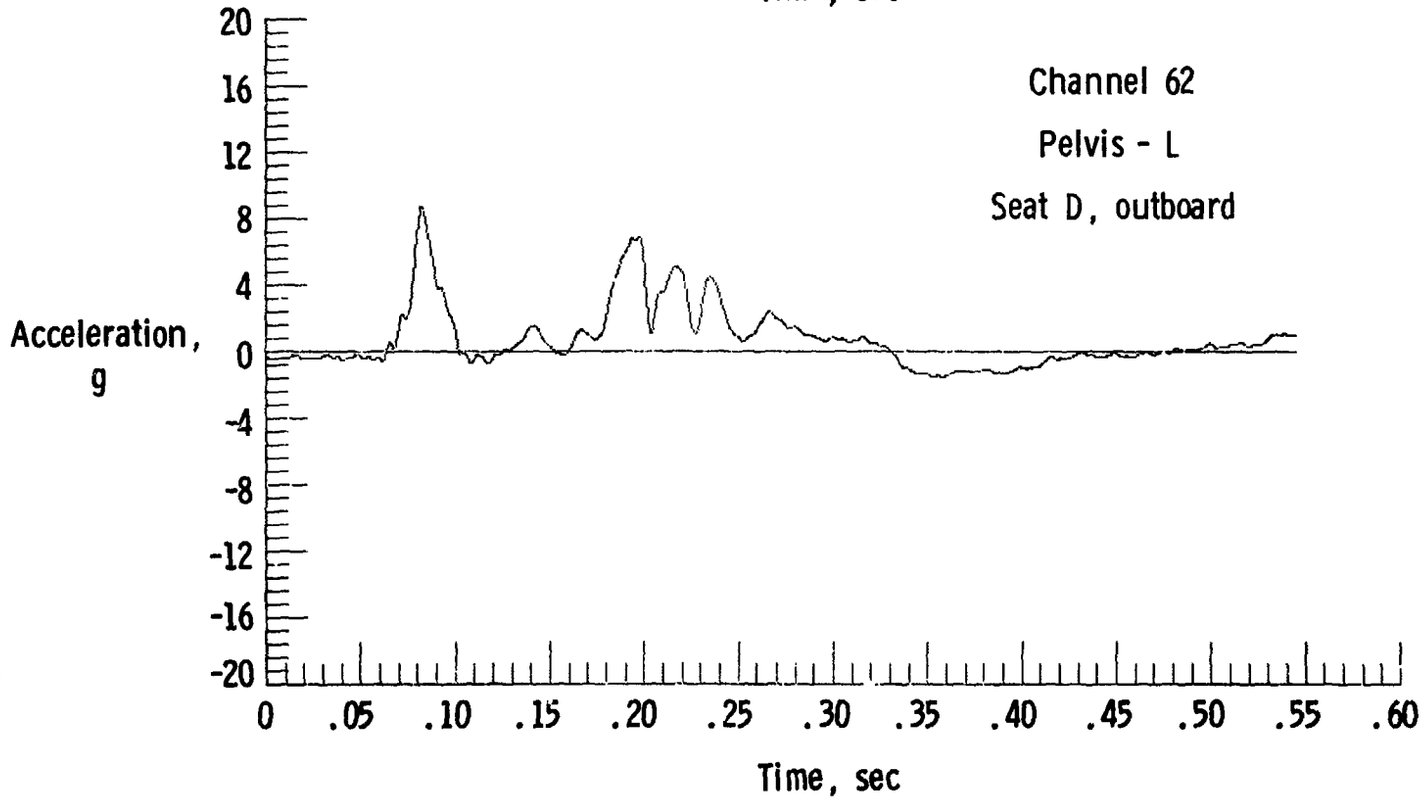

(1) Occupant accelerations.

Figure 10.- Continued.

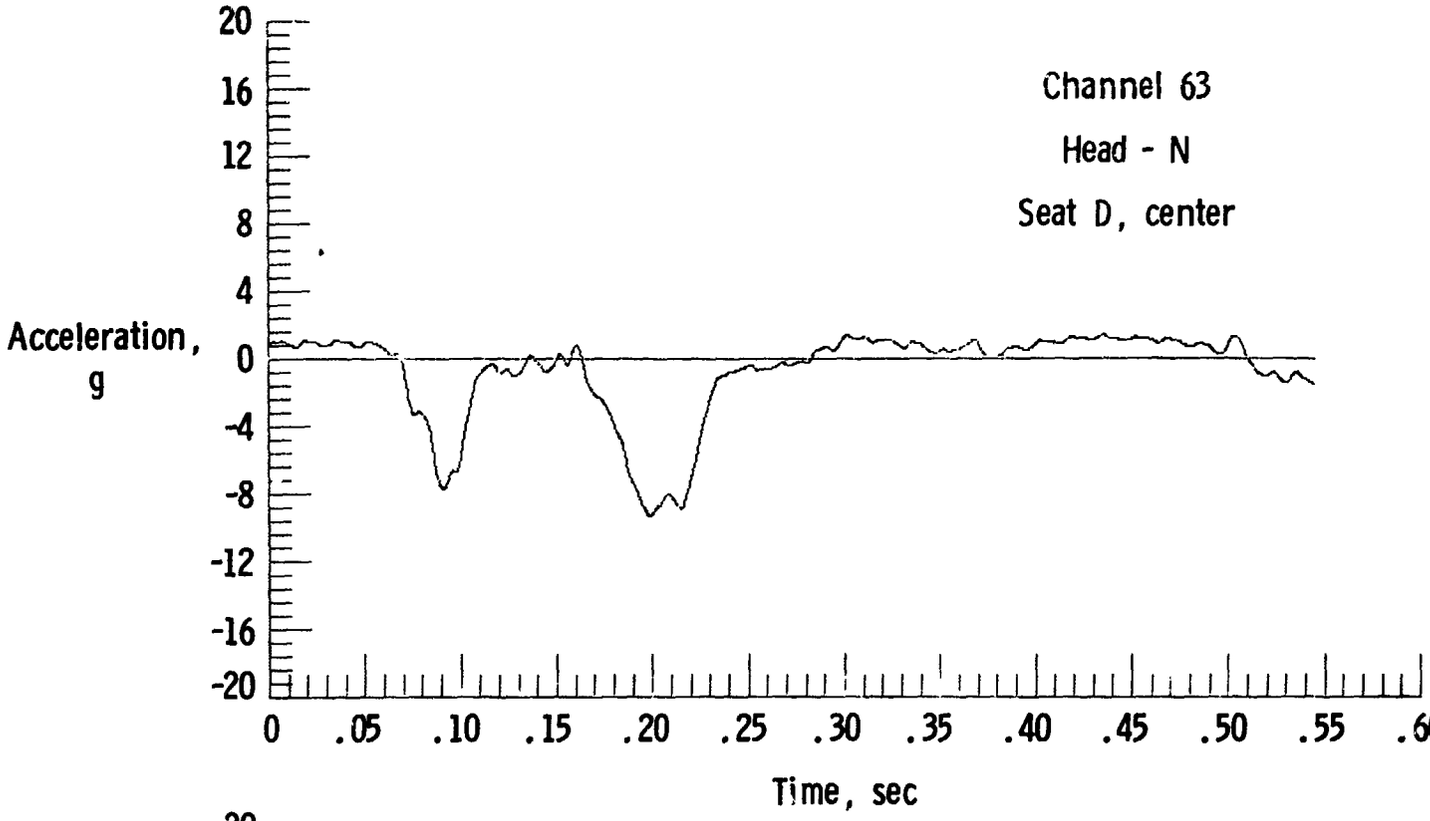

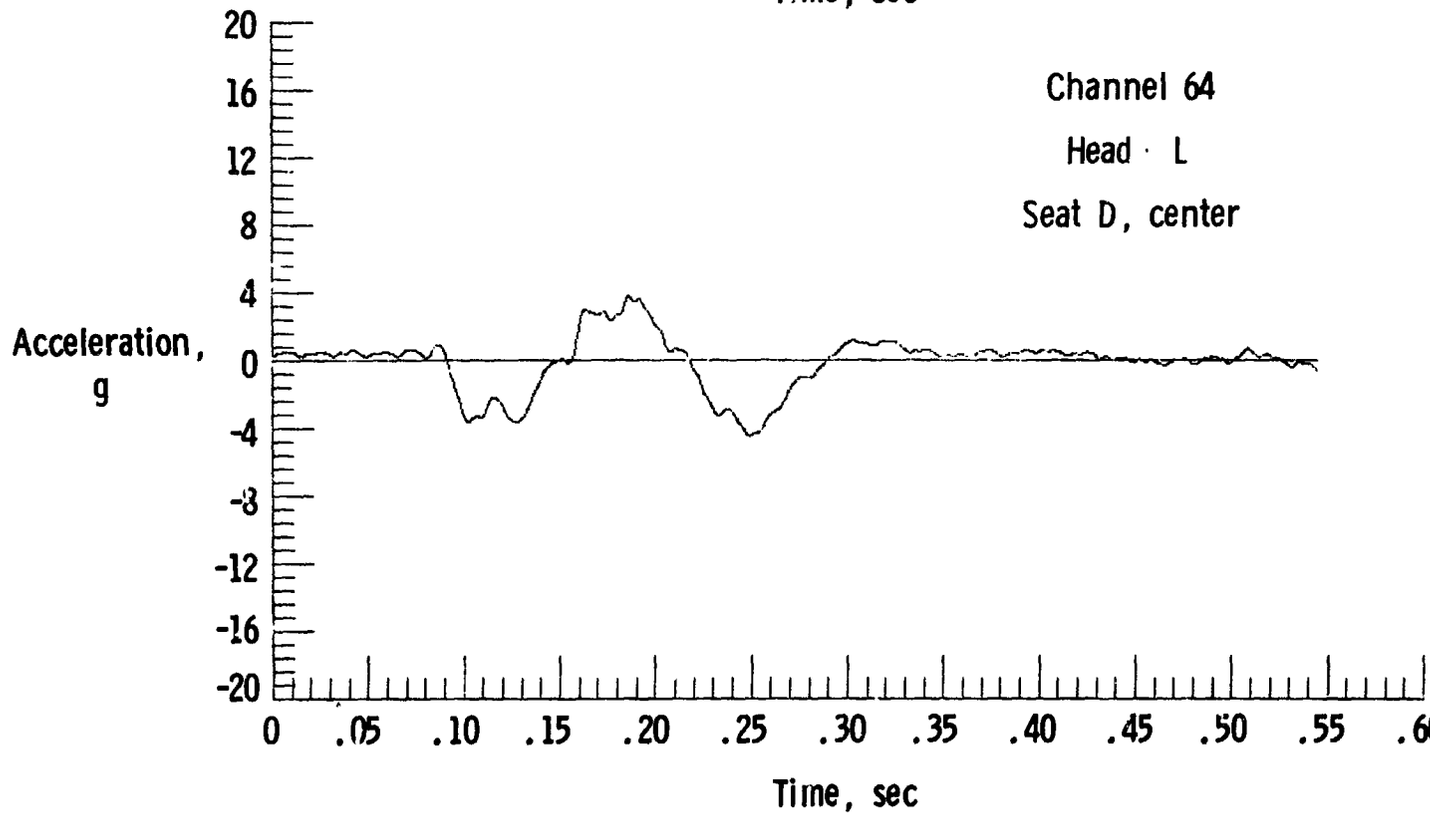

(m) Occupant accelerations.
Figure 10.- Continued.

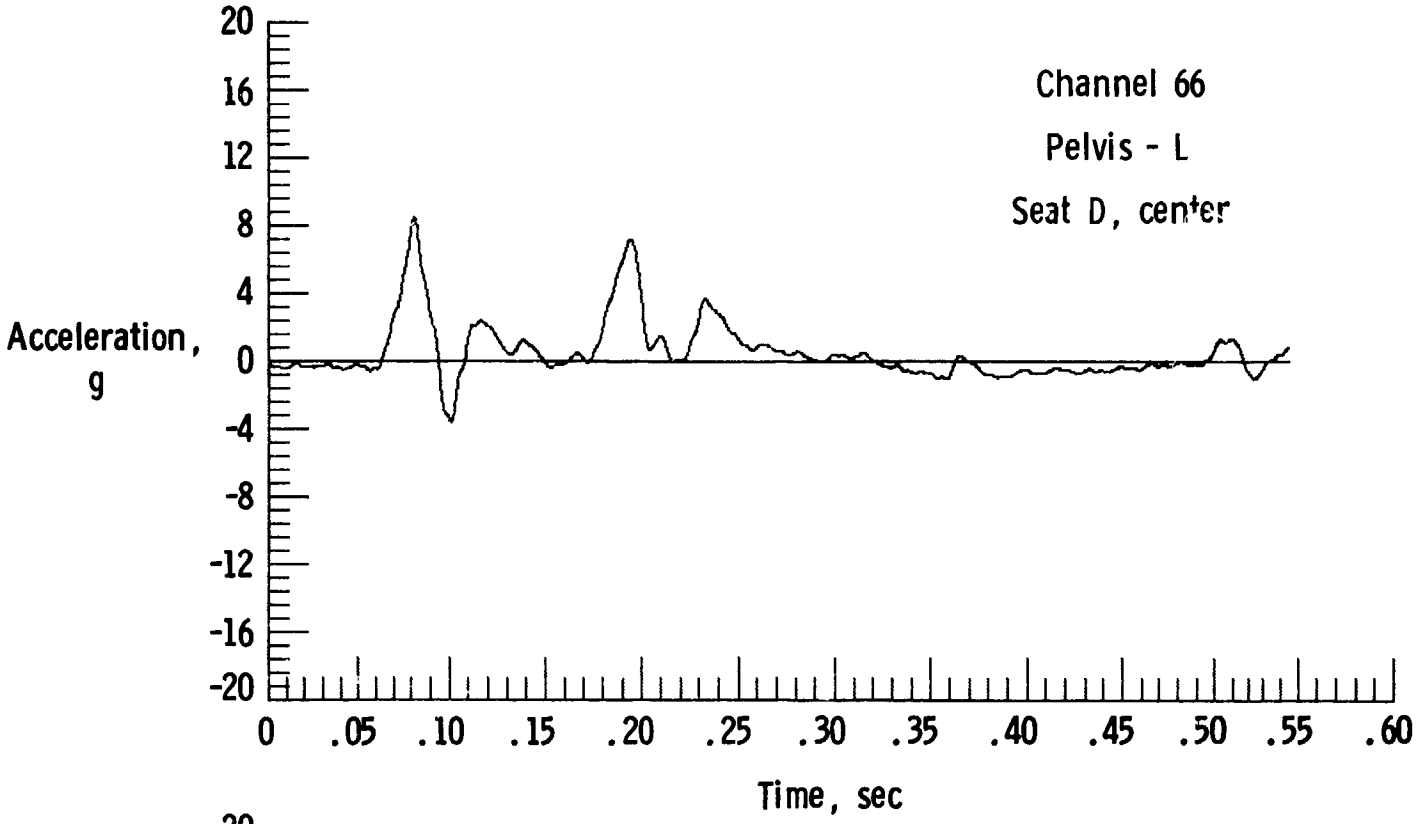

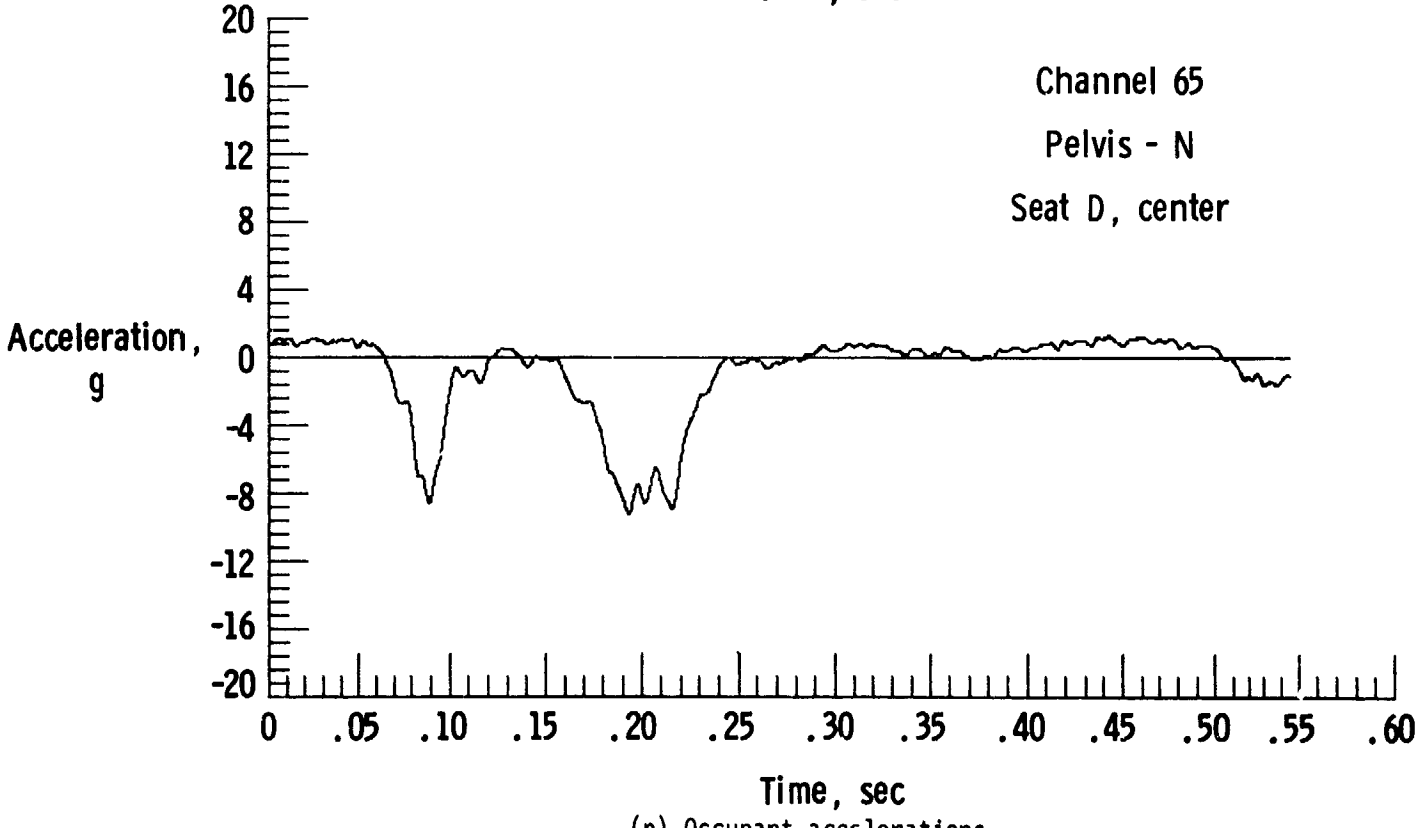

(n) Occupant accelerations.

Figure 10.- Continued.

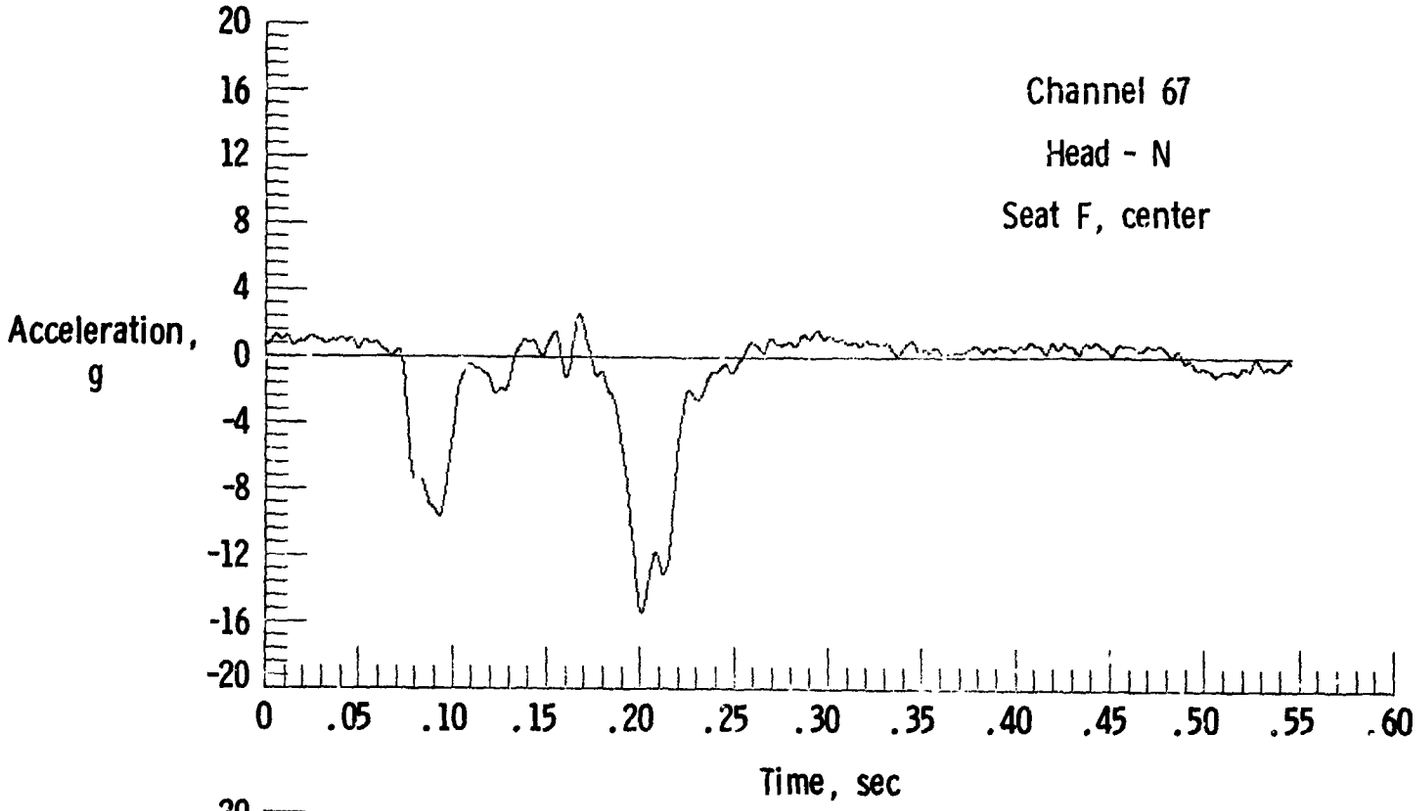

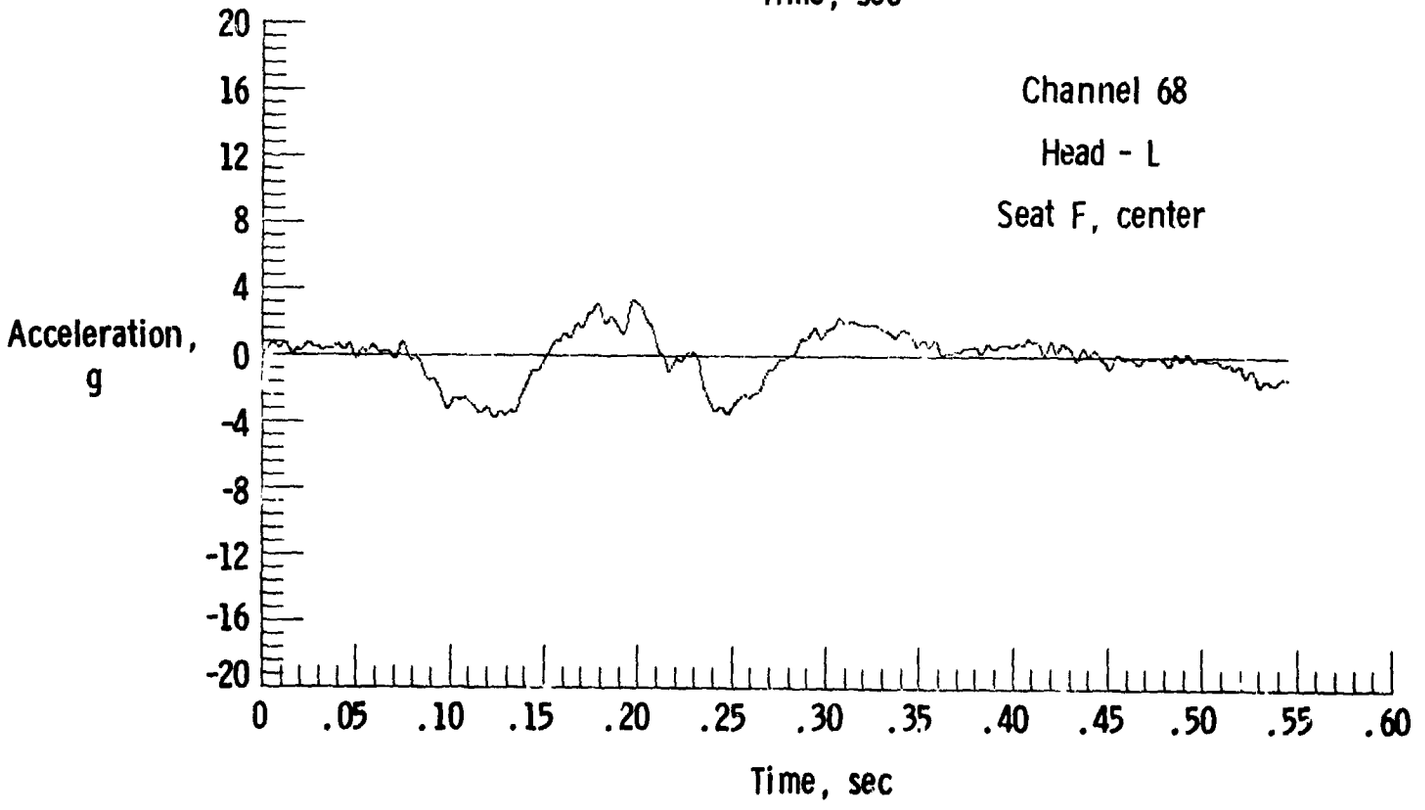

(o) Occupant accelerations.
Figure 10.- Continued.

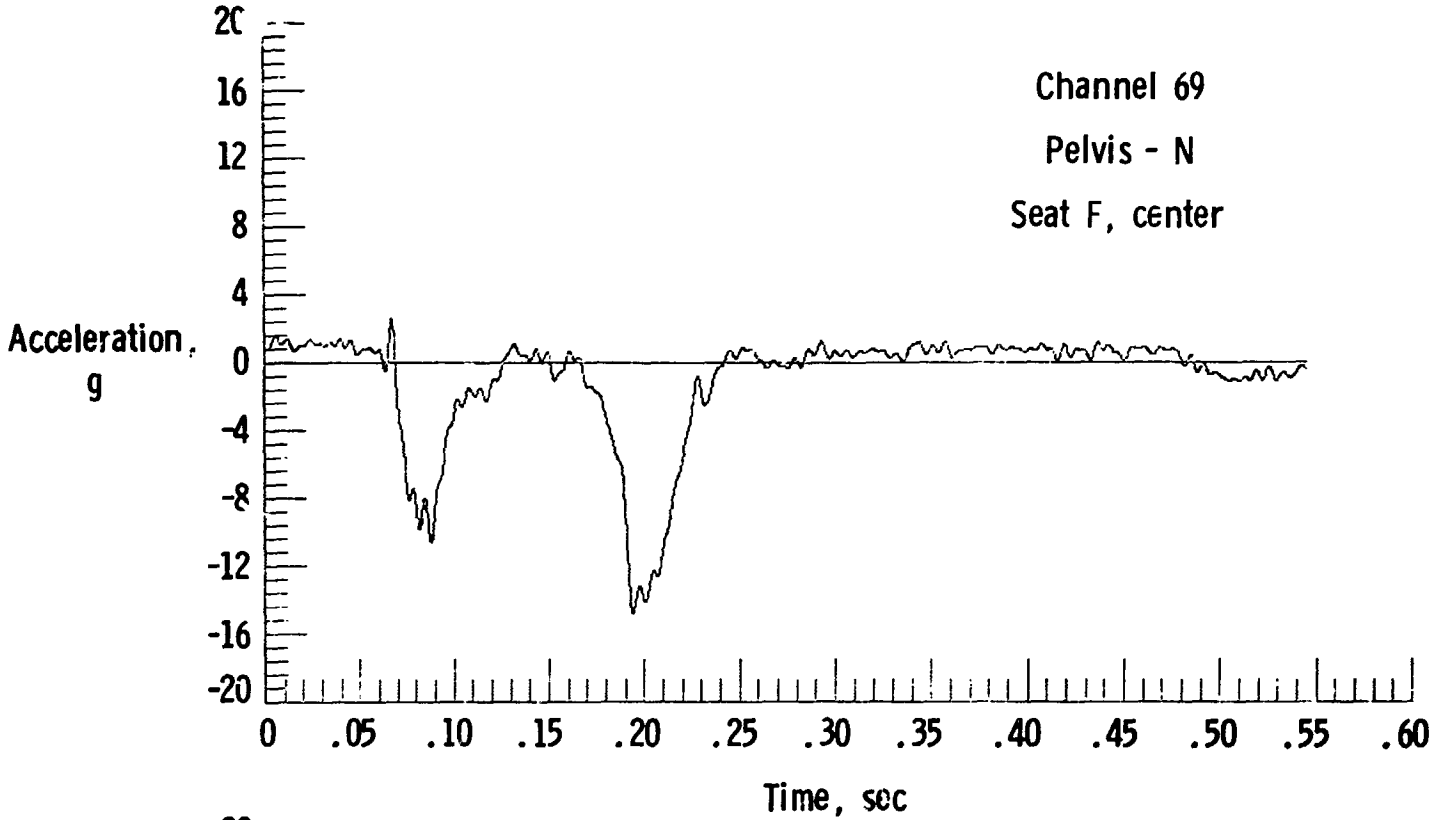

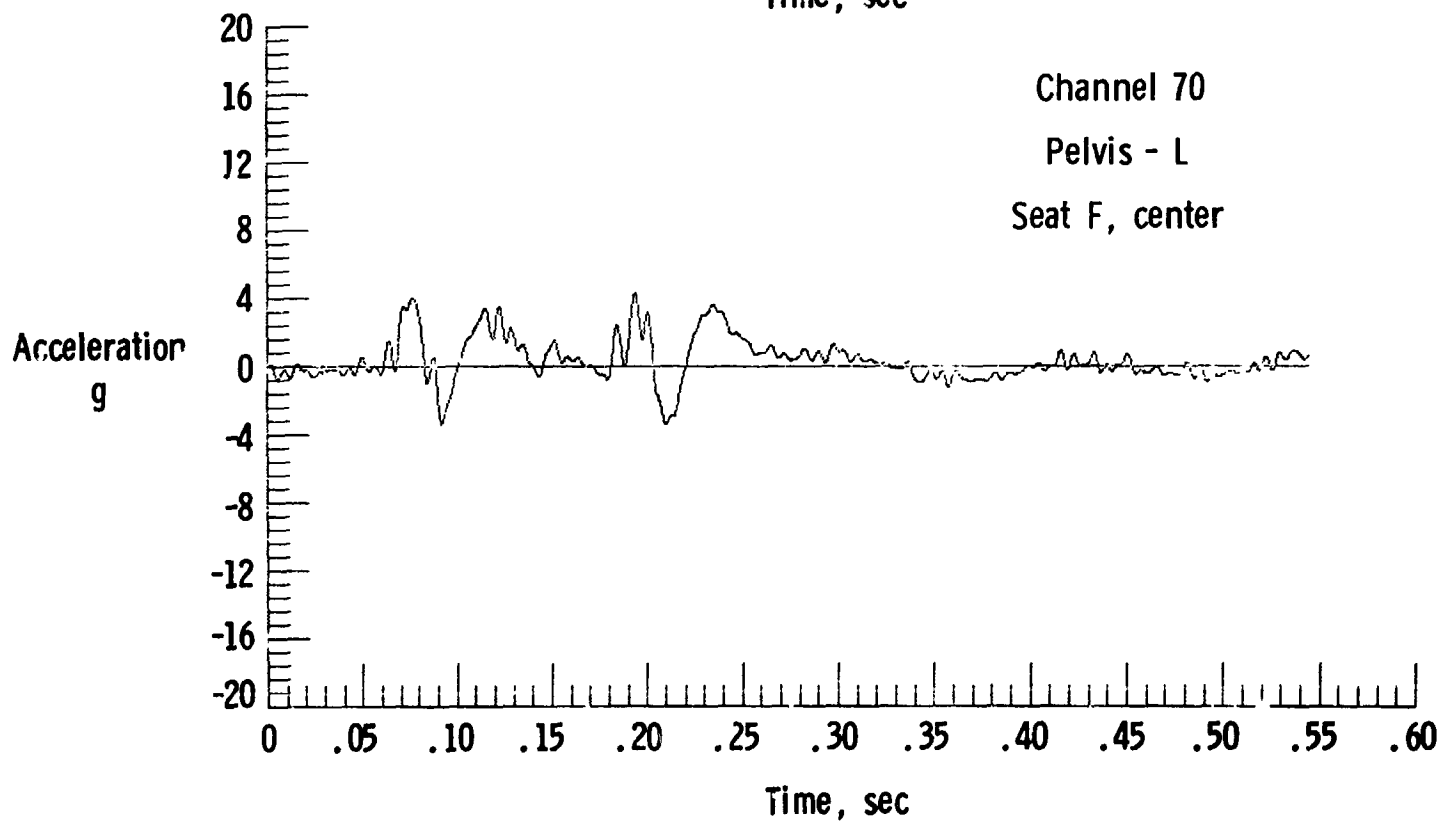

(p) Occupant accelerations.

Figure 10.- Concluded.